Facies and sedimentary architectures in the Upper Silurian Ringerike Group, Eastern Norway

Master's Thesis in Geodynamics and Basin Studies

Daniel Bergsagel Høie

Department of Earth Science

University of Bergen

June 2022

Abstract

The Upper Silurian Ringerike Group in Eastern Norway consists of alluvial-marginal marine deposits and is divided into the Sundvollen and Stubdal Formations. The formations were likely deposited in a piggyback basin adjacent to the advancing Caledonides and are in the study area limited to alluvial deposits, exposed in discontinuous outcrops. Deposits exhibit characteristics of a proximal distributary fluvial system, with minor amounts of mudstone beds in between the amalgamated sandstone bodies deposited by what has previously been recognised as meandering and braided rivers. Updated studies about the Ringerike Group are lacking and this thesis therefore provides a new facies and sedimentary architectural analysis of the Ringerike Group in which can aid to better understand proximal alluvial subsurface reservoirs. Field work, rock sampling and drone data acquisition with subsequent photogrammetry modelling have been utilised in order to interpret the deposits using facies analysis, sedimentary logs, microscopic techniques and sedimentary architecture analysis on virtual outcrops.

This study shows contrasting deposits in the Ringerike Group, with a more mudstone/siltstone-rich Sundvollen Formation compared to the almost exclusively sandstone represented Stubdal Formation. Fluvial deposits are however very similar, with amalgamated sandstone bodies represented in a multi-storey complex with internal cross-cutting of bed surfaces. Differentiation of fluvial styles between the two formations is furthermore argued, as facies and sedimentary architecture analyses show little evidence supporting such a distinction. 2D exposures of proximal fluvial deposits are known to be misinterpreted as the distinction between braided and meandering river deposits in proximal alluvial systems is a complicated task.

The Ringerike Group has overall very good connectivity and high net to gross values, thus displaying an analogue of excellent reservoir qualities. However, mudstone baffles are present and can impose troubles on the channel belt to channel belt connectivity. Moreover, the arid/semi-arid environment in the scarcely vegetated Late Palaeozoic combined with a tectonically active foreland basin system have further implications for the reservoir characterisation of the Ringerike Group.

This study only focuses on 2D architectural elements and further studies giving more attention to 3D sedimentary architectures and small-scale heterogeneities of proximal alluvial systems are proposed to further aid our understanding of such systems related to reservoir characterisation.

Acknowledgements

This thesis is a part of my master's degree in the Geodynamics and Basin Studies Research Group at the Department of Earth Science, University of Bergen. In this section I would like to give my appreciations to those made this thesis possible.

First and foremost, I would like to express my deepest gratitude to my main supervisor, Associate Professor Christian Haug Eide (University of Bergen) for the great discussions and excellent guidance during these last two years. Thank you for your great support, feedback and encouragement. In addition, I would like to express my gratitude to my co-supervisor, Dr. Gijs Allard Henstra (Aker BP) for jumping on the project mid-thesis, for your great guidance and feedback and for helping me during the field work.

Special thanks to Andreas Lambach Viken for making the many thin sections used for this thesis and to Martin Kjenes for helping me with the photogrammetry modelling. Big thanks to Atle Rotevatn for letting me loan the drone in the field. Also, thanks to Leif-Erik Rydland Pedersen for instructing me on how to use the stereoscope. Thank you to Johan Petter Nystuen for providing helpful literature.

I would also like to thank my fellow students for the interesting discussions, memories and social events during these great years although slightly spoiled during the Covid-19 pandemic. Special thanks to Håvar Sæther for assisting me during the field work and for enduring the cold first night in the cabin. Additionally, thanks to Tor-Sebastian for proofreading.

Finally, thank you to my friends and family for supporting me during these exciting years.

Daniel Bergsagel Høie

Bergen, June 2022

Table of Contents

1.0 Introduction

1.1 Motivation

Alluvial deposits are very common in the stratigraphic record and are frequently present in the subsurface as reservoirs for hydrocarbons (e.g. Miall, 2006) and can also work as reservoirs for carbon dioxide sequestration (e.g. Förster et al., 2010) and water exploitation in relation to the geothermal energy industry (e.g. Donselaar et al., 2015), for drinking water (e.g. Amoros et al., 1987) and for irrigation (e.g. Belmar et al., 2013). The alluvial deposits are often mostly represented by fluvial systems, which are controlled by allocyclic factors such as tectonism, climate and eustasy. Moreover, vegetation is another significant factor in the fluvial systems, factoring into the stability of riverbanks and confinement of the active channels (Gibling et al., 2018). Vertical and lateral stacking patterns of the fluvial systems are directly linked to basin accommodation and sediment load, generating a variance of deposits in response to the interplay between sediment load and accommodation (Lang et al., 2001).

Recent studies regarding alluvial sedimentology (e.g. Moscariello, 2018; Paredes et al, 2018; Swan et al., 2018) have pointed to the complexity of the alluvial architecture and reservoir characterisation of related deposits. Connectivity between neighbouring sandstone bodies can be problematic to elucidate, as the distinction between storeys with amalgamated erosive sandstone bodies and storeys with stacked belts due to rapid aggradation can influence connectivity and fluid flow in the subsurface in different ways (Willis et al., 2018). However, such a distinction is not always easy to determine in neither the subsurface nor in outcrop analogues.

Prior to the development of abundant vegetation in the Palaeozoic, proximal alluvial systems with amalgamated sandstone bodies were often deposited from braided rivers in the alluvium (Gibling et al., 2018). However, there remains some knowledge gaps in studies of such proximal alluvial systems as new depositional models have been mostly focusing on more distal alluvial systems (Cyples et al., 2020). For instance: 1) the effect vegetation had on bank stability before terrestrial plants were widespread, 2) the distinction between fluvial styles in outcrop analogues and 3) the arrangement of the channel belts and the intersection of these in proximal alluvial systems in order to assess reservoir performance and connectivity are all subjects which are not

properly understood in proximal alluvial systems (e.g. McMahon & Davies, 2018; Swan et al., 2018; Willis et al., 2018).

The Upper Silurian Ringerike Group in Ringerike, Eastern Norway which are comparable to the Devonian Old Red Sandstones (Davies et al., 2005a) is an example of such proximal alluvial systems. The Ringerike Group was deposited in a foreland basin system adjacent to the Caledonian fold and thrust belt and comprises marginal marine to alluvial deposits which in the study area is represented by two formations: the Sundvollen Formation and the Stubdal Formation (Turner, 1974a; Davies 2005a). The deposits are exposed in large outcrops and can be used as an analogue to subsurface reservoirs with a proximal alluvial character. A detailed study of the deposits in the Ringerike Group can therefore provide a better understanding of proximal alluvial systems and their potential as reservoirs for e.g. hydrocarbons, carbon dioxide and water. Sedimentary architectures are displayed well in the outcrops, though sedimentary structures and grain sizes are on the other hand more difficult to determine in the field due to diagenetic and weathering processes, requiring microscopic analyses.

Previous work has mostly focused on the stratigraphy and geochronology of the Ringerike Group and trace fossils of the underlying marine formations (e.g. Størmer 1954; Whitaker, 1965; Davies et al., 2005a; 2005b: 2006; Kristoffersen et al., 2014). Scientific studies regarding the sedimentology of the alluvial deposits however are scarce, where the last in depth published and peer-reviewed research of the alluvial system came from Turner (1974a; 1974b).

1.2 Aims

Through a combination of field and laboratory work, this thesis will provide a new and detailed study of the Ringerike alluvial system, both on the macro scale through studying outcrops and on micro scale through studying thin sections sampled from the field. The aims of the thesis are therefore to 1) describe the outcrops in terms of architectural elements and sand connectivity according to the sand/mud, 2) examine the textural and structural properties of the sampled thin sections, 3) provide an integrated interpretation and discussion of the alluvial system through the macro and micro results, 4) discuss the differences in deposits between the Sundvollen and Stubdal Formations, 5) discuss how the Ringerike Group and similar deposits in the subsurface would act as reservoirs and 6) discuss the influences of climate, vegetation and tectonics on the studied interval.

1.3 Study area

The study area for this master's thesis is located in the municipality of Hole in Eastern Norway (Fig. 1.1), with the closest town being Sundvollen. The alluvial deposits crop out discontinuously on the sides of the E16 road southward from Sundvollen, where in total five outcrops (Fig. 1.2) have been investigated. An overview of the outcrop locations is given in Fig. 1.2, where outcrop length varies from approximately 10-440 metres. Additionally, outcrop height varies from approximately 5-20 metres across the outcrop locations.
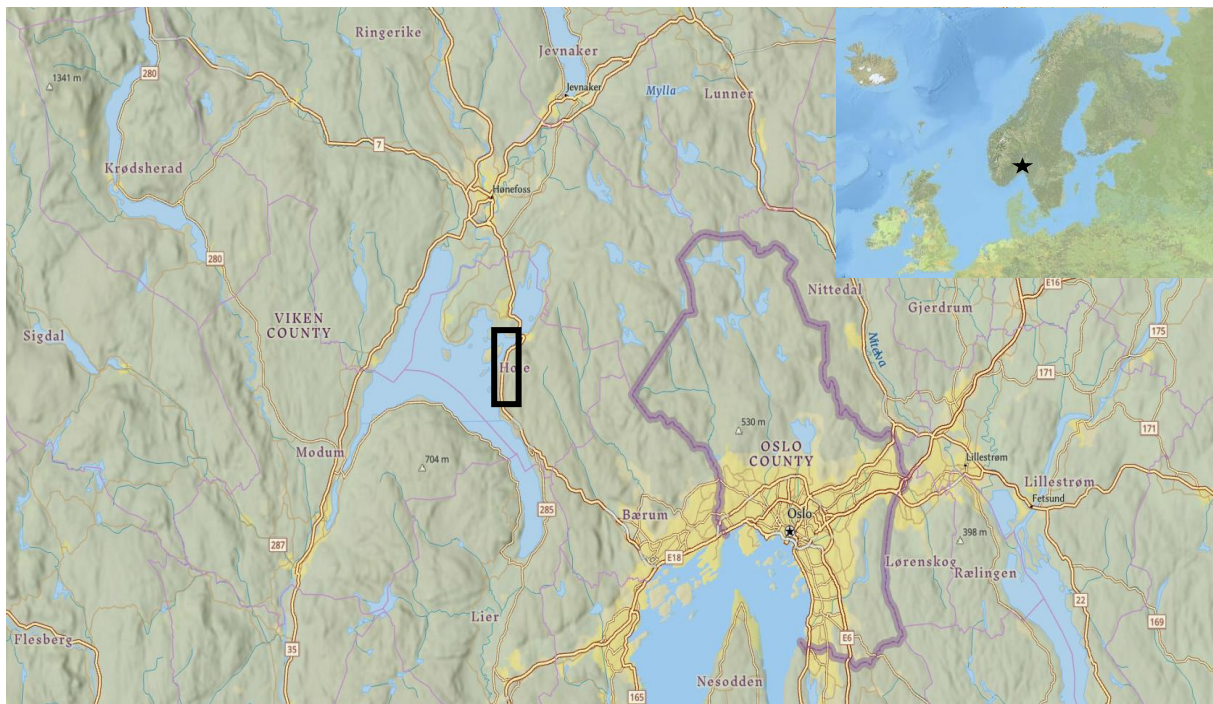
Figure 1.1. Map of Europe in the upper right figure with the study area represented by the black star, and zoomed-in map of Eastern Norway with the study area within the black outlined box in the bigger figure. (Photos from ArcGIS).

Figure 1.2. Maps of the outcrop locations in the study area. From south to north are outcrop 3 (O3), outcrop 4 (O4), outcrop 2 (O2), outcrop 1 (O1) and outcrop 5 (O5). A) shows locations of outcrop 3-5, B) shows locations of outcrop 1 and outcrop 5, C) shows locations of the outcrops throughout the study area. (Photos from Google Earth).

2 Geological setting

The objective of this chapter is to give a general background of the study area including the basin configuration, stratigraphic setting, lithologies which are present in the Ringerike Group, tectonic setting, depositional environments in the Ringerike Group and palaeoclimate conditions in the study area.
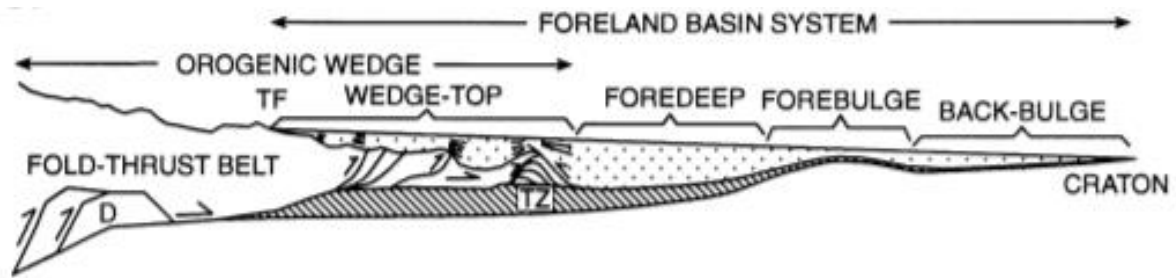
2.1 Foreland basin

An example of a sedimentary basin which undergoes significant subsidence and has good preservation potential is the foreland basin. Foreland basins are a product of tectonic and sedimentary loading which decompresses the lithosphere (Ingersoll, 1988), where an isostatic compensation is present due to collision and/or subduction of a lithospheric plate. Convergence of lithospheric plates will in both cases of continental-continental and continental-oceanic lithospheric plate collision lead to subduction of the densest lithospheric plate, resulting in an orogeny which will contribute to a thickened continental crust. Regional isostatic compensation thus occurs as the flexural rigidity in the crust will lead to lithospheric flexure (Beaumont, 1981). In an unfilled foreland basin system the deepest zone will thus be located nearest the fold and thrust belt (Fig. 2.1).

The term *foreland basin* was first introduced by Dickinson (1974) in which a division of two main types; peripheral (pro)- and retro-arc foreland basins, was suggested. DeCelles and Giles (1996) later provided a model of the foreland basin system (Fig. 2.1) and divided the foreland basin system into four depozones. Adjacent to the fold and thrust belt is the wedge top, followed by the foredeep, forebulge and back-bulge toward the craton as shown in Fig. 2.1. However, in some instances the forebulge and backbulge depozones may be poorly developed or not present in foreland basin systems (DeCelles & Giles, 1996). Furthermore, the proximal part of the foreland basin often contain additional smaller sedimentary basins named piggyback basins after Ori & Friend (1984), which forms due to moving thrust sheets in the wedge-top zone (DeCelles & Giles, 1996). The Ringerike Group is an example of deposits which has previously been interpreted to have been deposited in such piggyback basins (e.g. Bruton et al., 2010).

Deposits in the foreland basin may range from deep marine gravity deposits such as flysch to shallow marine and fluvial deposits, where the fine-grained flysch deposits are the oldest

deposits and the shallow marine-fluvial more coarse-grained deposits are the youngest deposits (Allen et al. 2009).

Figure 2.1. Conceptual and idealised model of the foreland basin system defined by DeCelles & Giles (1996). Between the fold and thrust belt and the craton lies the wedge top, foredeep, forebulge and back-bulge which develop cratonward. Note that the wedge top lies both within the orogenic wedge and the foreland basin system. D = duplex, in the fold and thrust belt. TF = topographic front of the fold and thrust belt. TZ = triangle zone.

2.2 Stratigraphic setting

The Upper Silurian Ringerike Group is divided into two geological formations: the Sundvollen and Stubdal Formations. It stretches discontinuously from Ringerike in the north to Skien further south (Fig. 2.7). Fig. 2.3 shows a stratigraphic chart of the Ringerike Group in the Ringerike area, where the underlying marine Steinsfjorden Formation is conformably overlain by the Sundvollen Formation, which progressively grade into the overlying Stubdal Formation. However, as shown in Fig. 2.3, new formations are introduced in the Ringerike Group further south (Davies et al., 2005a), meaning the areas of interest are located solely in Ringerike.
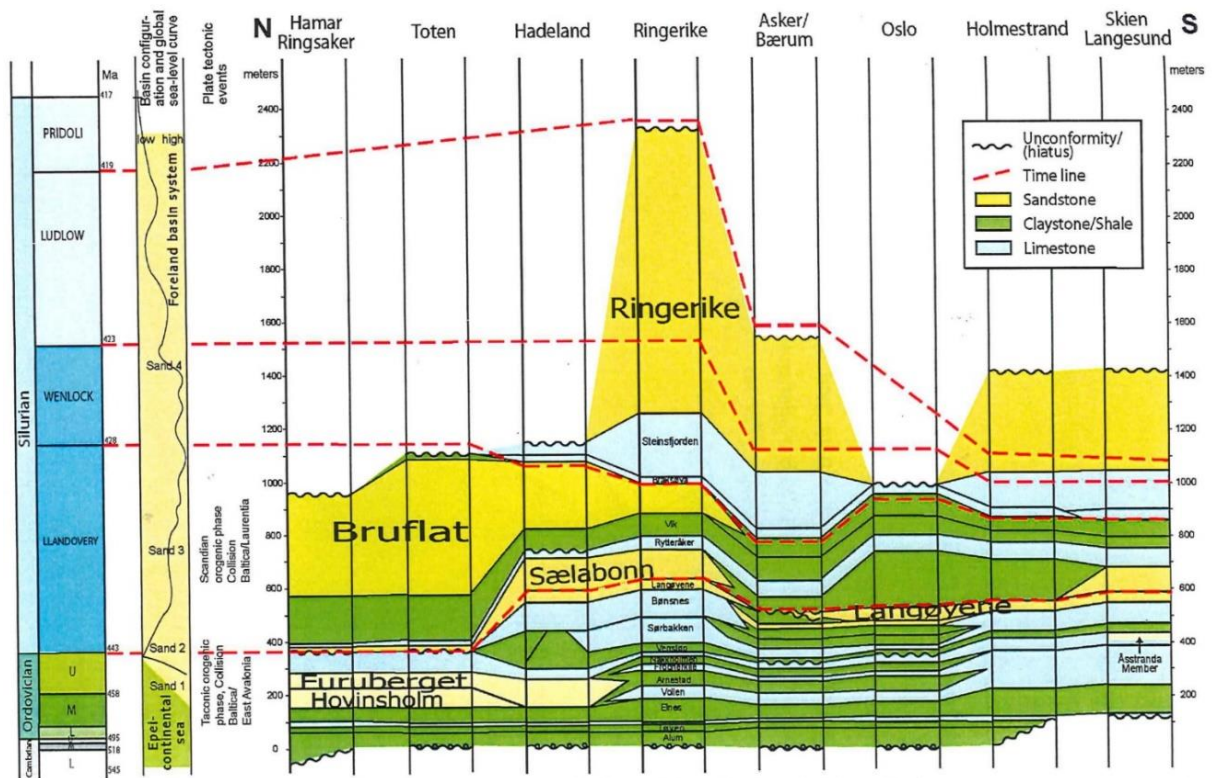
Figure 2.2. Stratigraphic chart of the Lower Palaeozoic sedimentary succession in the Oslo region, from Hamar/Ringsaker in the north from Skien/Langesund in the south. Additionally shown is the basin shift from an ephemeral continental sea to a foreland basin system with a related accommodation curve. Modified from Halvorsen (2003).
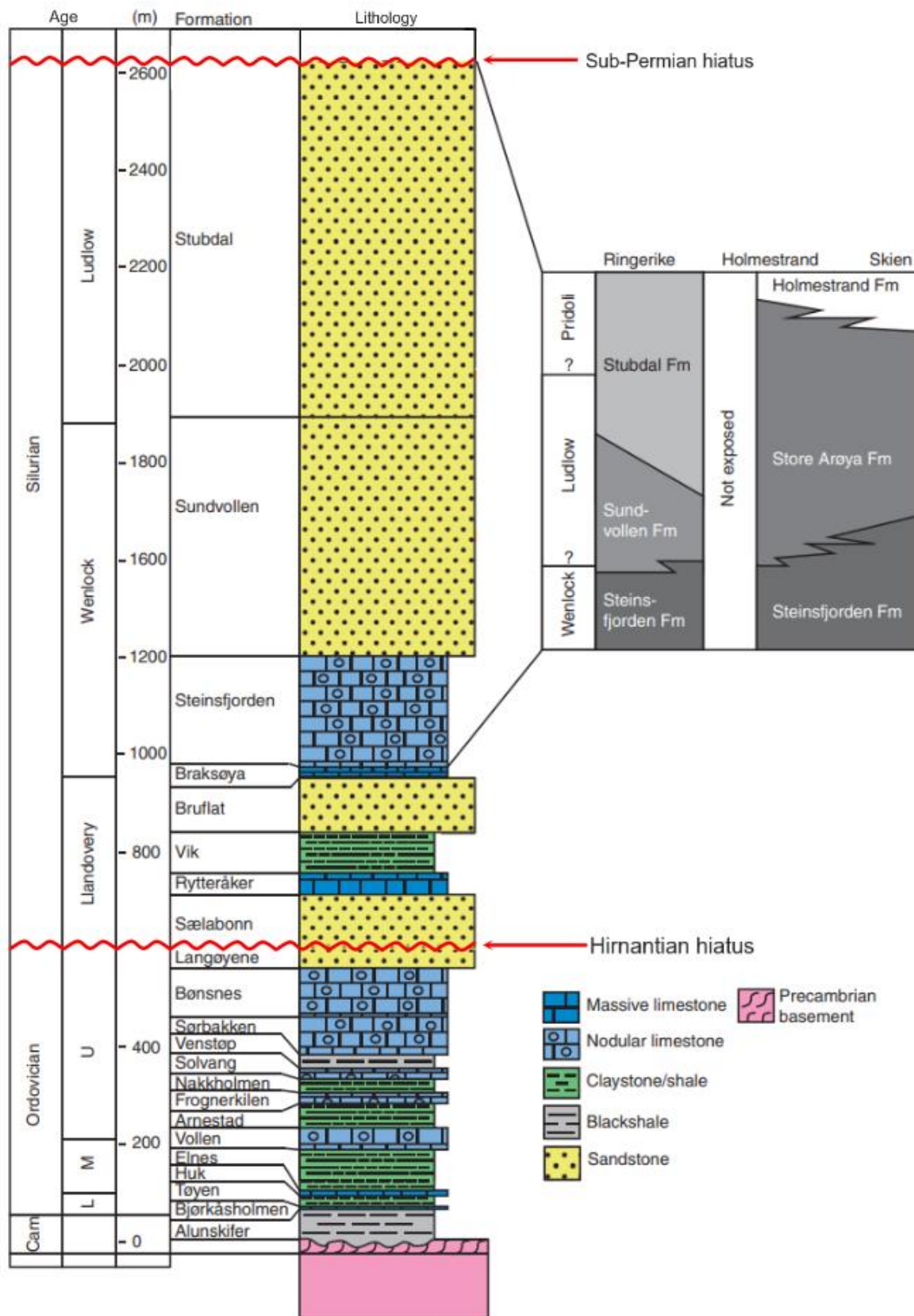
Figure 2.3. Stratigraphic chart of the Lower Palaeozoic sedimentary succession at Ringerike. The two unconformities: Hirnantian- and Sub-Permian hiatus are defined by the wavy red lines. Above the Sub-Permian hiatus lie the Permian magmatic rocks. Modified from Kristoffersen et al. (2014).

Table 2.1. Geological formations depicted in Figure 2.2 and which geological group the formations are assigned to.

Geological group (oldest to youngest)	Geological formations (oldest to youngest)
Røyken	Bjørkåsholmen
	Tøyen
	Huk
	Elnes
Oslo	Vollen
	Arnestad
	Frognerkilen
	Nakkholmen
	Solvang
	Venstøp
	Sørbakken
	Bønsnes
	Langøyene
Bærum	Sælabonn
	Rytteråker
	Vik
	Bruflat
Hole	Braksøya
	Steinsfjorden
Ringerike	Sundvollen
	Stubdal

The stratigraphic setting of the Lower Palaeozoic sedimentary succession in Ringerike is somewhat complex due to the tectonic history of the foreland basin system. Nevertheless, a stratigraphic chart (Fig. 2.2) have been constructed throughout the depozones from the Hamar/Ringsaker area in the north to the Skien/Langesund area in the south. Geological formations vary significantly throughout the Oslo region (Fig. 2.2), which in the Ringerike area (Fig. 2.3) is comprised of the Middle Cambrian-Lower Ordovician Alum Shale Formation followed by the Lower Ordovician-Upper Silurian Røyken Group, Oslo Group, Bærum Group, Hole Group and ultimately the Ringerike Group with associated formations listed in Table 2.1.

Unconformities in the Cambro-Silurian succession include the Hirnantian hiatus (Bruton et al., 2010) and the Sub-Permian hiatus between the Ringerike Group and the overlying Upper Carboniferous-Permian lavas (Henningsmoen, 1978).

The stratigraphy of the Ringerike Group in the study area is nonetheless well understood, where the marine Steinsfjorden Formation is conformably overlain by the marginal marine to fluvial Sundvollen Formation which correspondingly is overlain by the Stubdal Formation. However, the ages of the formations are debated. Various papers regarding the Ringerike Group have carried out different dating methods on the Sundvollen and Stubdal Formations, generating a variety of age intervals. Early work from Kiær (1908) and Whitaker (1964; 1965; 1980) suggested an Early Devonian age for the Ringerike Group, albeit with either unspecified or estimated ages. Other work utilising biostratigraphic dating or palaeomagnetic data have suggested earlier ages for the formations, with mainly Wenlock-Ludlow age intervals (Douglass, 1988; Heintz, 1969; Spjeldnæs, 1966; Størmer, 1954; Turner, 1974b; Worsley, 1983). According to the Geological Survey of Norway (2022b), ages for the Ringerike Group are defined by the work of Turner (1974a) with a Wenlock-Ludlow age for the Sundvollen Formation and a Ludlow-Pridoli age for the Stubdal Formation.

2.3 Lithologies

Differences in the lithological content from the underlying Steinsfjorden Formation to the overlying Ringerike Group is considerable and is easily recognisable in the field. Marine sedimentary rocks where carbonates, marls and mudstones are present comprise the Steinsfjorden Formation. Additionally, the rocks are highly fossiliferous which are easily spotted in outcrops. The Ringerike Group however is quite different from the Steinsfjorden Formation as the Sundvollen and Stubdal Formations are mostly alluvial, sandstone abundant and less fossiliferous (Davies et al., 2006). Nevertheless, the formations can be differentiated in the field due to the substantial amounts of mudstones and also the minor amounts of calcarenites in the Sundvollen Formation in comparison to the Stubdal Formation, which has very small amounts of mudstones and a complete absence of calcarenites. Moreover, the Stubdal Formation is slightly coarser in grain size (Turner, 1974a), albeit grain sizes are hard to differentiate between in the field due to the outcrops being weathered.

2.4 Tectonic setting

In Late Cambrian-Silurian, the subduction of the Iapetus Ocean and subsequently the collision between the Laurentian and Baltican plates transpired, forming the Scandian phase of the Caledonian orogeny (Davies et al., 2005b). The uplift of the Caledonides formed a foreland basin system to the east on Baltica, where eroded sediment of Lower Palaeozoic age was deposited throughout the Silurian (Worsley et al., 1983; Bruton et al., 2010).
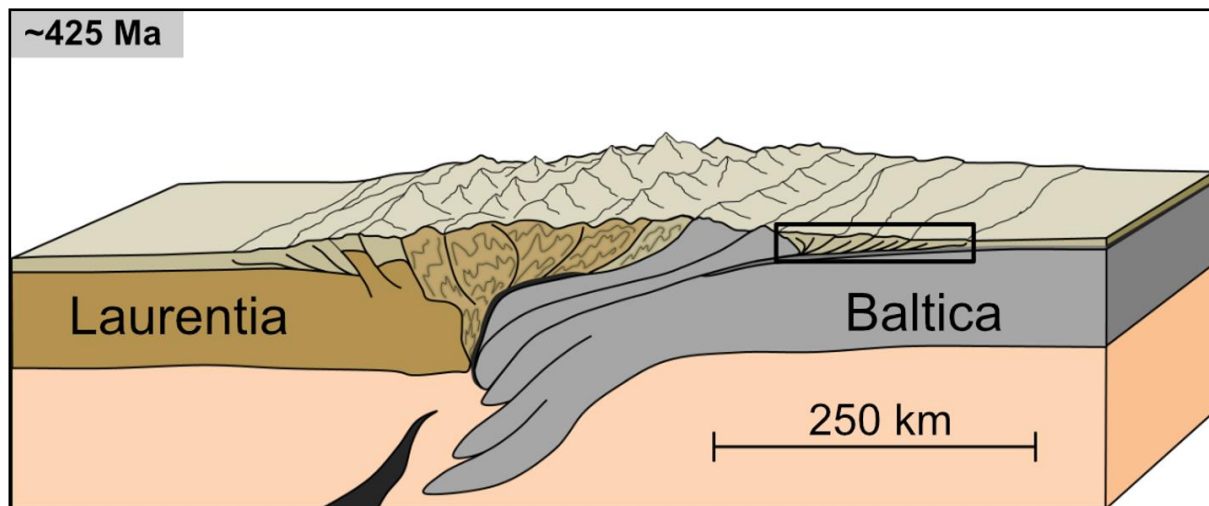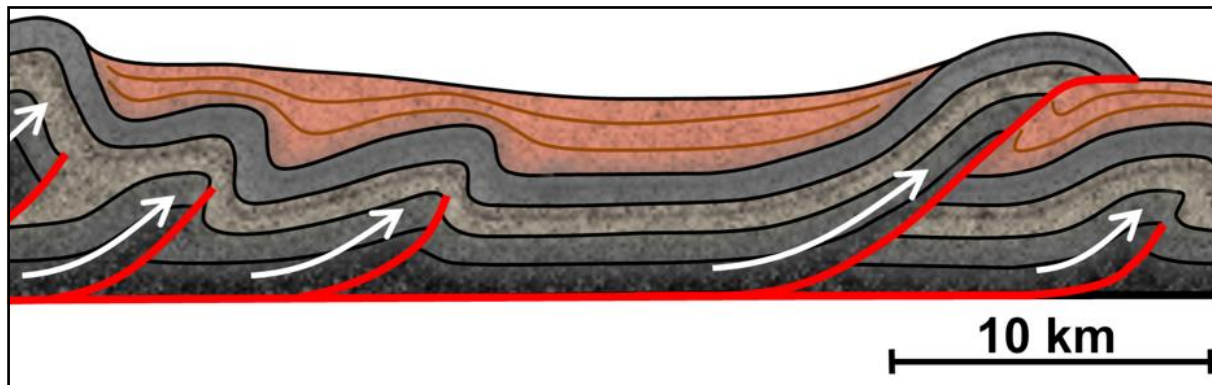

Figure 2.4. Conceptual model of the Caledonian orogeny at approximately 425 Ma. The black outlined box represents the foreland basin in the Oslo region. Modified from Henstra (2018).

Lower Palaeozoic sedimentary rocks are in the Oslo Region firstly represented by the dark shales in the Middle Cambrian-Lower Ordovician Alum Shale Formation, overlying the Proterozoic and pre-Caledonian Vangsås Formation in the Lake Mjøsa area and basement rocks in the Oslo region, with a north-south diachronous signature from Ringsaker/Toten (oldest) to Skien/Langesund (youngest). A stable platform within an epicontinental sea is believed to be the depositional environment for the alum shales and the subsequent Bjørkåsholmen, Tøyen and Huk Formations of Early-Middle Ordovician ages. Earliest siliciclastic inputs with increasing sedimentation rates, hence indicating a shift from an epicontinental sea to a foreland basin, is marked by the sandstones and siltstones of the Elnes Formation believed to have a northwestern source from the terrestrial "Telemark Land" (Bruton et al., 2010). The foreland basin system hereafter develops throughout the Ordovician with an increasing subsidence (Bjørlykke, 1983), allowing further marine sedimentation in the basin until the Ordovician-Silurian boundary as the Hirnantian hiatus, either in response to tectonic events or a regressive phase of glacio-eustatic origin, occurs (Bruton et al., 2010).

A major transgressive phase is indicative in the Lower Silurian succession in the Oslo region, likely explained by crustal subsidence due to tectonism as sedimentation rates were high. The Bruflat Formation however represents the start of a regressive phase, moving from a deep marine siliciclastic to a shallow marine carbonate environment (Bruton et al., 2010). Worsley et al. (1983) however argues there existed a minor transgression in Wenlock, as lagoonal facies are interbedded by carbonate platform facies. Progradation in the foreland basin ultimately results in alluvial sediments being deposited near the Wenlock-Ludlow boundary when the shallow marine to tidal Steinsfjorden Formation was conformably overlain by the Sundvollen and Stubdal Formations. The Ringerike Group were the final sediments deposited in the Oslo region, thus ending the Lower Palaezoic sedimentary succession.

Caledonian tectonism in the Oslo region can firstly be linked to the deposition of the Bruflat Formation due to a rapid subsidence in the foreland basin (Bjørlykke, 1983). The Osen-Røa Nappe Complex after Nystuen (1981) converged in a south-easterly direction toward the Oslo region (Bjørlykke, 1983), displacing the Cambrian sediments. Convergence of the Caledonides is represented by the low-angle Osen-Røa thrust which can be traced from the Caledonian front in the Lake Mjøsa area to the Oslo region. It is not exactly clear where the thrust dies out though it is believed to die out as a blind thrust in the Langesund/Skien area. The Osen-Røa thrust lies within the allochthonous/parautochthonous-autochthonous Alum Shale Formation and is termed as a décollement from which imbricate thrust faults splay upwards, forming duplex structures in the overlying Ordovician-Lower Silurian (Bruton et al., 2010). As the Caledonian fold and thrust belt persists through the Silurian and to the Devonian (e.g. Andersen, 1998; Corfu et al., 2014), the entire Lower Silurian succession is affected by the related tectonism and crustal shortening in Ringerike was approximately 27-50 % (Morley, 1986). The youngest Ringerike Group is moreover thought to be deposited in piggy-back basins, from which thrusts have separated into different piggy-back basins. The Ringerike Group is deposited in what now appears as syncline structures due to the south-southeasterly moving fold and thrust belt. However, it is only the marine sedimentary succession which is strongly folded and faulted as the Ringerike Group is more mechanically competent (Bruton et al., 2010).

Figure 2.5. Conceptual model of the Caledonian fold and thrust belt affecting the Lower Palaeozoic sedimentary succession at Ringerike, forming a duplex structure. Red lines and white arrows show the movement of the thrusts. The uppermost Ringerike Group in faint red colour are the least affected by tectonics. Modified from Henstra (2018).
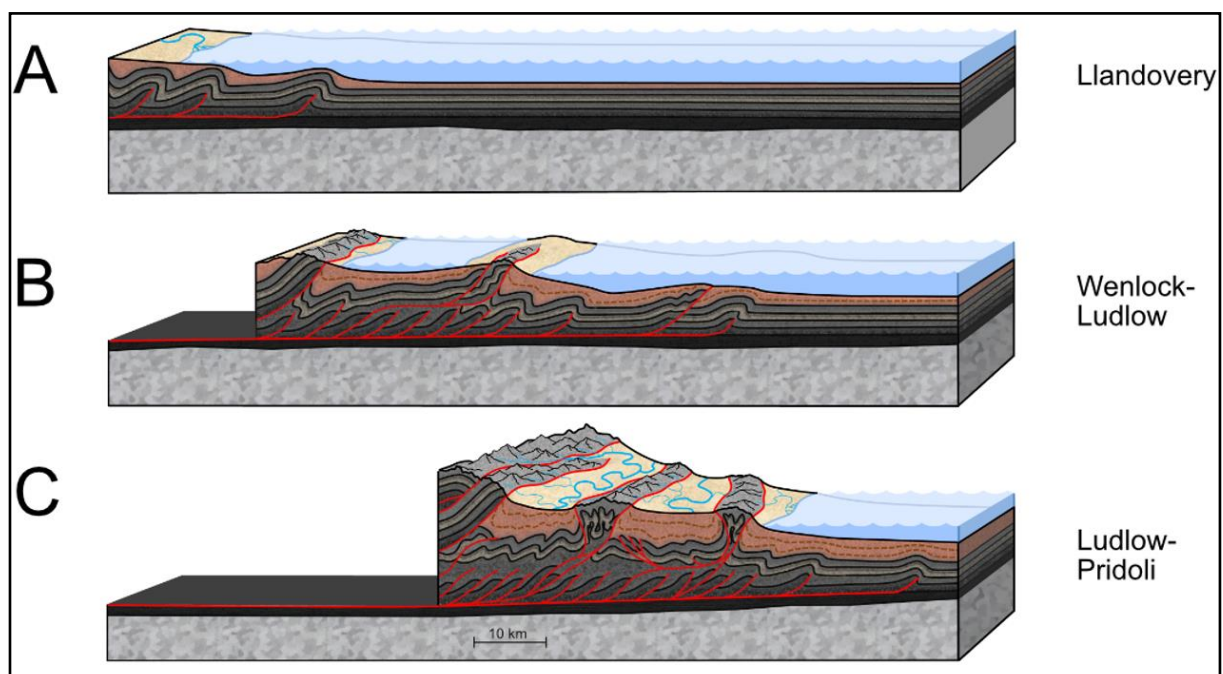
Figure 2.6. Conceptual model of the tectonic development in the foreland basin system in the Silurian, where grey colours represent the Cambrian-Middle Silurian marine strata and red colours represent the Upper Silurian Ringerike Group. Red lines mark the thrusts in the foreland basin system. Note the bottommost Osen-Røa thrust. A) Earliest tectonic impact on the sedimentary succession in Llandovery, forming duplex structures in the Cambrian and Ordovician strata. B) Continued S-SE movement of the fold and thrust belt in Wenlock-Ludlow, from which more folding and faulting occurs. Upward moving thrusts lead to the formation of a piggy-back basin, where deposition of the marginal marine-fluvial Sundvollen Formation occurred. C) Continued advancement of the fold and thrust belt led to further shortening of the Lower Palaeozoic sedimentary succession and formed new piggy-back basins in Ludlow-Pridoli, depositing the fluvial Stubdal Formation. Modified from Henstra (2018).

Moreover, contact metamorphosis caused by plutonic and volcanic rocks overlying the succession has additionally altered the Lower Palaeozoic succession at a later stage in the Upper Carboniferous Permian. These magmatic rocks are formed due to the formation of the Oslo Graben, linked to the Variscan orogeny causing rifting in the Oslo region (Dahlgren & Corfu, 2001). Subsidence in the Oslo Graben (e.g. Oftedahl, 1978; Bjørlykke, 1983) prevented erosion of the Lower Palaeozoic succession which is today preserved within the boundaries of the graben (Turner, 1974b) (Fig. 2.7).
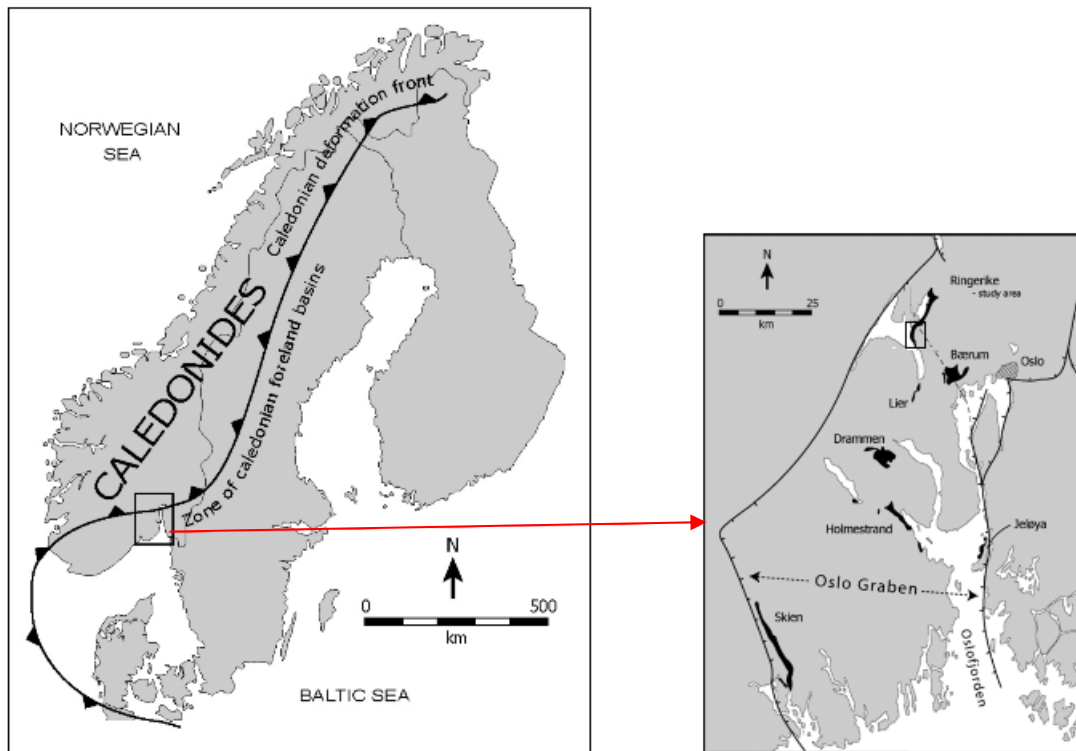
Figure 2.7. Map of Scandinavia with the maximum reach of the Caledonian front on the figure to the left with foreland basins further south. The figure to the right shows a zoomed-in map of the Oslo Region with the study area shown by the black outlined box, preserved within the boundaries of the Oslo Graben. Deposits in the Ringerike Group is shown by the black-coloured areas. Modified from Halvorsen (2003).

2.5 Depositional setting

Contemporaneous with the development of the Caledonides, a meandering river system in an alluvial setting is thought to be deposited in the Ringerike area in Wenlock-Ludlow (Turner, 1974a; 1974b). The base of the Sundvollen Formation, lying conformably over the Steinsfjorden Formation, consist of fluvio-deltaic sandstones, mudstones and limestones when the terrestrial system still was in contact with the sea (Turner, 1974a; Worsley et al., 1983). Continuous progradation throughout Wenlock shifted the depositional environment to strictly alluvial, where sandy and muddy sediment was deposited in alluvial architectural elements such as point bars, crevasse splays and oxbow lakes referred to as the Sundvollen Formation transpired. Lacustrine and aeolian depositional environments are also believed to be represented in the formation (Turner, 1974a; 1974b; Worsley et al., 1983; Halvorsen; 2003).

Subsequently, as progradation continued throughout Ludlow-Pridoli, the river system changed from a meandering to a braided river system (Turner, 1974b; Worsley et al., 1983; Davies et al., 2005b). The sandstone abundant braided river system is referred to as the Stubdal Formation lying comformably over the Sundvollen Formation (Fig. 2.3), which deposited alluvial sediments in the Ringerike area throughout the Ludlow-Pridoli timespan (Turner; 1974a; 1974b; Davies et al., 2005a).

2.6 Palaeoclimate

The study area was in the Late Silurian situated on Baltica in the southern latitudes, approximately at 15-20 ° S in the subequatorial zone according to Torsvik & Cocks (2013). Fig. 2.8 shows location of the study area in Wenlock (430 Ma) and Pridoli (420 Ma).

Furthermore, the climate in Ringerike was at the time of depositing the Ringerike Group warm and arid (Worsley et al., 1983; Davies et al., 2005b) and terrestrial vegetation in the Late Silurian was scarce and not well developed (Davies & Gibling, 2010; Gibling et al., 2014). Kiipli et al. (2016) argues that physical weathering in the easterly adjacent Baltoscandian foreland basin was the dominant weathering force in the Wenlock-Pridoli, which can also be applied to the slightly more northerly foreland basin Ringerike area in the same timespan.
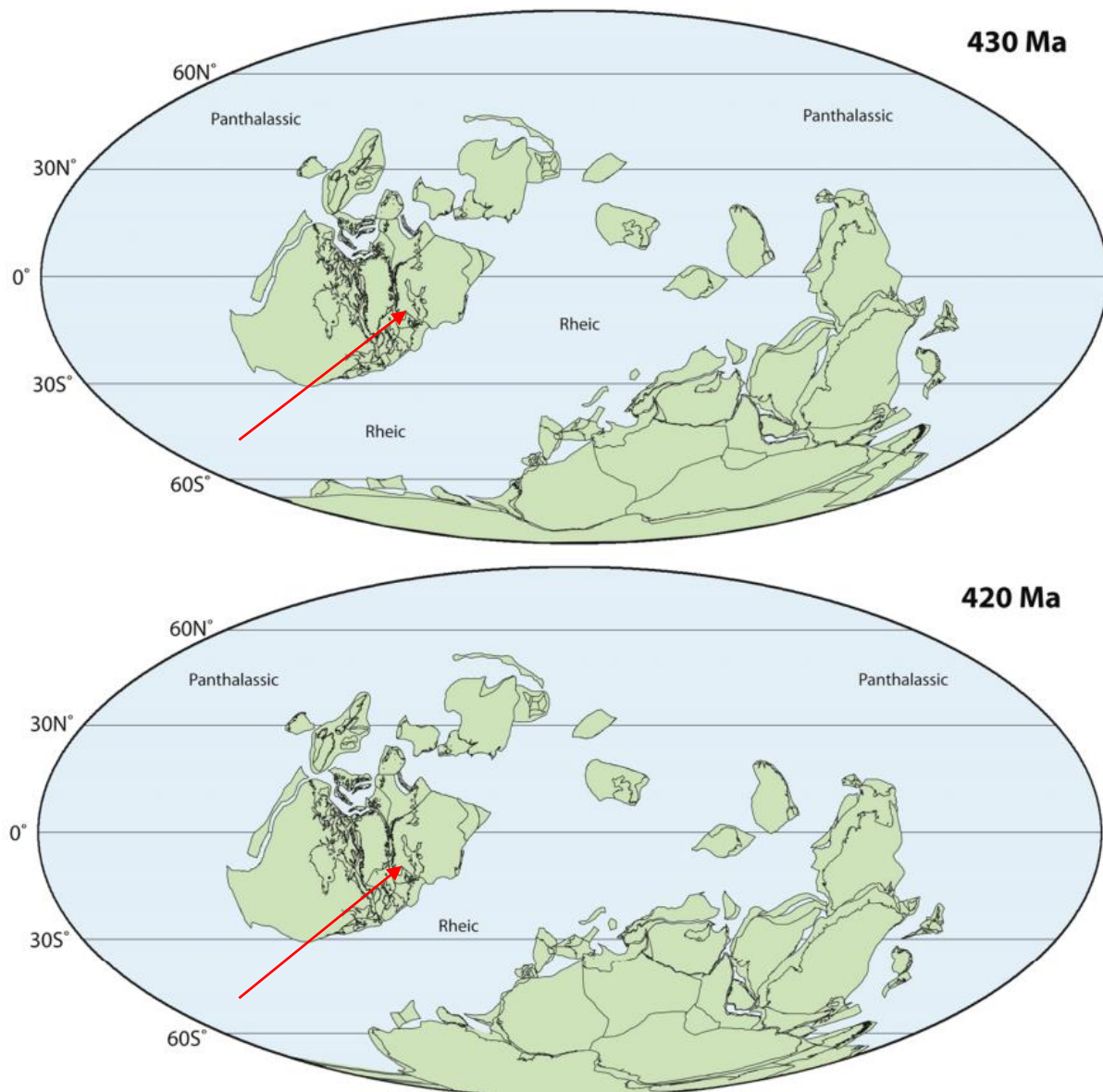
Figure 2.8 Palaeogeographical map of the world transpiring from Wenlock (430 Ma) to Pridoli (420 Ma). Red arrows mark the approximate palaeogeographical location of the study area which was situated on Baltica in Late Silurian. Modified from Torsvik & Cocks (2013).

3.0 Sedimentological concepts

In the following subchapters, sedimentological terms and concepts will be frequently used and the purpose of this chapter is therefore to explain these terms and concepts. Both concepts and terms regarding meandering and braided river systems will herein be clarified.

3.1 Point bars

The *point bar* is a geomorphological landform created by the deposition of sediment in the meandering river. In the point bar, sediments are deposited as the stream competence of the river is diminished in the inner bank, which after a series of lateral accretion results in a fining-upward sequence. On the other hand, the outer bank or cut bank is a place of erosion rather than deposition (Fig. 3.1). The basal part of the sequence is often represented by a lag of gravel or sand with intraformational rip-up mud clasts whereas the uppermost part is composed of mud (e.g. Donselaar & Overeem; Ghinassi et al., 2016). An idealised model of the point bar deposit is shown in Fig. 3.2.
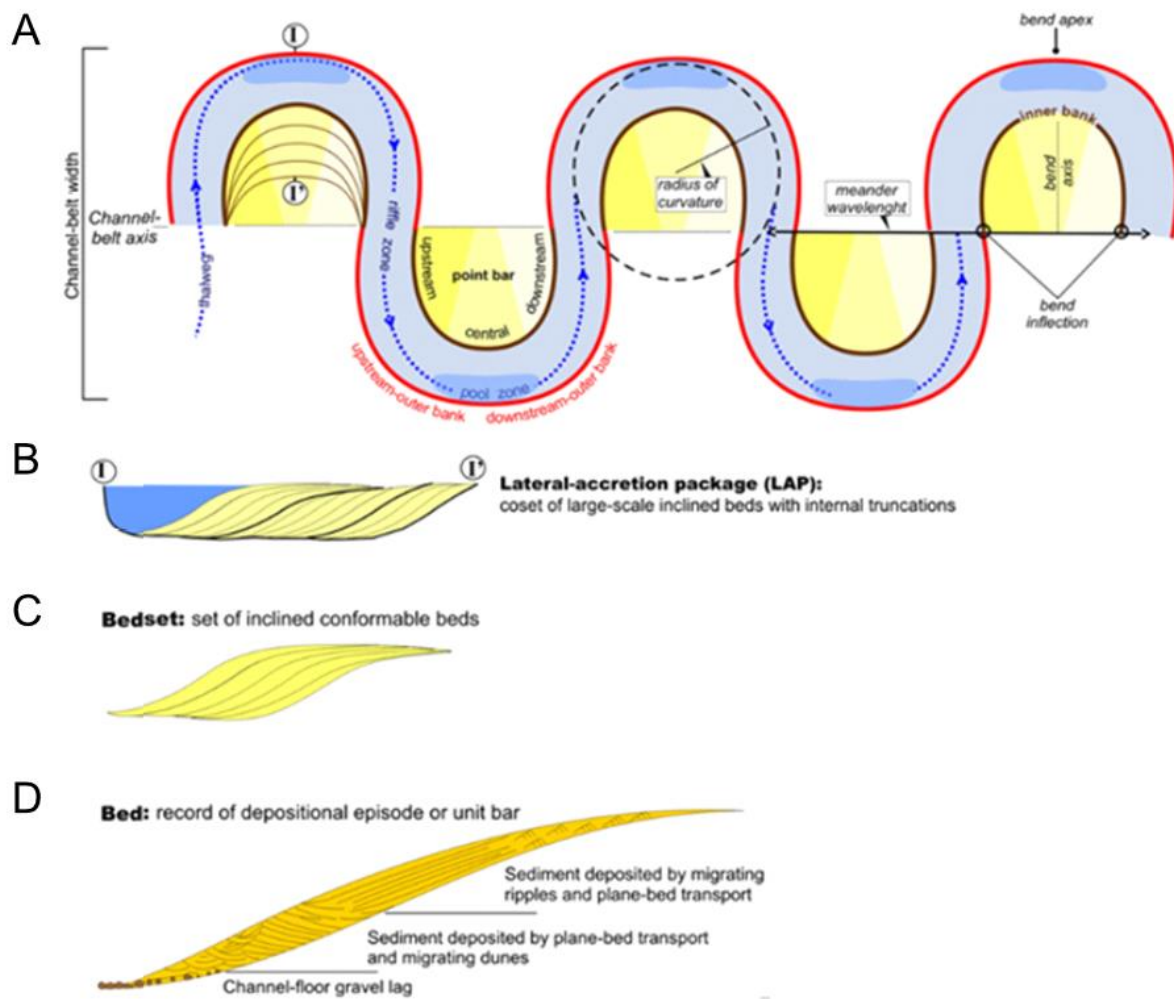
Figure 3.1. Meandering river models. The uppermost model shows the architecture of the sinuous meandering river, with an inner and outer bank. Deposition of sediment occur in the inner bank, while erosion occur on the outer bank. Models B-D shows the deposits from a meandering river, where model B shows a profile of I-I' in model A. The lateral accretion of the beds are depicted here. Model C shows the bedset terminology, compiled of several beds. Model D shows a single bed, where the point bar deposit is visible. Modified from Ghinassi et al. (2016).
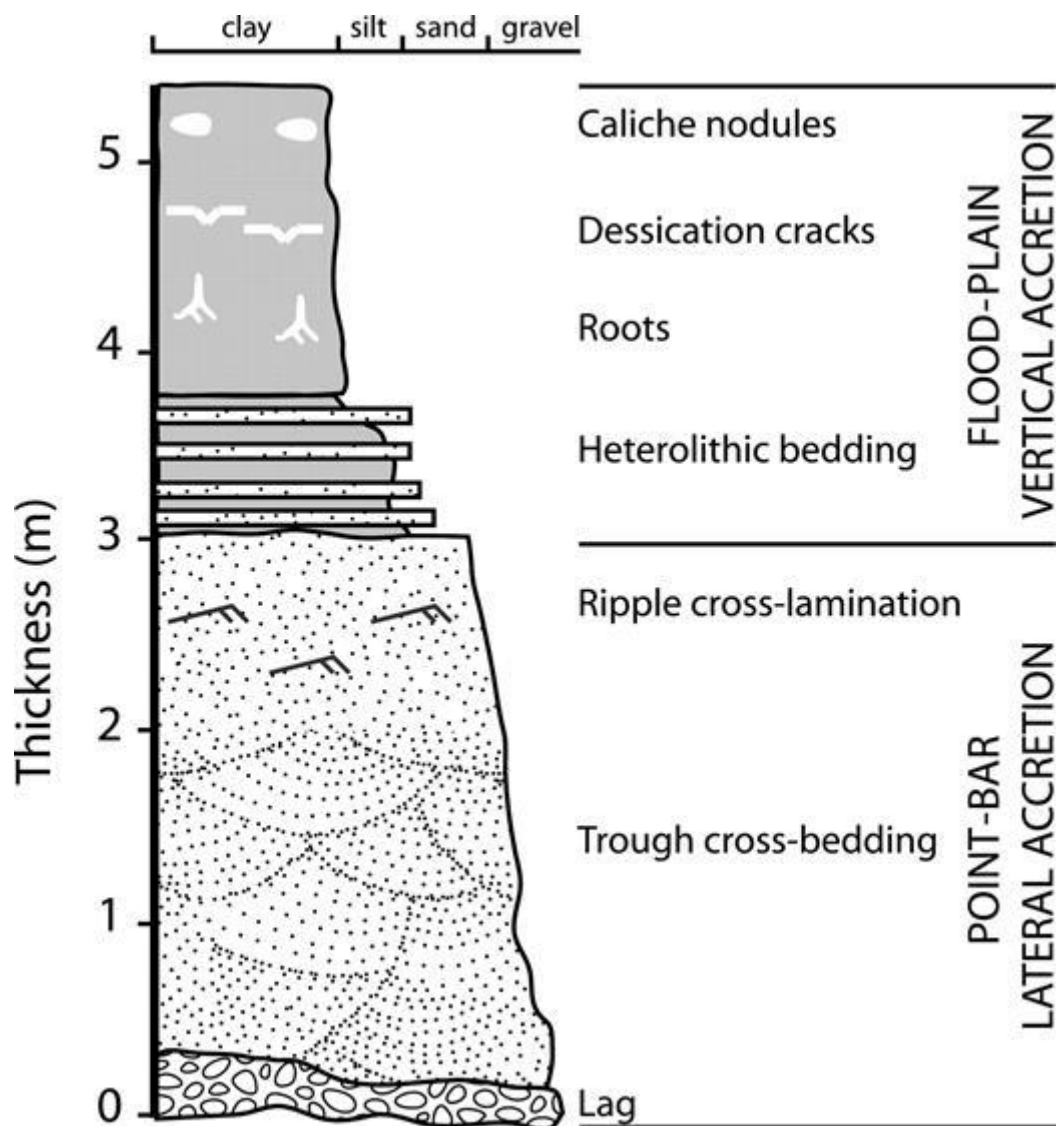
Figure 3.2. Idealised model of a meandering river deposit, showing a fining upward sequence from bottom to top. A basal conglomerate lag is often present followed by sandstone grading up from plane-parallel stratification to cross-bedded stratification to current ripple lamination and finally to the floodplain facies association at the top. The floodplain deposit furthermore often contains crevasse splay deposits, root traces, desiccation cracks and caliche nodules. From Donselaar & Overeem (2008).

3.2 Braid bars

The *braid bar* on the other hand, is a landform created by the deposition of sediment in the braided river. Braid bars are deposited in the middle of the laterally shifting braided river system as the strength of the levees are lesser than in meandering rivers. Braid bars are slightly more complicated than point bars, and no single idealised model explains the upward facies evolution of the braid bars as braided river facies varies significantly among deposits. However, idealised

models of the sedimentary architecture of braided river facies are shown in Fig. 3.3. Due to the higher flow energies commonly found in braided rivers combined with frequently laterally shifting and bifurcating channels with more bedload compared to suspended load, floodplain deposits are scarce and amalgamated sandstone bodies are more common (Bridge & Lunt, 2006).
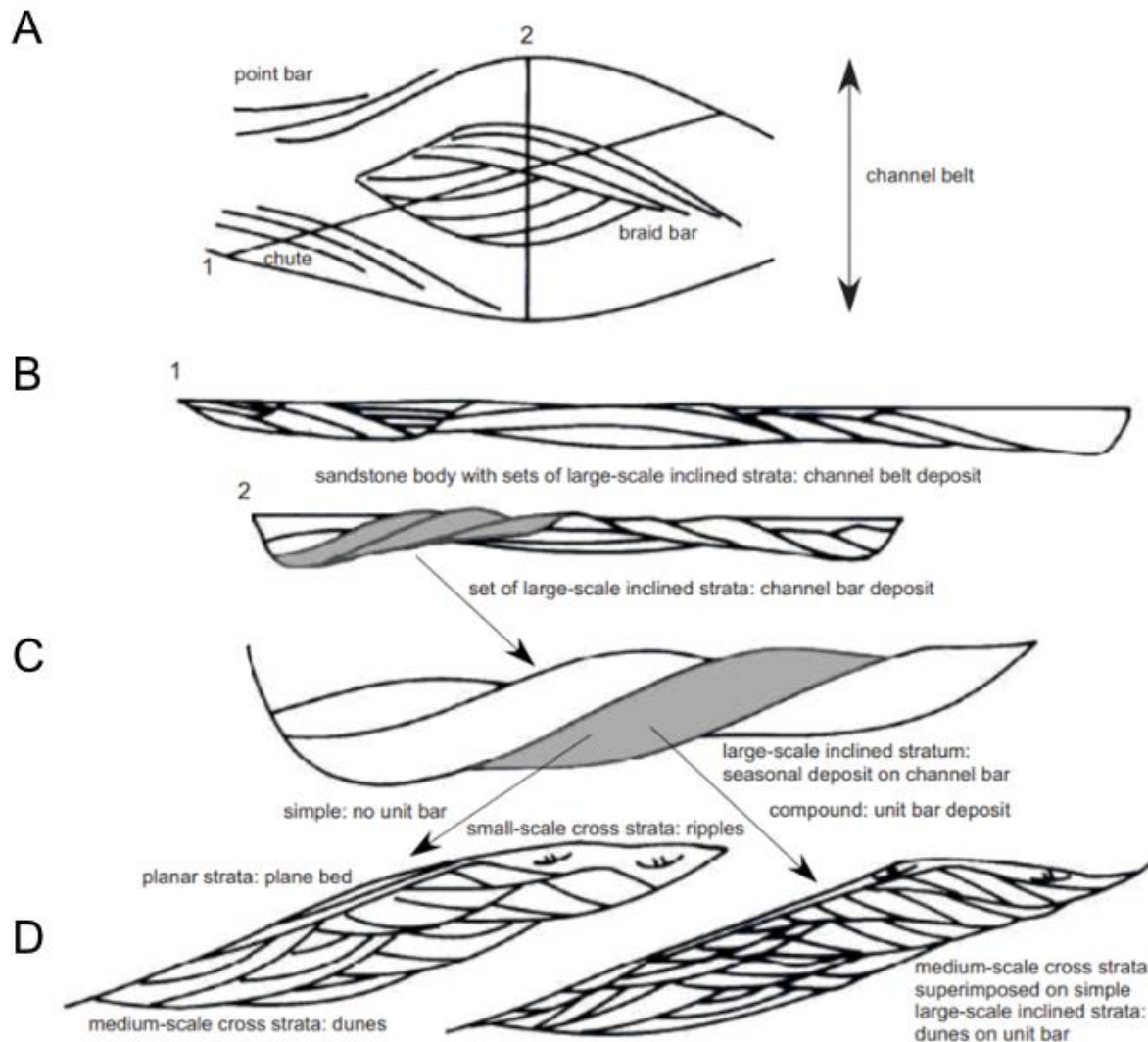
Figure 3.3. Model of the braided river system. A) Surface architecture of the braided river, with clear stream diffluence and confluence zones accompanied by the braid bar in the middle. B) 1: Idealised profile across the chute, channels and braid bar showing the internal architecture of a typical channel belt deposit. 2: Idealised profile of the channels and braid bar showing the internal architecture of a typical braid bar deposit. Each deposit type exhibit large scale inclined strata. C) Close-up of a braid bar with inclined strata. D) The large-scale inclined strata can be simple (deposited under a single flood) or compound (deposited under one or more floods as a unit bar), containing plane-parallel stratification, cross-bedded stratification and current ripple lamination. Modified from Bridge (2006).

3.3 Crevasse splays

During floods, sediments are deposited outside of the channel belt as the levees are breached, exposing the floodplain directly to the channel. The result is the formation of the crevasse splay, where sandy – often fine-grained – sediment is deposited. Deposition most often occurs as lobe shaped deposits (Fig. 3.4) where sandstone deposits are located normally close to the channel. In the field, this is easily recognised by a layer of sand between floodplain deposits. The size of the crevasse splay deposits varies and depends on the length and strength of the individual floods (Burns et al., 2017).
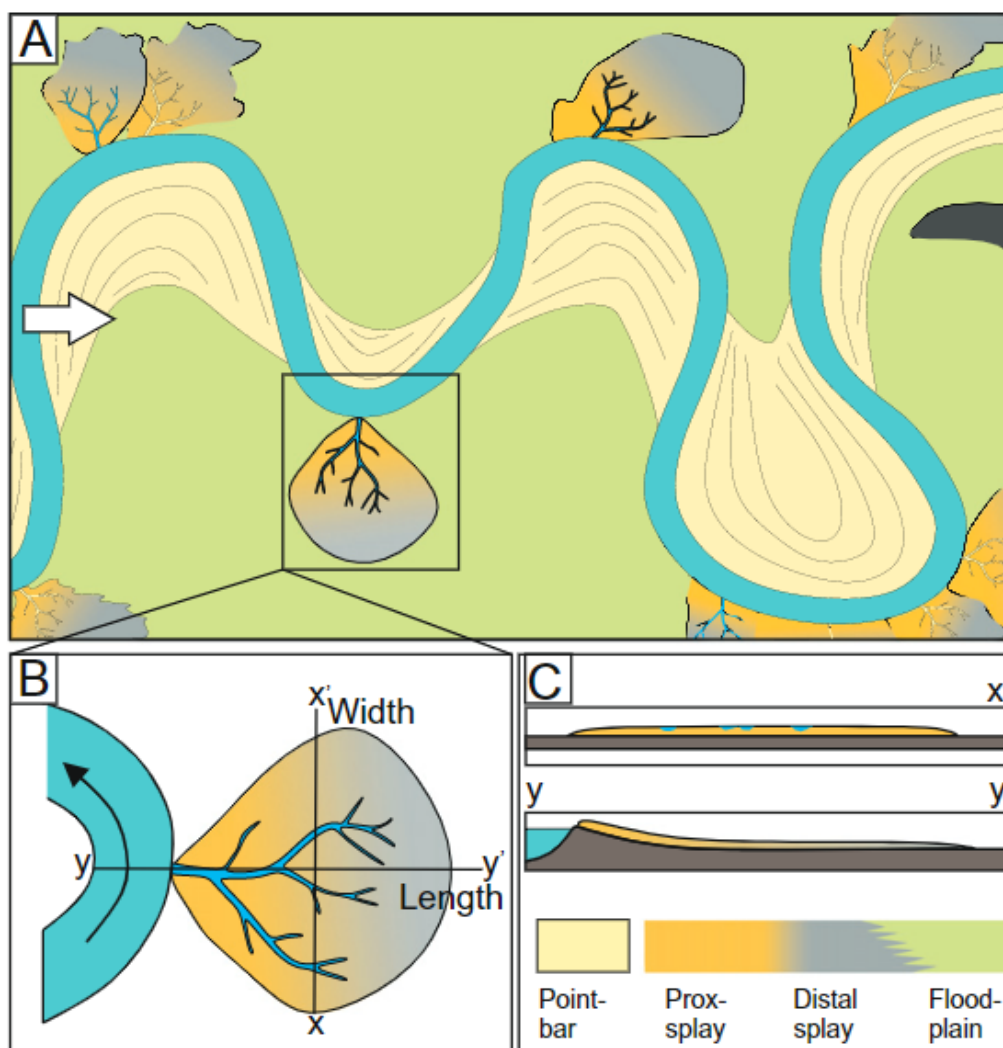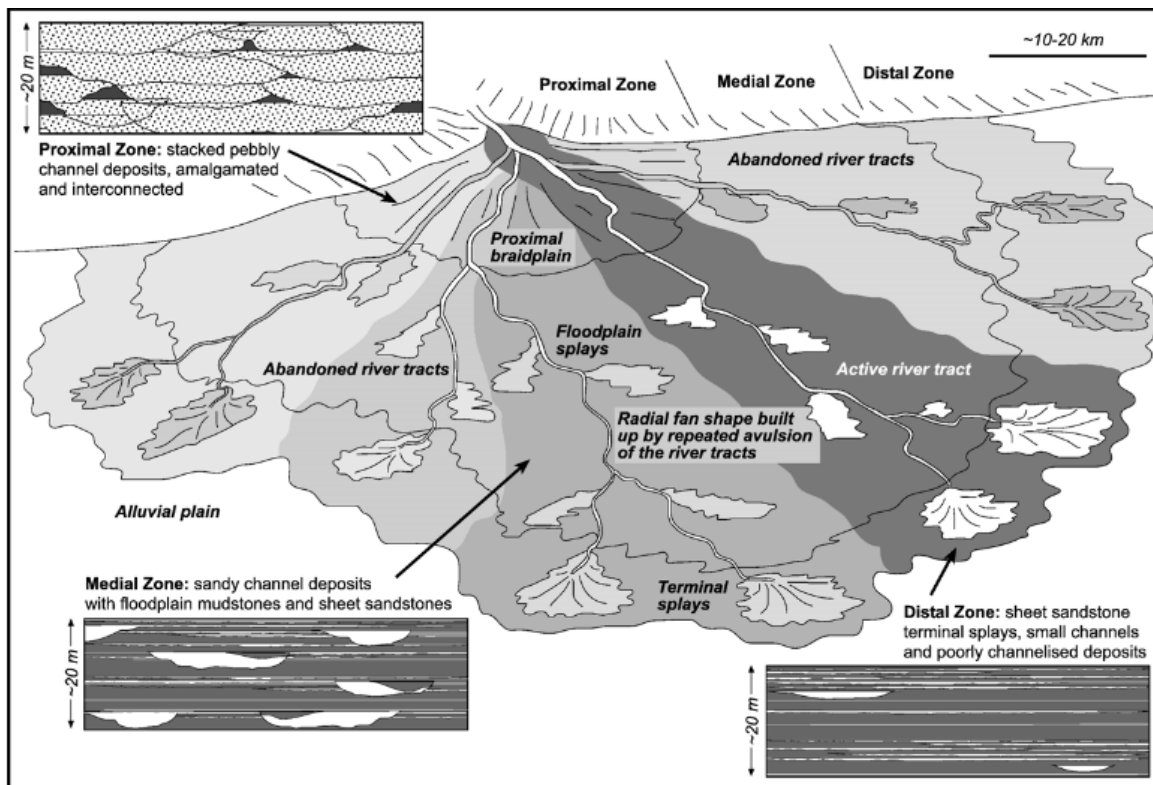
Figure 3.4. Model of the crevasse splay morphology. Crevasse splays are deposited as lobes from the river levees (A) and deposit most amounts of sand adjacent to the channel belt and diminish in size farther onto the floodplain, as shown by B) and C). From Burns et al. (2017).
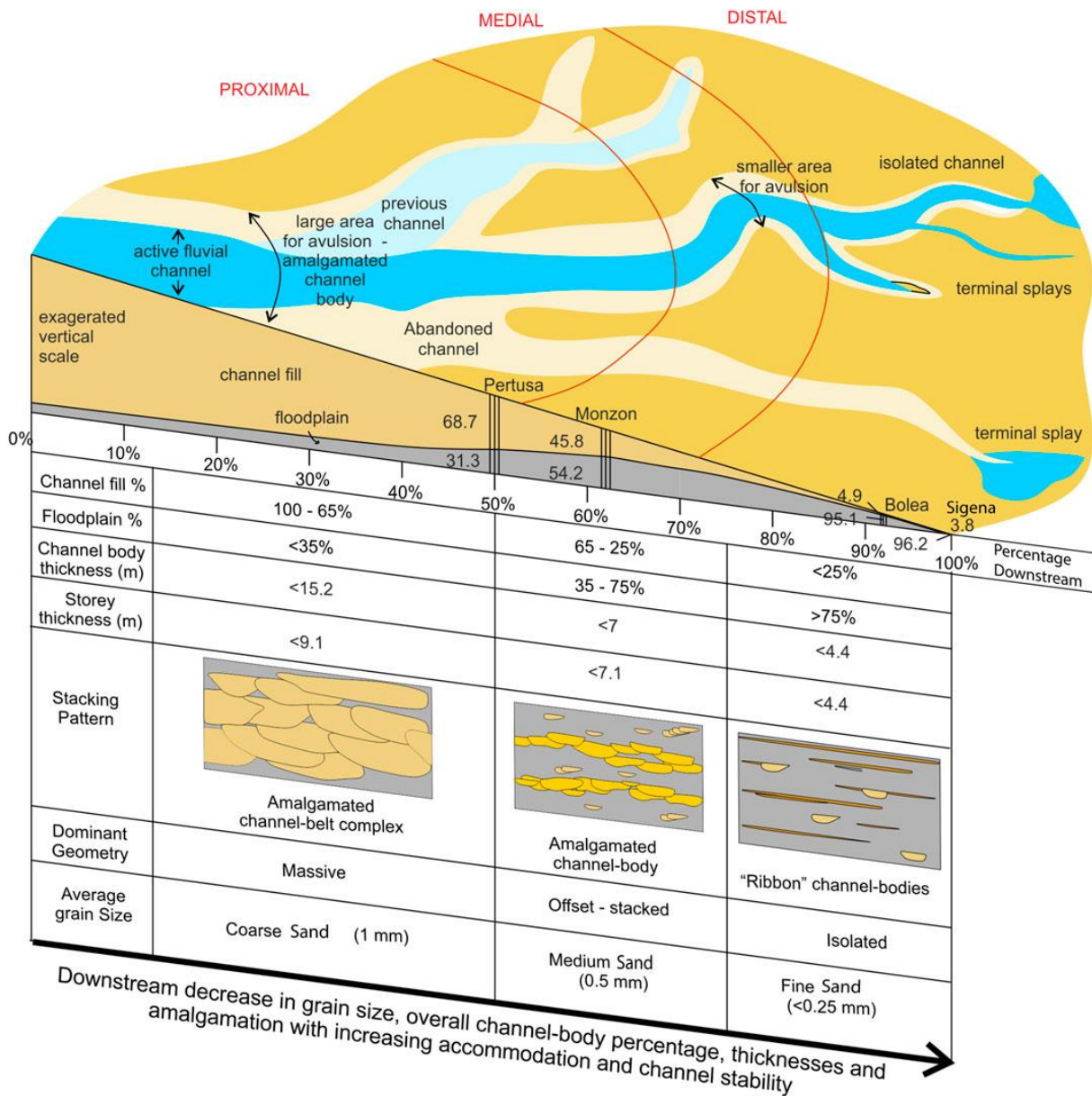
3.4 Distributary fluvial system (DFS)

The distributary fluvial system (DFS) is the most common type of fluvial deposits and constitutes the majority of fluvial deposits in modern sedimentary basins. Contrary to the degradational tributary river system, the DFS is aggradational and thus have a greater preservation potential. The DFS is spread out from an apex where the stream in the alluvial system is confined in a valley and thereafter becomes unconfined when entering the sedimentary basin (Weismann et al., 2010). As the channel enters the sedimentary basin, it can actively migrate across the basin, ultimately displaying a radial pattern of river channels (Fig. 3.5). Fan-shaped lobes of crevasse splay deposits are characteristic features of the DFS and are formed due to the many avulsions of the river channels downstream in the sedimentary basin (Nichols & Fisher, 2007). Moreover, the DFS can be separated into three parts: the proximal, medial and distal zone. These zones are established chiefly due to 1) the change in the style of deposits – from amalgamated sands poor in floodplain mud in the proximal zone to the floodplain-rich and poorly channel-shaped deposits in the distal zone, 2) grain size decreases downstream in the sedimentary basin, 3) floodplain deposits are increasingly preserved further downstream in the basin and 4) channel size and distance variation between the migrating channels (Nichols & Fisher, 2007; Weismann et al., 2010; Martin et al., 2021). Fig 3.6. shows an example of the Huesca DFS in the Ebro basin where the statements described over are supported, with a sand-mud ratio, grain size and channel size decrease downstream in the Ebro basin.

Additionally, a common feature adjacent to the DFS is the axial river system which flow transversely to the rivers in the DFS, often reworking the toes of DFS (Weismann et al., 2010).

Figure 3.5. Conceptual model of the DFS where the proximal, medial and distal zones are shown in the sedimentary basin along with their individual examples of deposits. Additionally shown are the fluvial fans along with the crevasse splays which are splayed from the ancient and active river channels. From Nichols & Fisher (2007).

Figure 3.6. Model of the Huesca distributary fluvial system. The red lines mark the shift from the proximal to the medial to the distal zone, where channel fill percentage, floodplain percentage, channel body and storey thickness clearly differ in the DFS zones. Furthermore, stacking pattern, dominant geometry and average grain size are also depicted in the different DFS zones. From Martin et al. (2021).

Depending on the basin and river size, DFSs can exhibit great variation in length, to < 1 km in the smallest to > 700 km in the largest. Some of the largest modern DFSs are found in foreland basins, e.g. the Pilcomayo DFS in the Andean foreland basin (Weismann et al., 2010).

4 Methods

4.1 Field work and data acquisition

To acquire data from the study area, field work was an essential part of the thesis. Two field seasons has therefore been conducted in October 2021 and March 2022 as well as reconnaissance work in June 2021. As the outcrops are situated along the road E16 south of Sundvollen, they were easily accessible. 91 samples from the outcrops were acquired and brought back for thin section preparation. Additionally, 25 sedimentary logs with a total vertical length of 111.5 metres, with the largest being 6.2 metres vertically, were acquired from the outcrops. Grain sizes, sedimentary structures and bed contacts were recorded in the sedimentary logs.

For this thesis, it was necessary to get a full overview of the outcrops in order to examine the sedimentary architecture of the study area. Hence, outcrop images were taken on the other side of the road with an unmanned aerial vehicle (UAV). The UAV used in the field work was a multirotor UAV of the four-rotor rotorcraft type, informally known as a quadcopter drone. Of the quadcopter drones, a DJI Mavic 2 Pro was used for outcrop photography, installed with a Hasselblad L1D-20c camera. Additional camera equipment includes a 1-inch CMOS sensor and 10-bit Dlog-M colour profile (DJI, 2022). Images were taken from across the road approximately 25 meters from the outcrops, and in order to get continuous outcrop models, overlapping images had to be taken in the field. The resolution, i.e. the smallest visible geological feature, ranges from 8 mm to 10 cm in the outcrops.

Due to regulatory limitations, flying was not permitted in the study area as motorised vehicles drove on the road close to the outcrops. UAV images were therefore acquired by holding, lifting and pointing the UAV camera toward the desired image locations.

4.2 3D outcrop modelling

UAV images taken of the outcrops were gathered and processed on the computer to produce 3D virtual outcrop models (Appendix IV). The photo processing software Agisoft Metashape was used to construct the 3D models. The images were exported to Agisoft Metashape for model processing. To achieve continuity within the model, unclear or unfitting images due to

e.g. different lighting conditions were omitted. Some of the channel deposits are stretching out for 40-50 meters and continuity in means of similar clear images are thus desired. Nonetheless, challenging UAV photography conditions in the field resulted in one of the models having slightly different lighting conditions throughout the model. The process of constructing the 3D models is shown in Fig. 4.1 and is simply explained (Agisoft Metashape, 2021) in the following subchapters. Virtual outcrop details are listed in Appendix IV.
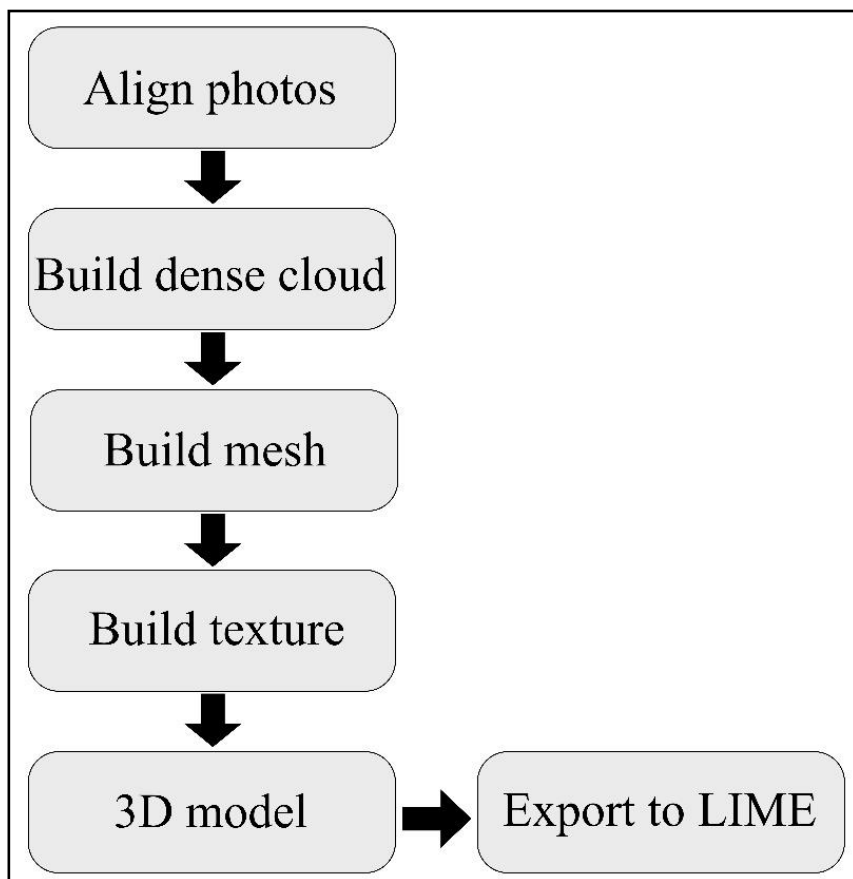
Figure 4.1. Workflow of the virtual 3D outcrop modelling.

4.2.1 Aligning images

After selecting the suitable UAV images, the images had to be aligned. Alignment of the images is necessary to get certain amount of tie points between the overlapping photos. For the models, key points up to 4,000 and a tie point value of zero were selected along with a high accuracy to produce the best image alignment.

4.2.2 Build dense cloud

The next step was to build a dense cloud by using the aligned images. In this process, depth information from the images is gathered, producing dense points cloud which resembles the actual outcrop. Dense clouds were produced with a medium quality and with a mild depth filtering. Point artifacts were prevalent in the dense clouds and several points therefore needed to be removed before continuing with the next task in the workflow.

4.2.3 Build mesh

Polygonal meshes were subsequently constructed, using the dense clouds as the reference points. The polygonal mesh model is a collection of faces, vertices and edges, generating a shape of the polyhedral object – in this case a virtual outcrop. The mesh models were produced with an arbitrary surface type, medium face count and with interpolation enabled.

4.2.4 Build texture

To produce the final 3D models, the last task in the workflow was to add texture to the mesh models. Texture was added by using a generic mapping mode and a mosaic blending mode with a texture size of 4096 px. After the 3D models were constructed, the next step was to export the models to LIME.

4.3 Interpretation in LIME and Affinity Designer

The finished virtual outcrops were exported to LIME, a virtual outcrop visualization suite (Buckley et al., 2019, which together with Affinity Designer, a vector graphics program, acted as the software used for interpretation. Due to Affinity Designer being more convenient for drawing in sedimentological features on the outcrops, it was the desired program for interpretation. Screenshots of the outcrops were taken in LIME in an orthographic projection and exported as a jpeg-file with a size of 8000 pixels, which ultimately was pasted in on an artboard in Affinity Designer.

4.4 ImageJ

After interpreting the different facies observable in the outcrops in Affinity Designer, the facies distribution in the five outcrops were portrayed by ImageJ, an image processing program (National Institutes of Health, u.y.). Facies were attributed to different tones of grey in 8-bits, which were analysed by ImageJ and later generating a histogram of the grey tones. The peaks of the histogram showed the facies associations and the height of the peaks portrayed the amount of pixels represented by a facies association in an outcrop, which in turn were copied to Microsoft Excel for quantitative analyses. Facies association distribution in the outcrops were displayed as percentages in bar charts, thus representing the pixel counts. However, due to uneven facies boundaries, the pixel counts are slightly inaccurate as the anti-aliasing filter was not available when the outcrops were exported from Affinity Designer.

4.5 Thin section preparation and microscopic analyses

A total of 91 samples were acquired in the field for thin section preparation. Firstly, slabs were cut off from the samples by using the Isomet 5000 linear precision saw. Secondly, the Astera Grinding Robot with diamond embedded metal wheels was used for grinding the samples down to a size of 30 microns. Lastly, Struers Polishing machines were used to obtain a smooth and polished surface on the thin sections (University of Bergen, 2022).

The petrographic microscope Nikon ECLIPSE E200 POL was used for thin section analyses and is equipped with 4x, 10x and 40x magnification objectives. For the sake of this thesis, thin sections were analysed by means of 4x and 10x magnification. Both plane polarised- and cross polarised light techniques were used in the microscopic analyses of the thin sections. Images of the thin sections were taken using the Nikon ECLIPSE LV100POL petrographic microscope together with the NIS-Elements 6.11.01 64-bit software. Additionally, the stereo microscope (also known as stereoscope) Leica MZ APO with 8x magnification (1x magnification object) was used for thin section analyses. Images of the thin sections were taken using a Leica DFC420 camera together with the LAS V3.8 software.

5.0 Results

This chapter consists of three parts and presents results from 1) analysis of virtual outcrops and logs, which yields distribution of facies associations and sedimentary architecture, 2) facies and facies association determination and microscopic analyses and 3) proportions of the different facies associations in the different studied outcrops.

5.1 Facies and facies associations

5.1.1 Facies

In the study area, twenty-two sedimentary facies have been identified and are present in the sedimentary logs taken during the field seasons (Appendix I). As the study area comprises a sandstone-rich alluvial system, the majority of the facies comprise various types of sandstone that are distinct in texture and fabric. The facies are listed in Table 5.1 coupled with a brief description of the individual facies. In this thesis, the terms 'stratification' and 'lamination' are differentiated by a 1 cm threshold in which lamination is defined as < 1 cm and stratification is defined as > 1 cm. Furthermore, grain sizes are classified in concordance with Wentworth (1922).

The colours of the deposits appear arbitrary and vary locally from green to red to drab colours due to shifting reduction and oxidation states in response to the water table position at the time of deposition (Turner, 1974a) and are therefore not included in the facies descriptions. Furthermore, facies herein are determined solely by lithologies and sedimentary structures as no biogenic structures or fossils have been identified in the deposits in which can aid facies analysis.

Table 5.1. Facies in the study area with a brief description of each facies.

Facies	Description
F1 – Plane-parallel stratified very fine sandstone	Very fine-grained sandstone with plane-parallel stratification (PPS). Strata are very thin (2-3 cm) and are slightly inclined (as they follow the dipping bed architecture) and occasionally horizontal.
F2 – Plane-parallel stratified fine sandstone	Fine sandstone with plane-parallel stratification (PPS). Strata are very thin (2-3 cm) and are slightly inclined (as they follow the dipping bed architecture) and occasionally horizontal.
F3 – Plane-parallel stratified medium sandstone	Medium-grained sandstone with plane-parallel stratification (PPS). Strata are very thin (2-3 cm) and are slightly inclined (as they follow the dipping bed architecture) and occasionally horizontal.
F4 – Current-rippled very fine sandstone	Fine-grained sandstone with current ripple stratification. Strata are approximately 5 cm and are horizontal and slightly inclined.
F5 – Current-rippled fine sandstone	Fine-grained sandstone with current ripple stratification. Strata are approximately 5 cm and are horizontal and slightly inclined.
F6 – Current-rippled medium sandstone	Fine-grained sandstone with current ripple stratification. Strata are approximately 5 cm and are horizontal and slightly inclined.
F7 – Cross-bedded stratified fine sandstone	Fine-grained sandstone with cross-bedded stratification. Strata are gently dipping in the bottomset and is defined as through cross-bedded.
F8 – Cross-bedded stratified medium sandstone	Medium-grained sandstone with cross-bedded stratification. Strata are gently dipping in the bottomset and is defined as through cross-bedded.
F9 – Plane-parallel stratified fine sandstone with mud clasts	Fine-grained sandstone with plane-parallel stratification and intraformational rip-up mud clasts (MC). MC size varies from a couple of millimetres to ~20 cm.

F10 – Plane-parallel stratified medium sandstone with mud clasts	Medium-grained sandstone with plane-parallel stratification and intraformational rip-up mud clasts (MC). MC size varies from a couple of millimetres to ~20 cm.
F11 – Current-rippled fine sandstone with mud clasts	Fine-grained sandstone with current ripple stratification and intraformational rip-up mud clasts (MC). MC size varies from a couple of millimetres to ~5 cm.
F12 – Very fine sandstone with mud clasts	Very fine-grained sandstone with intraformational rip-up mud clasts (MC). MC size varies from a couple of millimetres to ~20 cm.
F13 – Fine sandstone with mud clasts	Fine-grained sandstone with intraformational rip-up mud clasts (MC). MC size varies from a couple of millimetres to ~20 cm.
F14 – Medium sandstone with mud clasts	Medium-grained sandstone with intraformational rip-up mud clasts (MC). MC size varies from a couple of millimetres to ~20 cm.
F15 – Massive very fine sandstone	Very fine-grained sandstone with no visible structure.
F16 – Massive fine sandstone	Fine-grained sandstone with no visible structure.
F17 – Massive medium sandstone	Medium-grained sandstone with no visible structure.
F18 – Current-rippled fine sandstone with mud clasts	Muddy sandstone with current ripple stratification and intraformational rip-up mud clasts (MC). MC size varies from a couple of millimetres to ~5 cm.
F19 – Muddy sandstone	Muddy sandstone.
F20 – Laminated siltstone	Laminated siltstone with wavy and horizontal lamination.
F21 – Sandy mudstone	Sandy mudstone, rhizocretions sometimes present.
F22 – Mudstone	Mudstone with flaky appearance in outcrops.

5.1.2 Facies associations

A total of five facies associations (FA) have been recognised in the study area, through sedimentary architectural elements combined with facies that were found to be closely associated and are interpreted to represent a specific depositional environment.

These include:

- FA1 – Channel belt facies association
- FA2 – Crevasse splay facies association
- FA3 – Abandoned channel facies association
- FA4 – Floodplain facies association
- FA5 – Loess facies association

Table 5.2 gives a brief overview of the facies associations and their individual architecture, together with associated facies and thin sections, whereas the following subchapters comprise detailed descriptions and interpretations of the individual facies associations. Moreover, Fig. 5.1 shows the legend for sedimentary logs which are attached in the following subchapters.

Table 5.2. Overview of the facies associations and the related sedimentary architecture and facies.

Facies association	Sedimentary architecture	Facies
FA1 – Channel belt facies association	Lens-shaped, erosive, laterally extensive storeys with cross-cutting bed surfaces	Plane-parallel stratified-, current rippled-, cross-bedded- and massive sandstones and muddy sandstone (F1-F19)
FA2 – Crevasse splay facies association	Thin (5-20 cm) and laterally extensive sandstone bodies	Current rippled- and massive sandstone (F4, F5, F14, F15, F17)
FA3 – Abandoned channel facies association	Lens-shaped, erosive or tabular, laterally extensive	Sandy mudstone (F21)
FA4 – Floodplain facies association	Thin (1-20 cm), often laterally extensive	Muddy sandstone, sandy mudstone, mudstone (F19, F21, F22)

FA5 – Loess facies association	Thickly bedded, tabular bed boundaries, laterally extensive	Laminated siltstone (F20)

Legend

≡ Planar-parallel stratification

Current ripples

Tangential cross-bedding

Intraformational rip-up mud clasts

Sandstone

Mudstone

Mud content

Figure 5.1. Legend for the sedimentary logs which are attached in the following subchapters.
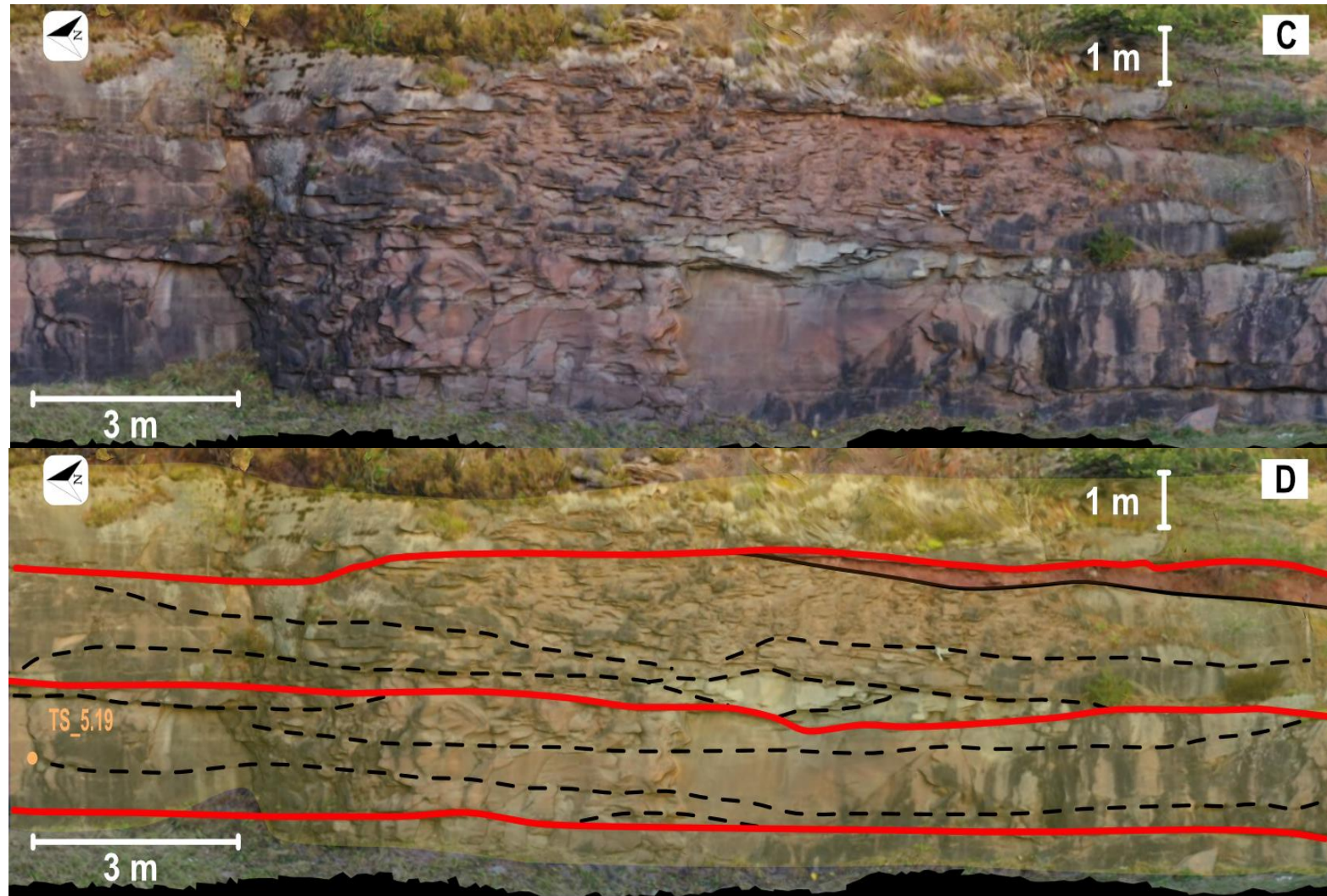
5.1.2.1 FA1: Channel belt facies association

The FA1 is the most abundant facies association and is found in outcrops 1-4 (Fig. 1.2), in both the Sundvollen Formation and the Stubdal Formation. Most of the identified facies are found herein as shown in Table 5.1, however very fine-fine-medium- grained sandstone with plane-parallel stratification, very fine-fine-medium-grained sandstone with current ripple stratification, fine-medium-grained sandstone with mud clasts and massive very fine-fine-medium-grained sandstone (Fig. 5.3) are the dominating facies in the facies association.

Deposits in the outcrops consist of amalgamated sandstone bodies represented in multi-storeys, with storeys ranging from 32-262 metres in width and 1-3 metres in thickness. The sandstone bodies in the storeys have erosional boundaries and beds are cross-cutting each other. The storeys display a lens-shaped sedimentary architectural style, although with a complex internal structure (Fig. 5.2). The horizontal edges of the storeys are rarely seen, and these are likely eroded or buried in the subsurface. True total thicknesses are therefore not possible to determine. The stories commonly comprise smaller erosional surfaces which crosscut each other in different directions, separating the sand bodies. Due to the lesser lateral extensivity of outcrop 1 compared to outcrop 2 & 3 (Fig. 1.2), architectural styles in outcrop 1 differs slightly from outcrop 2 & 3, which additionally is affected by a 15.5 metre break in the outcrop coupled with a fault (Fig. 5.19).

Grain size trends are difficult to determine in the field because of a very limited grain size range in the deposits, and only a few fining upward trends have therefore been recognised in the logs. Furthermore, the individual bedsets containing very fine- to medium-grained sandstone are frequently separated by 1-2 cm thin mudstone beds (Fig 5.4). Rip-up mud clasts are often present in the base and occasionally also found in the middle of the sandstone bodies. Additionally, muddy sandstone beds are often present between the sandstone bodies.
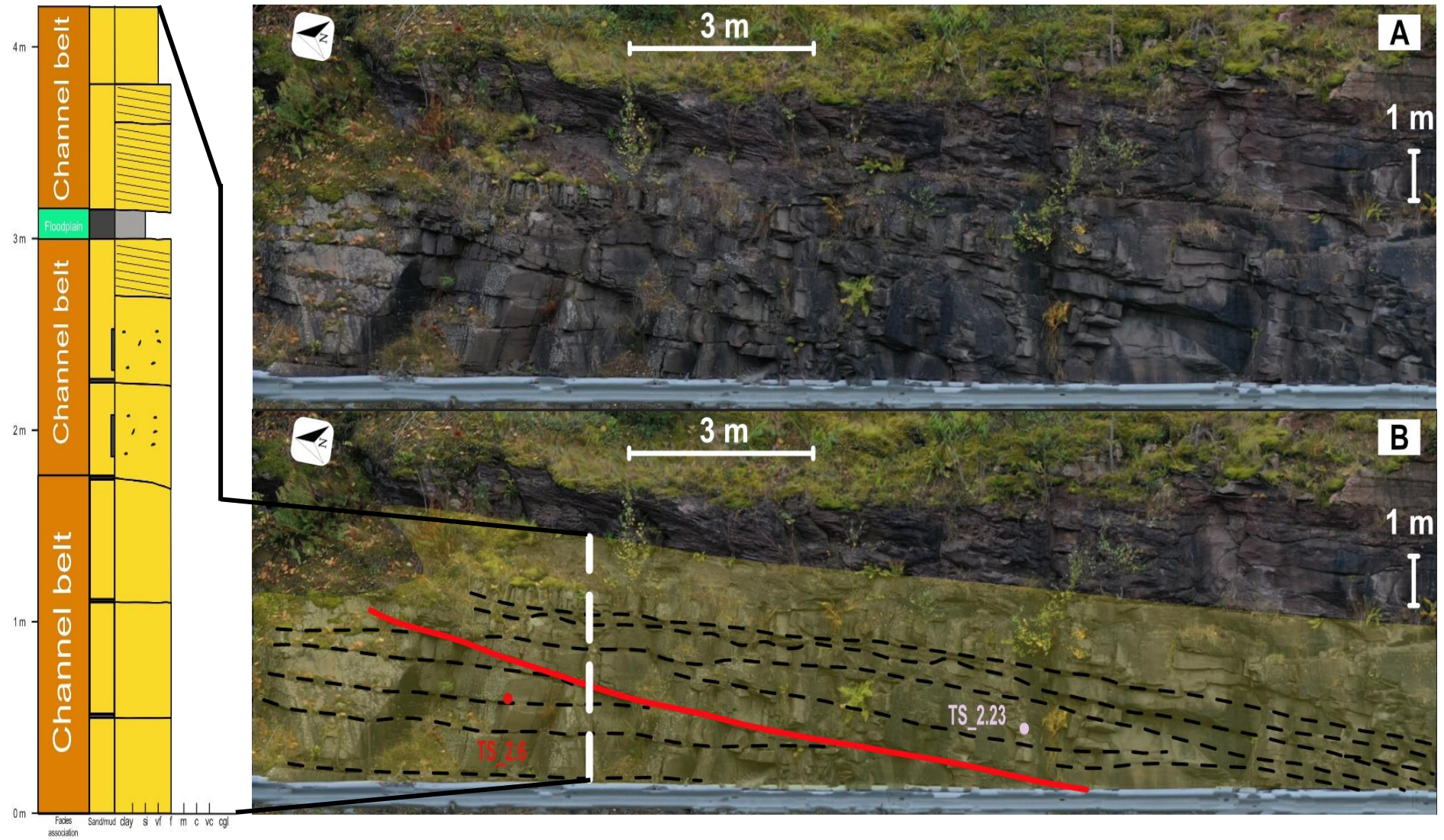
Figure 5.2. Examples of architecture in FA1 – channel belt facies association. The yellow colour marks the channel belt deposits. Red line colour marks the storeys and black stippled line colour marks the bedding planes. White stippled line shows the location of the adjacent sedimentary log. A) and B) are from the Sundvollen Formation at outcrop 1 and C) and D) are from the Stubdal Formation at outcrop 3.
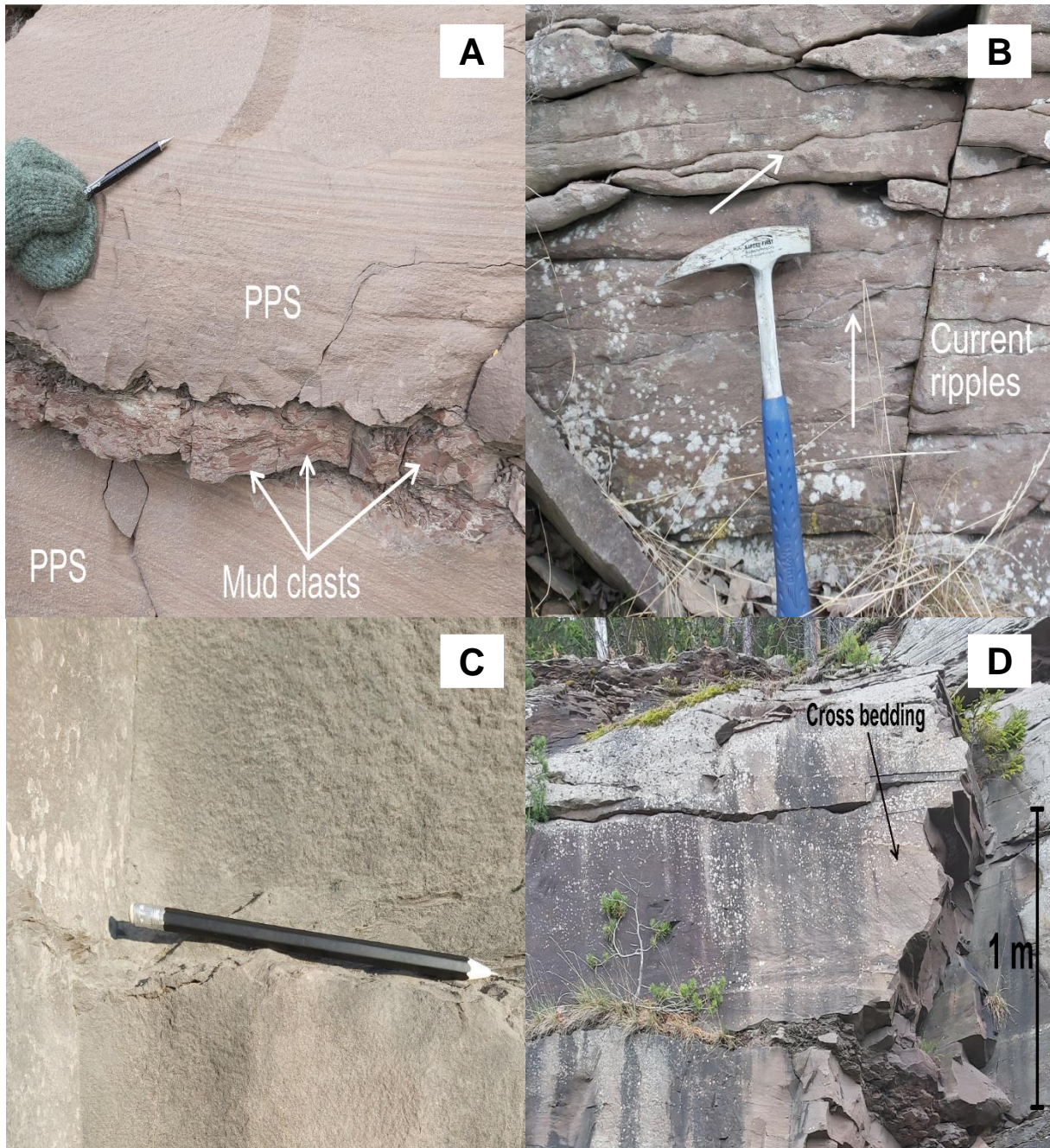
Figure 5.3. Examples of commonly occurring facies and sedimentary structures in FA1 – channel belt facies association. A) F1-F3 plane-parallel stratified sandstones and F12-F13 sandstones with mud clasts at outcrop 3. B) F4-F6 current rippled sandstones at outcrop 4. C) F14-F16 massive sandstones at outcrop 2. D) F7-F8 cross-bedded sandstones at outcrop 3.

Figure 5.4. Example of the channel belt facies association at outcrop 1 with thin mudstone layers (red arrows) separating the sandstone bodies.

5.1.2.1.1 Thin section analyses

Thin section analyses show mostly fine to medium-grained sandstone (Fig. 5.5), however a sample in outcrop 1 contains very fine-grained sandstone. The facies association is interpreted as quartz-arenitic in composition as quartz grains comprise ~ 95 % of the samples. Clay minerals (mud clasts), opaques, plagioclase and chlorite comprise the rest of the mineral composition, while natrolite and fluorite often occur as accessory minerals. The grains in the samples are largely subangular-subrounded and often covered in a reddish stain. Mud clasts appear as dark-coloured and can occupy large areas of thin sections (Fig. 5.6), often containing smaller silt-very fine-grained sand grains composed of quartz within. White coloured veins are also common in the mud clasts. Grain size sorting related to sedimentary structures is occasionally observed in thin section (Appendix II). Plane-parallel stratification in fine- and medium-grained sandstone (facies F2 and F3), as well as current ripple cross-lamination in fine- and medium-grained sandstone (facies F5 and F6) has been identified in thin section, supporting the facies identification in the field.
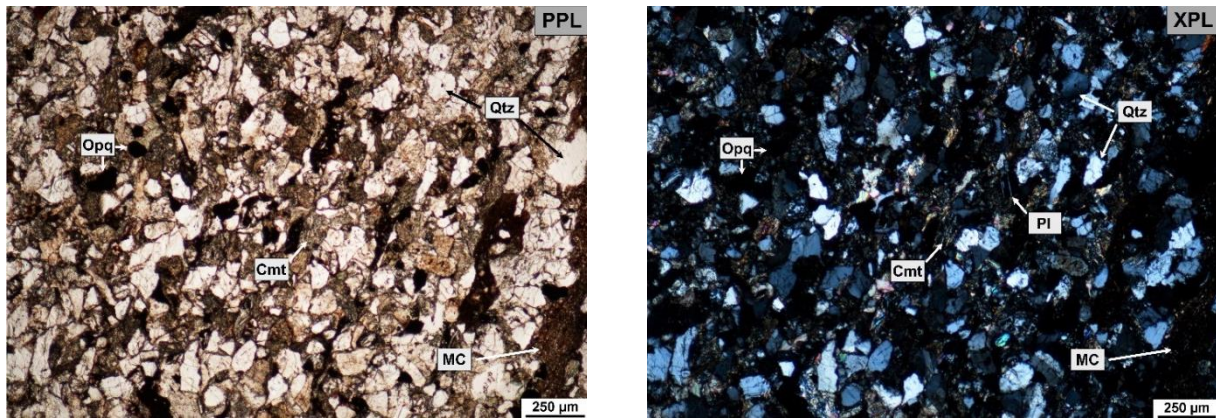
Figure 5.5. Thin section TS_2.2 in plane-polarised light (PPL) and cross-polarised light (XPL). Grain sizes and sorting analyses show a typical deposit in FA1, with subangular-subrounded fine-medium sand grains and moderately-poorly sorting. Deposits are moreover strongly cemented. Abbreviations: Qtz = quartz, Pl = plagioclase, MC = rip-up mud clast, Opq = opaque minerals, Cmt = cement.
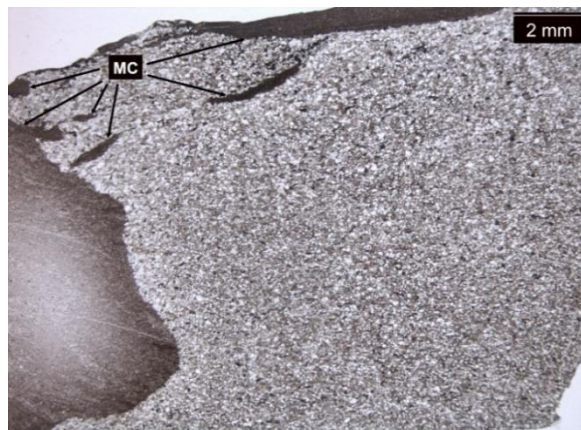
Figure 5.6. Stereoscope image of thin section 6.5. Present in the sample are rip-up mud clasts. Abbreviations: MC = rip-up mud clasts.

5.1.2.1.2 Interpretation

The sandstone bodies in this facies association comprise several depositional elements linked to unidirectional currents such as plane-parallel-, cross-bedding- and current ripple stratification and rip-up mud clasts. Where current ripple stratification represents lower flow regime sedimentary structures, the other structures represent upper flow regime sedimentary structures, indicating sandstone bodies deposited by powerful flows (e.g. Fielding, 2006). Furthermore, the sedimentary architectures with wide storeys up to 263 metres with internal cross-cutting bed surfaces separated by thin mudstone beds indicate consistent and erosive sedimentation (e.g. Mitten et al., 2020). As no biogenic structures and oscillatory currents are present in the

deposits, a delta front depositional environment is unlikely (e.g. Plint & Wadsworth, 2003; Carmona et al., 2009). Given the alluvial character of the Ringerike Group, the deposits are likely fluvial deposits with amalgamated sandstone bodies. This facies association is therefore interpreted as a channel belt facies association.

5.1.2.2 FA2: Crevasse splay facies association

This facies association is found in both the Sundvollen Formation and the Stubdal Formation, yet rather scarcely in outcrops 1-4 (Fig. 1.2). It occurs as thin sand layers intercalated by mudstones and are easily spotted on the outcrops (Fig. 5.7). Deposits are thin (~ 20 cm) yet laterally extensive – and often pinching out in both sides into the channel belt facies association. Sandstone beds in this facies association display lengths of maximum 84 metres. Very fine- to fine sandstone beds with current ripple stratification (facies F4-6) and very fine- to fine-grained sandstone beds with mud clasts (F12-F14) are found herein adjacent to sandy mudstone- and mudstone beds (F21-F22). Sedimentary structures were in some places not possible to determine in the field, though was however later revealed by thin sections. Bed boundaries are notably less erosive (see Fig. 5.13) compared to the channel belts in FA1. Rip-up mud clasts are additionally present, up to 10 cm in length.
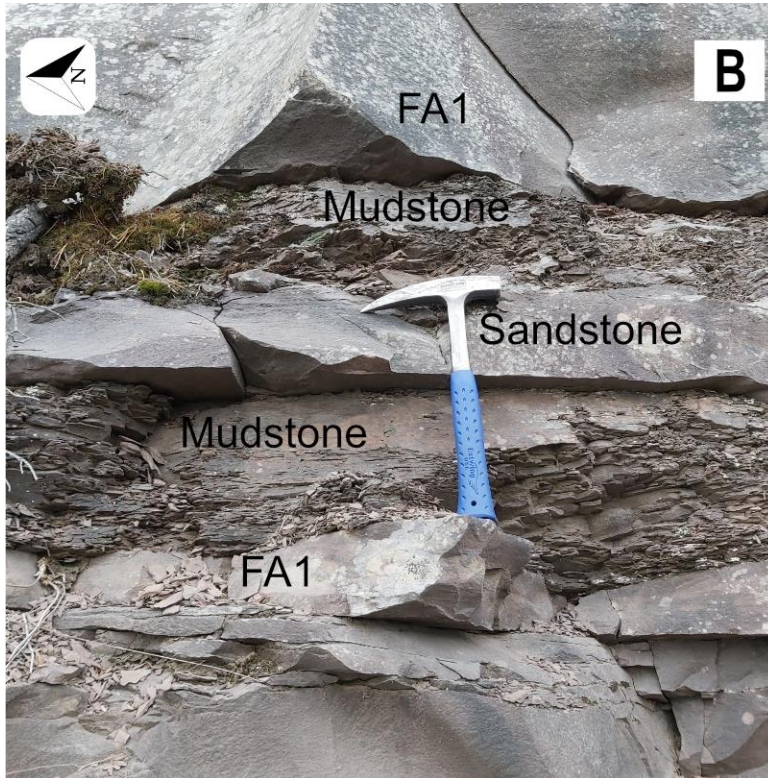
Figure 5.7. Typical expression of FA2 – crevasse splay facies association, from outcrop 3, with a thin sandstone bed intercalated by mudstone beds. Note the lesser erosive boundary compared to the FA1 – channel belt facies association.

5.1.2.2.1 Thin section analyses

Thin section analyses show very fine- to fine-grained subangular-subrounded grains in quartz-rich samples accompanied by smaller muddier horizons (Fig. 5.8), in clear contrast to the quartzarenitic, mud-poor and largely fine- to medium-grained sandstone beds in FA1. Clay minerals, chlorite and natrolite are additional identified minerals. A large rip-up mud clast is also visible in Fig. 5.8, containing subangular-subrounded silt- to very fine sand grains. Moreover, stereoscope analyses display current-ripple stratification in the samples (Fig. 5.9).
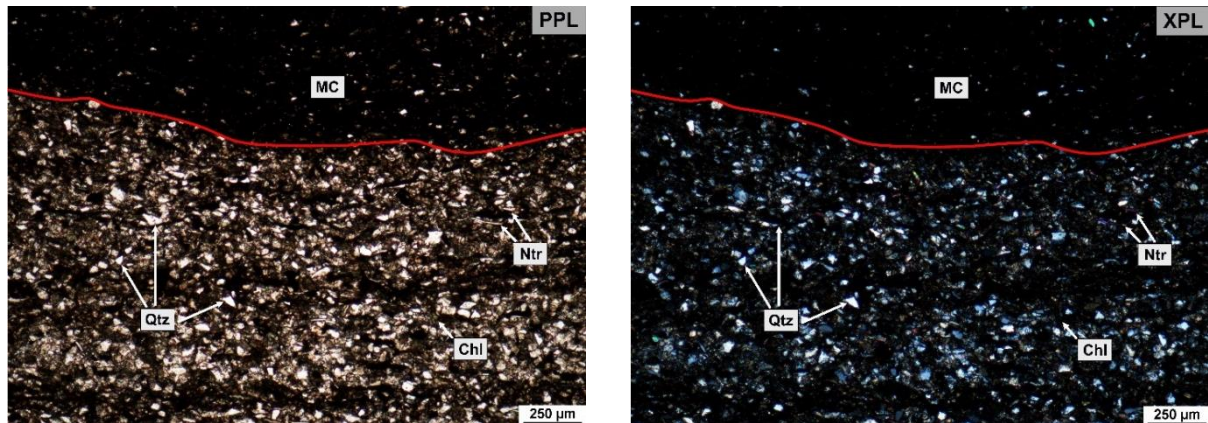
Figure 5.8. Thin section 2.11 in plane-polarised light (PPL) and cross-polarised light (XPL). Grain sizes and sorting analyses show a typical deposit in FA2, with subangular-subrounded very fine sand grains and moderate-poor sorting in a muddy matrix. Deposits are moreover strongly cemented. The red line separates the sandy part from the rip-up mud clast. Abbreviations: Qtz = quartz, Cl = chlorite, Ntr = natrolite, MC = rip-up mud clast.
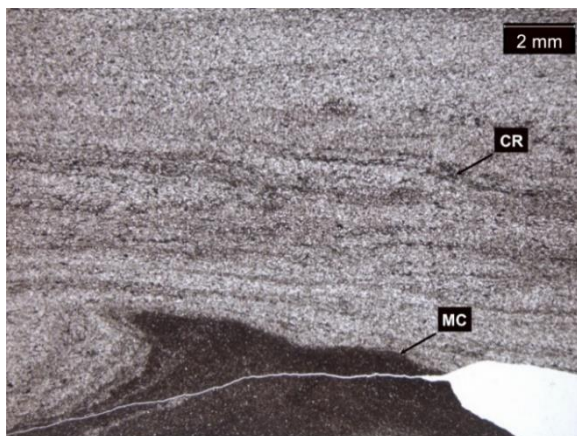
Figure 5.9. Stereoscope images of thin sections 2.11. Present in the samples are current ripples and rip-up mud clasts. Abbreviations: CR = current ripple stratification, MC = rip-up mud clast.

5.1.2.2.2 Interpretation

The presence of thinly bedded very fine- to fine-grained sandstone with current ripple stratification indicates deposition from a unidirectional current, however with less powerful current forces compared to FA1 as cross-bedding- and plane-parallel stratification is absent. Moreover, the intercalation of the thin sandstone beds with mudstone beds suggest deposition took place in a low-energy depositional environment. The sheet-form sedimentary architecture

with laterally extensive deposits furthermore indicates these sandstone beds were deposited largely unconfined.

Such deposits with sheet-formed and laterally extensive sandstone beds intercalated by mudstone beds suggest deposition took place on the floodplain due to breaching of a river levee, depositing overbank sediments in the form of crevasse splay. As deposition of crevasse splays is restricted to flooding events and deposit sandstone beds rather quickly by unidirectional currents, sedimentary structures are most often restricted to lower flow regime concurrent with the current ripple stratification identified (e.g. Gulliford et al, 2017). However, the presence of rip-up mud clasts might also suggest a more forceful unidirectional current (e.g. Bridge, 2006). Given the largely fluvial character of the Ringerike Group, this facies association is therefore interpreted as a crevasse splay facies association.

5.1.2.3 FA3: Abandoned channel facies association

This facies association is solely found in outcrop 1 (Fig. 1.2) in the Sundvollen Formation, where sandy mudstone (facies F21) comprises the facies association. Deposits (Fig. 5.10) are large and is measured as 19.4-81.3 metres long with heights from 1.8-6.2 metres, wedging out in the north and south. Colours herein range from black to reddish to drab coloured in response to the freshness of the outcrop. Moreover, the architectural style is very similar to a fluvial sandstone channel, with a clear lens shape, eroding into the underlying beds, however also occurring as tabular. The internal grain size evolution was difficult to determine in the field, as weathering processes has altered the outcrop surface.
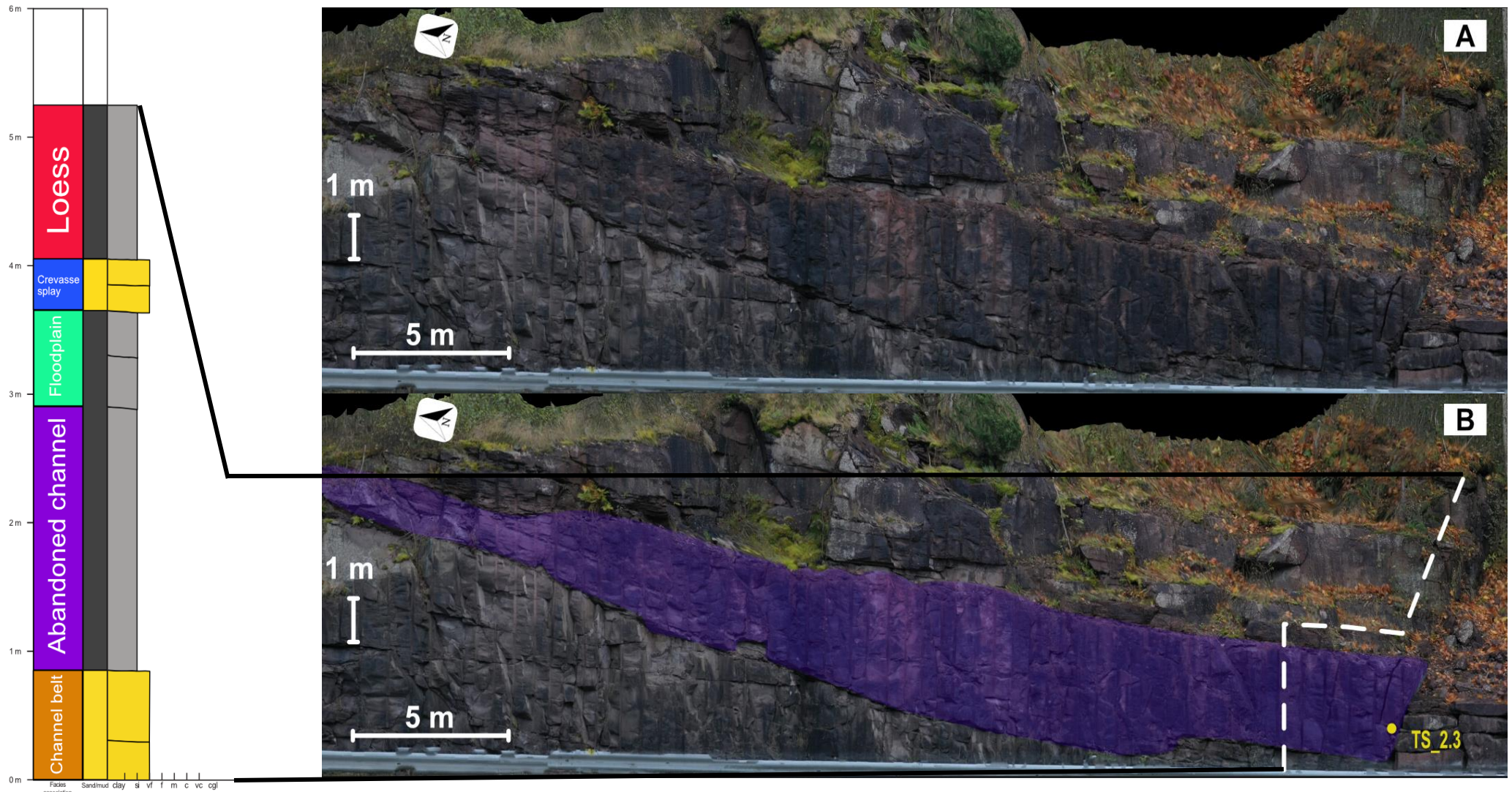
Figure 5.10. Example of the facies association at outcrop 1. The architecture of the deposits (marked in purple colour) is similar to a channel belt however composed of mudstone, indicating a more low-energy environment. A log through the facies association marked by the white stippled line is displayed to the left.

5.1.2.3.1 Thin section analyses

Thin section analyses show subangular-subrounded silt grains in a matrix of clay minerals, where quartz is the constituent mineral (Fig. 5.11). Additionally, very large grains are identified in a thin section, consisting of calcite due to the high birefringence. Fig. 5.12 shows a larger image of the thin section, which display these large calcite minerals in a chaotic manner together with the surrounded mudstone. Other minerals which are identified include plagioclase, chlorite and natrolite. A distinct area of the thin section containing more pronounced cementation is also present. Moreover, current ripples are observable in stereoscope analyses (Fig. 5.12).
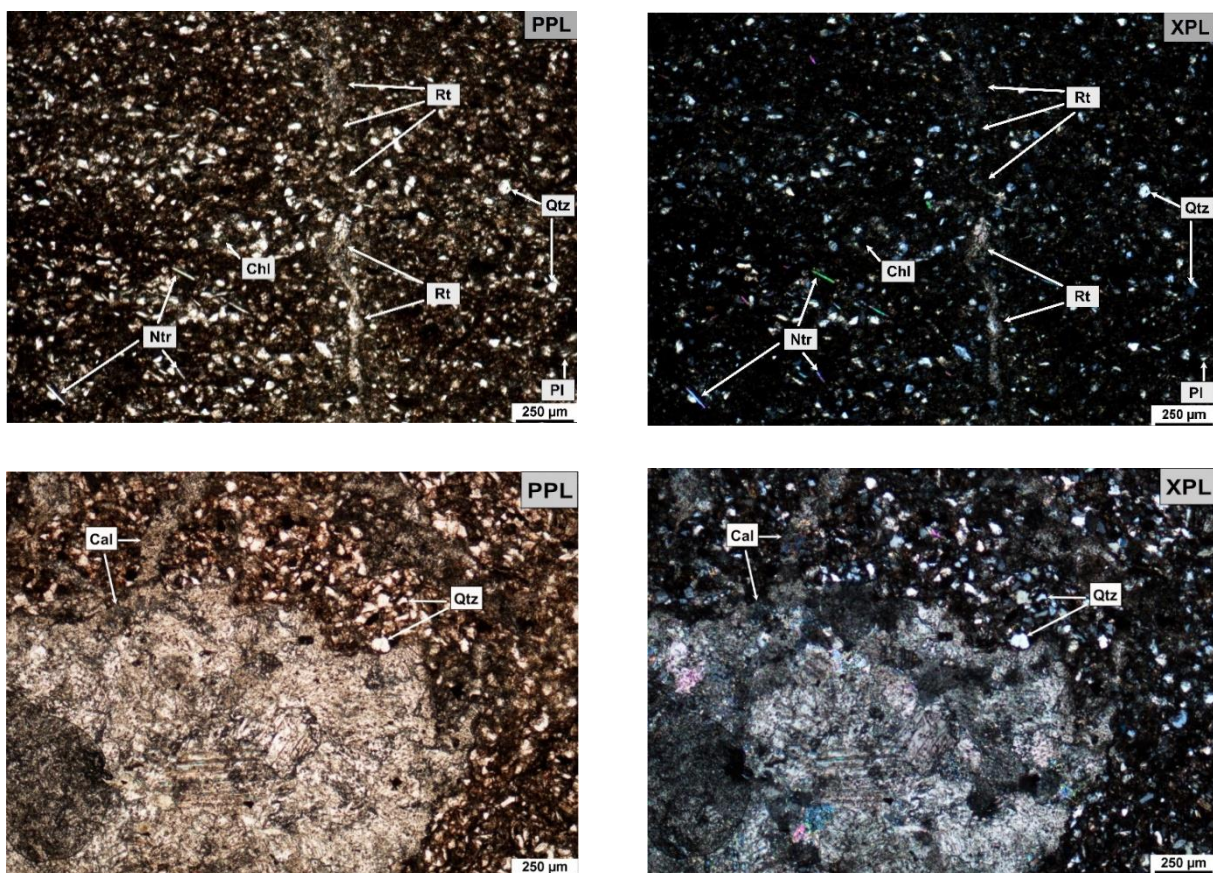
Figure 5.11. Thin section 2.3 (upper) and 2.17 (lower) in plane-polarised light (PPL) and cross-polarised light (XPL). Grain sizes and sorting analyses show a typical deposit in FA3, with subangular-subrounded silt-very fine sand grains and moderate-poor sorting in a muddy matrix. Deposits are moreover strongly cemented. A curved rootlet is also observable. Abbreviations: Qtz = quartz, Pl = plagioclase, Cal = calcite, Cl = chlorite, Ntr = natrolite, MC = rip-up mud clast, Rt = rootlet.
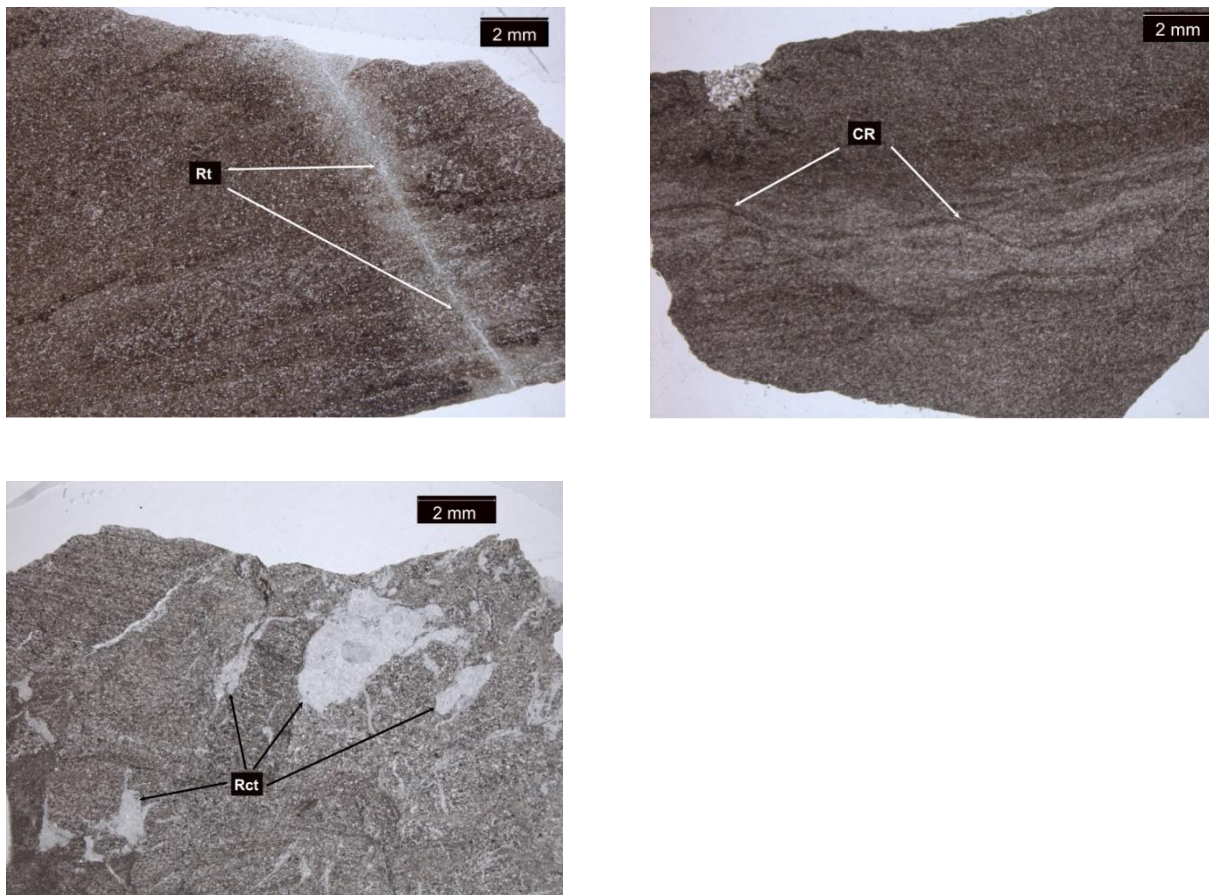
Figure 5.12. Stereoscope images of thin sections 2.3 (upper left), 2.7 (upper right) and 2.17 (lower left) showing the rootlet, current ripple stratification and rhizocretions. Note the small accumulation of sand grains also in the upper left corner on thin section 2.7 surrounded by muddy sediments. Abbreviations: Rt = rootlet, MC = rip-up mud clast, Rct = rhizocretions.

5.1.2.3.2 Interpretation

A low-energy environment can be deduced from the thin sections, consisting of silt and clays with no apparent sedimentary structure. Additionally, the presence of the pronounced cementation likely representing a rootlet in the thin sections is an indication of a calm terrestrial environment in which roots have likely penetrated the sediment. The large calcite grains are most likely caliche deposits, possibly also owing to root penetration and thus might display rhizocretions (e.g. do Nascimento et al., 2019). Moreover, the current ripple stratification indicates some outwash of running water.

The architectural elements concurrent with a channel belt, the presence of mudstone and indications of root activity suggest a depositional environment of an abandoned channel which

have been deposited largely subaerial (e.g. Nichols & Fisher, 2007). The current ripple stratification which was deposited subaqueous is possibly present due to flooding episodes of the likely adjacent active channel, inducing the current ripple stratification which only requires a few seconds to form (Bridge, 2006). This facies association is therefore interpreted as an abandoned channel facies association, collectively also termed as mud plug.

5.1.2.4 FA4: Floodplain facies association

This facies association is found in outcrops 1-4 (Fig. 1.2) in both the Sundvollen Formation and the Stubdal Formation. The facies association occurs frequently throughout outcrop 1-4 , separating the sandstone beds in the channel belts and crevasse splays in FA1 and FA2, respectively. Deposits are tabular and often very thin (normally 2-5 cm) though reach a maximum thickness of 60 cm and are often laterally extensive (up to 10-20 metres). Lithologically, the facies association is entirely composed of brown coloured mudstone beds with a flaky and recessive appearance in the field in clear contrast to the adjacent unbroken and more resistant sandstones (Fig. 5.13). Due to the flaky nature of the deposits, sedimentary structures have not been observed. Moreover, the mudstone beds are often eroded by the sandstone beds in FA1 and FA2.
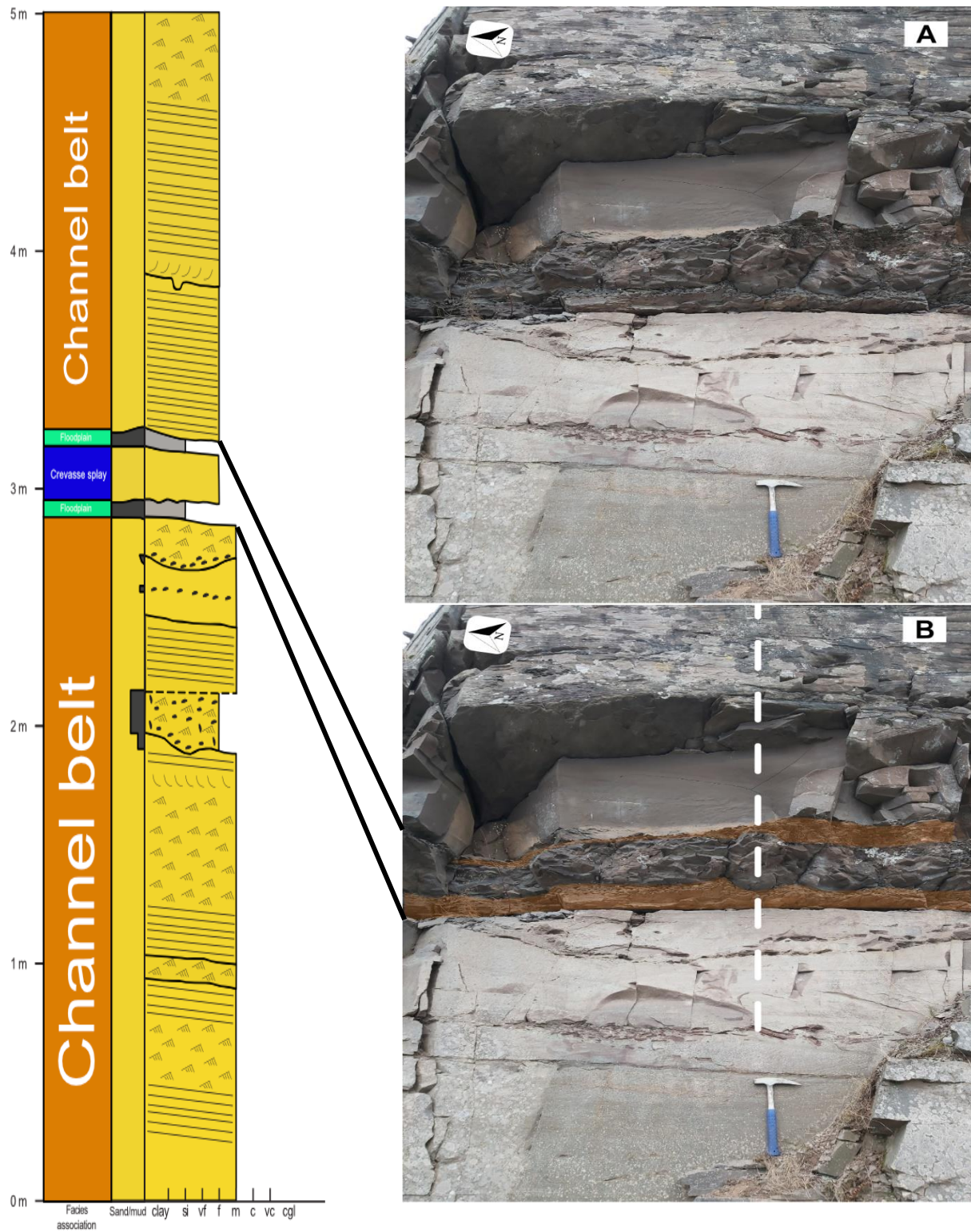
Figure 5.13. Example of the facies association at outcrop 4, shown by the brown colour. The mudstones herein are intercalated with sandstones in FA1 and FA2. A log through the facies association is shown to left.

5.1.2.4.1 Thin section analyses

Thin section analyses show a very fine-grained mudstone sample with what is assumed to be ~ 90 % clay minerals due to the dark colour and non-observable grains whereas silt grains compose the rest of the sample (Fig. 5.14). No apparent sedimentary structures are observable and grain roundness cannot be determined properly. However, grains can probably be assumed to be subangular-subrounded composed largely of quartz as all other grains in the rest of the samples (Appendix II) exhibit quartz-rich samples with subangular-subrounded grains.
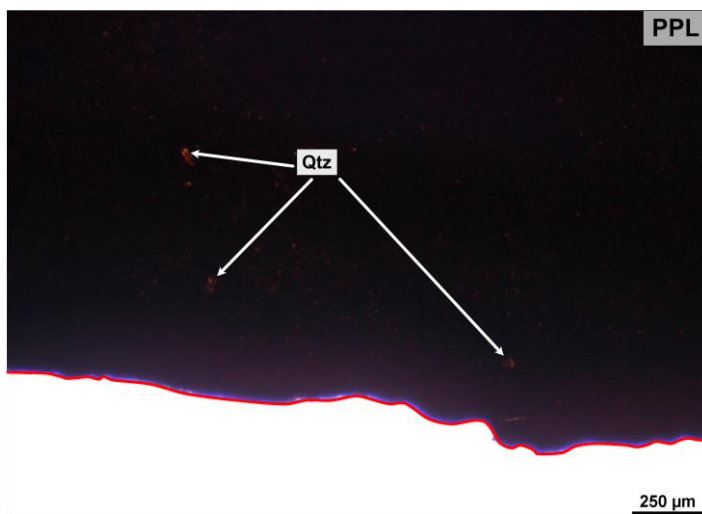
Figure 5.14. Thin section 2.28 in plane-polarised light. Grain sizes show a typical deposit in FA4, composed of clays and silts with no apparent sedimentary structures. Red line marks the end of the sample in order to give contrast in the image. Abbreviation: Qtz = quartz.

5.1.2.4.2 Interpretation

Mudstone deposits with no observable structures and a flaky appearance in the field suggest deposition by suspensive material. Relatively thin (1-60 cm) mudstone deposits indicate a low-energy environment, which combined with erosional truncations of the mudstone beds suggest a proximity to more high-energy environments (e.g. Thayer & Ashmore, 2016). Given the presence of channel belt and crevasse splay as interpreted in the previous subchapters with mudstones intercalated between these sandstone beds, this facies association is interpreted as floodplain facies association.

5.1.2.5 FA5: Loess facies association

The final facies association is only found in the Sundvollen Formation at outcrops 1 and 5 (Fig. 1.2). In the outcrops, the facies association is displayed by 2.3-3.25 metres thick beds with tabular bed boundaries, stacked on top of each other reaching a maximum thickness of 8.5 metres. The facies association is laterally extensive, stretching from the northernmost outcrop 5 to the more southern outcrop 1. Total lateral length is not clear, however it displays lengths up to 78 metres in outcrop 1. Bed boundaries are unequivocally tabular (Fig. 5.15) and sedimentary structures were not seen in the field. Dominant deposit colour is faint reddish and black. Facies F20 – laminated siltstone is the only facies which is present in the facies association.
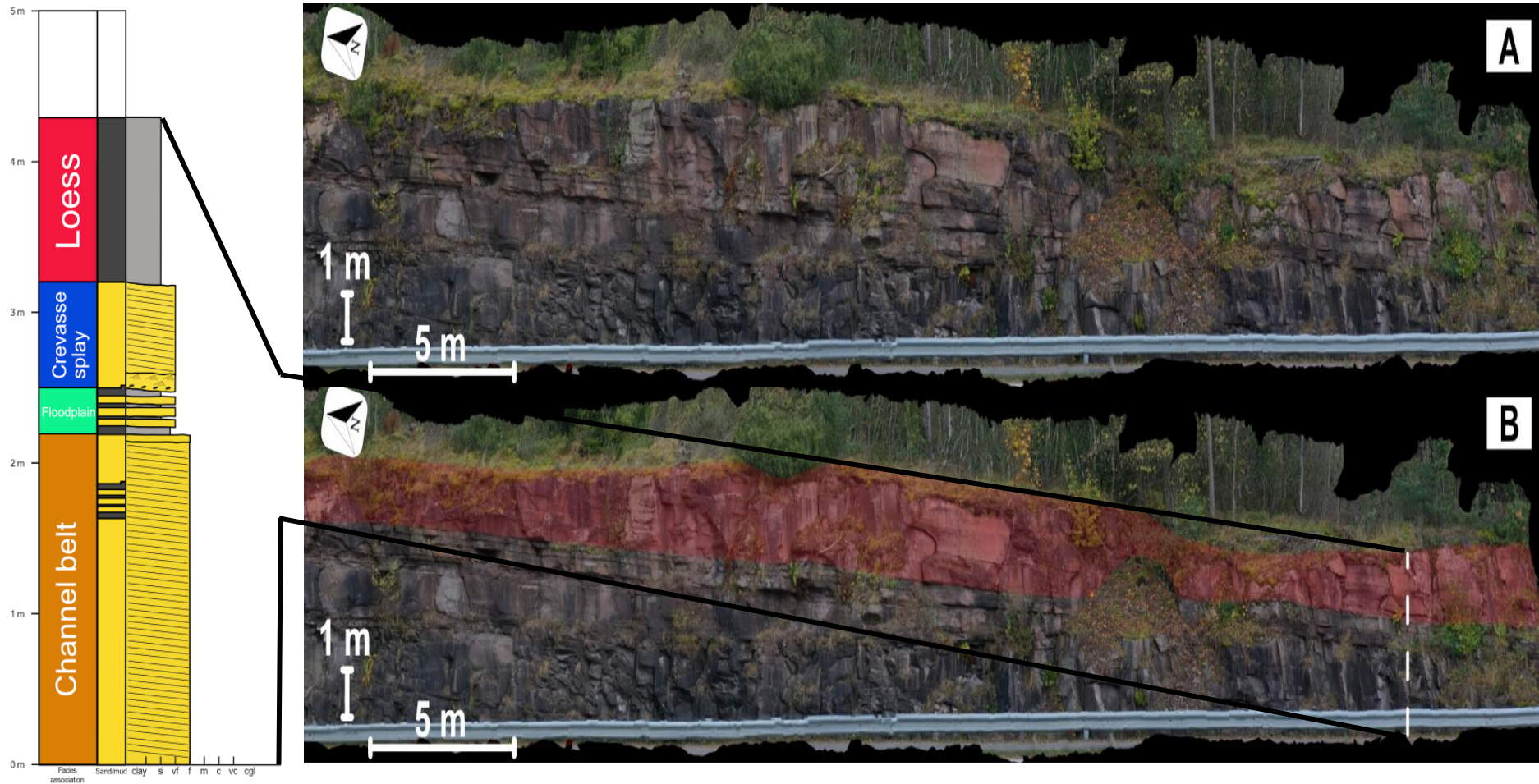
Figure 5.15. Example of the facies association at outcrop 1, shown by the red colour. The facies association lies over the sandstone beds in FA2. The white stippled line shows the location of the adjacent log.

5.1.2.5.1 Thin section analyses

Thin section analyses show a very fine-grained muddy sample, with subangular-subrounded silt grains with a mostly random grain fabric order (Fig. 5.16). Quartz and natrolite are identified and wavy lamination is seen in stereoscope analyses. Also note the muddier horizons in the stereoscope images (Fig. 5.17).
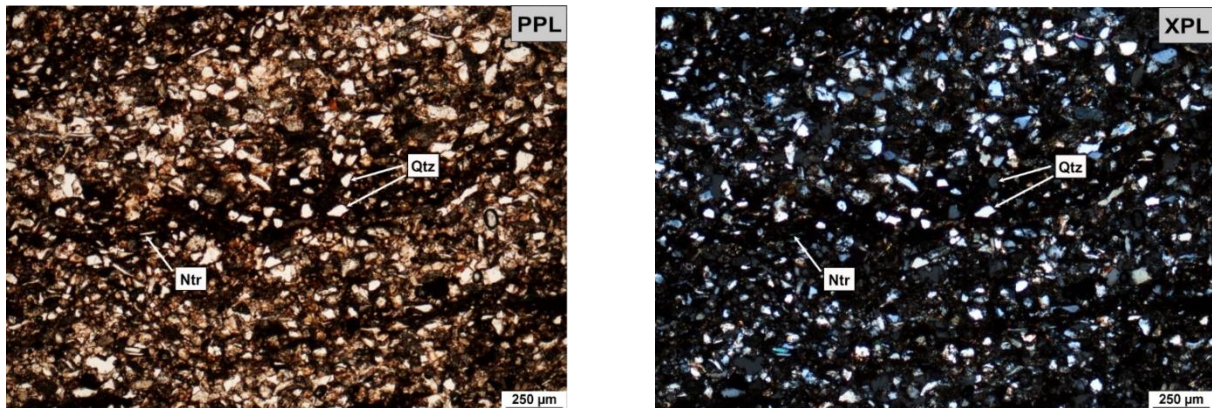
Figure 5.16. Thin section TS_2.21 in plane-polarised light (PPL) and cross-polarised light (XPL), showing a typical deposit in FA5, with subangular-subrounded silt grains and moderate-poor sorting. Abbreviations: Qtz = quartz, Ntr = natrolite.
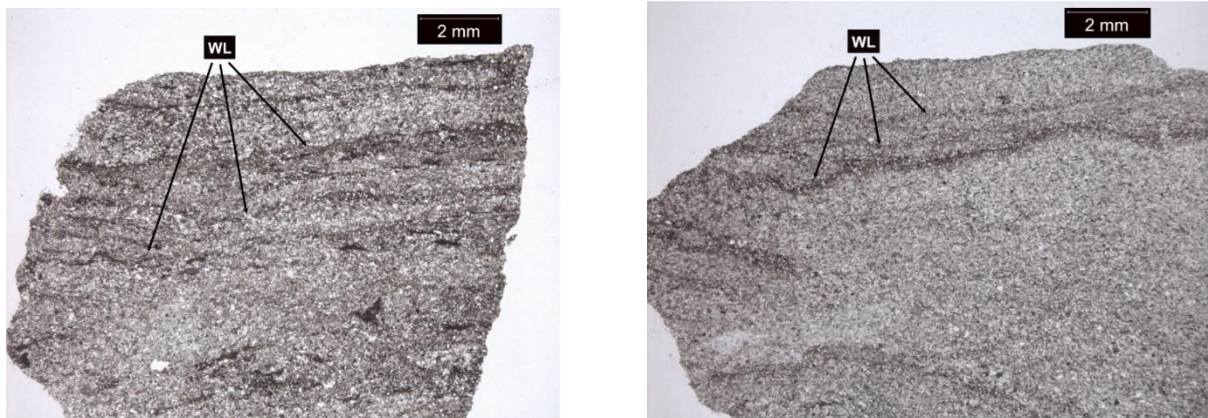
Figure 5.17. Stereoscope image of thin sections 2.21 (left) and 2.21 (right). The wavy lamination in the samples is shown by the black arrows. Abbreviation: WL = wavy lamination.

5.1.2.5.2 Interpretation

The tabular bed boundaries and the laminated siltstone are indicative of a relatively low-energy environment. Siltstones in the facies association display mostly random grain fabric which is in clear contrast to the sandstone deposits of FA1 and FA2 with unidirectional stratification and aligned grain fabric. A lacustrine deposit would similarly to the unidirectional currents display aligned grain fabric, which therefore suggest deposition with minor effect of water. Additionally, organic matter and bioturbation is absent, further contradicting a lacustrine origin of this facies association (e.g. Ghinassi et al., 2015). A subaerial depositional agent is hence likely, namely aeolian loess due to the random grain fabric and fine-grained deposit. However, as some of the silt grains display aligned grain fabric it is also possible that some pluvial reworking of the sediments (e.g. Wilkins et al., 2018) has occurred post-depositional, explaining the wavy lamination in thin sections.

The combination of the siltstones with random grain fabric and thickly tabular bedded deposits is indicative of loessites. This facies association is therefore interpreted as loess facies association.

5.2 Sedimentary architecture

The virtual outcrops which have been generated and interpreted are shown in the following sections, where the individual outcrops are shown firstly with no interpretation followed by a figure with facies interpretation and lastly shown by a figure with interpretations additionally including thin section and sedimentary log locations on the outcrops.

As the outcrops differ in length and height, resolution varies among the individual outcrops, where outcrop 4 has the highest resolution (smallest recognisable feature is 8 mm) and outcrops 2 and 3 have the lowest resolution (smallest recognisable feature is 10 cm and 5 cm, respectively). The longest outcrops thus show the architectural elements over a large area at relatively low resolution and no detailed interpretation of small elements such as thin mudstone layers and rip-up mud clasts have been made on these. On the other hand, the smaller outcrops include interpretation of these mudstone layers and rip-up mud clasts yet lack the larger architectural elements over longer distances.

5.2.1 Outcrop 1

This outcrop is composed of the Sundvollen Formation (Fig. 5.18) and is located near Rørvik Camping close to Sundvollen (Fig. 1.2). Of all the outcrops, outcrop 1 has the most abundance of facies and facies associations (Fig. 5.19). Stratigraphically, it is affected by a fault in the middle part of the outcrop represented by the break in outcrop, juxtaposing the channel belt facies association with the upper lying abandoned channel-, floodplain- and loess facies associations. Nonetheless, in the lowermost part of the outcrop on the northern side, unaffected by the fault, sandstone beds in the channel belt FA are separated by a mud plug in the abandoned channel FA. In total, ten storeys are identified in the channel belts ranging from 0.5-3.2 metres in thickness and 25-70 metres in width. Bed surfaces in the channel belts are arranged in several directions, displaying the erosional nature of the deposits.

Overlying the channel belts is the most prominent abandoned channel, stretching throughout large parts of the outcrop. The mud plug has a clear lens shape and pinches out in both sides of the outcrop. Floodplain mudstone beds overlie the mud plug which decrease in thickness from 95 cm in the north to 10 cm toward the south. Following the floodplain mudstones are the very fine-grained sandstones in the crevasse splay facies association, arranged in 4-5 sequences of beds ranging from 30 cm to 15 cm in thickness, separated by 1-2 thin mudstone layers. The uppermost deposits of the outcrop are the loessites in the loess facies association, ranging from 1.5-4 metres in thickness.

Altogether, seven sedimentary logs were taken at this outcrop and twenty-four thin sections represent samples taken in the field seasons. These are listed in Appendices I-II.
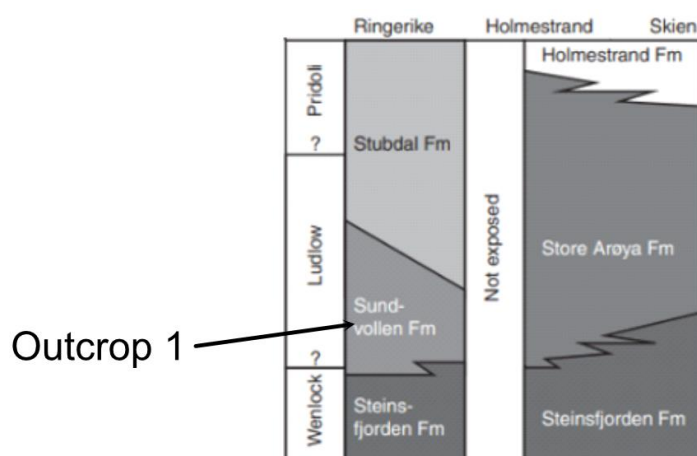
Figure 5.18. Outcrop 1 in the stratigraphic record in the Ringerike area. Modified from Davies et al. (2005a).
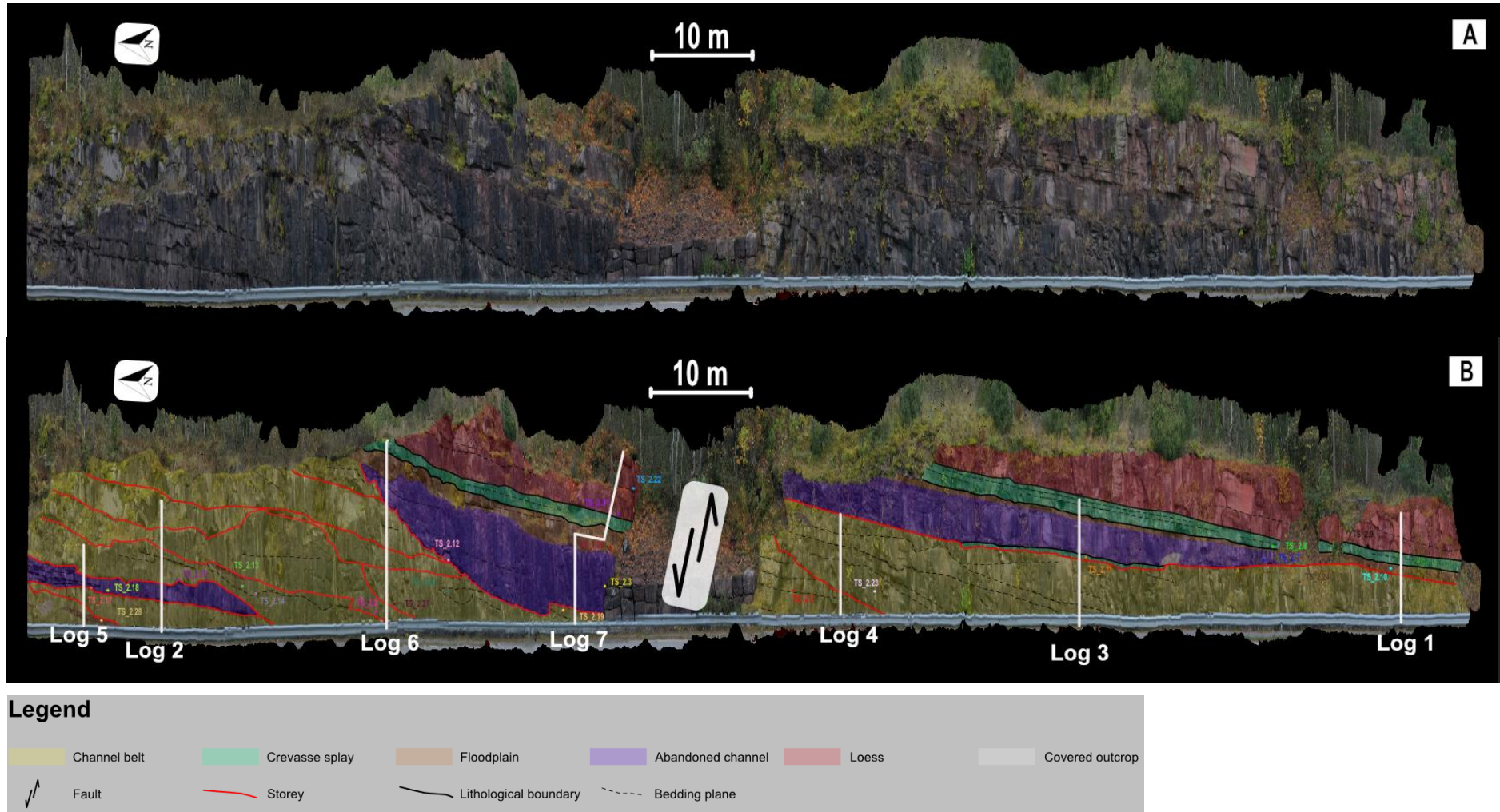
Figure 5.19. Outcrop 1 with 3x vertical exaggeration. The model is presented with A) no interpretation and B) interpretation with associated thin sections (TS) and sedimentary log location.

5.2.2 Outcrop 2

This outcrop is composed of the Stubdal Formation higher up in the stratigraphy (Fig. 5.20) and is located north of Trappa Parking near Utvika (Fig. 1.2). Outcrop 2, with a width of 437 metres, is the widest of all the outcrops studied and is restricted to the channel belt- and floodplain facies associations.

As shown in Fig. 5.21 the outcrop consists almost merely of sandstone bodies in the channel belt facies association, whilst mudstone beds in the floodplain facies association constitute 0.03 % of the outcrop. Similar to outcrop 1, the sandstones are comprised in multistorey channel belts, herein twelve storeys ranging from 1-3 metres in thickness and 36-262 metres in width. The bed surfaces in the channel belts herein appear very erosive, often cross-cutting each other – especially in the northern part of the outcrop as shown in Fig. 5.21. The southern part appears less chaotic and some clear-cut arcuate channel belts are identified here. The channel belts are vertically and laterally extensive, consisting throughout the entire outcrop. Large floodplain deposits are scarce, however 1-2 thin floodplain mudstones often present, separating the sandstone bodies.

Altogether, ten sedimentary logs were taken at this outcrop and thirty-five thin sections represent samples taken in the field seasons. These are listed in Appendices I-II.

Figure 5.20. Outcrop 2 in the stratigraphic record in the Ringerike area. Modified from Davies et al. (2005a).

Figure 5.21. Outcrop 2 with 3x vertical exaggeration. The model is presented with A) no interpretation and B) interpretation with associated thin sections (TS) and sedimentary log locations.
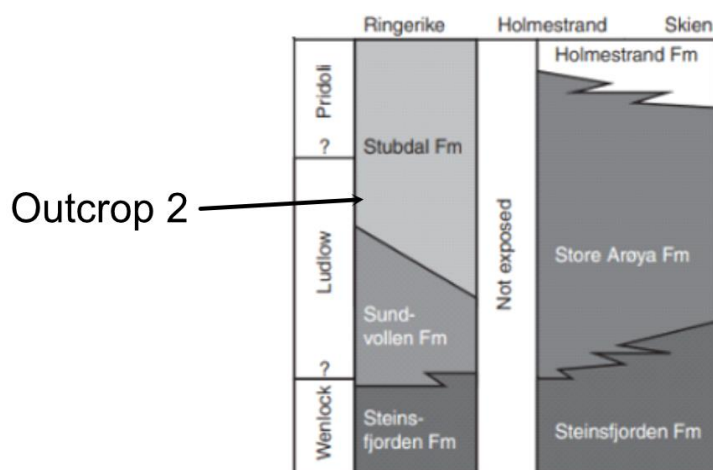
5.2.3 Outcrop 3

This outcrop is also composed of the Stubdal Formation (Fig. 5.22) and is located south of Jotaveien Parking near Utvika (Fig. 1.2). Outcrop 3, with a width of 429 metres, is the second largest of the outcrops studied and is similarly to outcrop 2 restricted to the channel belt- and floodplain facies associations (Fig. 5.23). The outcrop overlies outcrop 2 and is mostly constituted of sandstone bodies in the channel belt facies association, whilst the remaining 0.4 % consist of floodplain mudstone beds. Both the facies association proportion and sedimentary architecture resemble outcrop 2 as the outcrop is sandstone-rich and composed of multistorey channel belts. Herein, eleven storeys ranging from 0.5-3.5 metres in thickness and 53-147 metres in width are identified. Bed surfaces are cross-cutting each other frequently, yet it is more apparent in the northern part of the outcrop.

Contrary to outcrop 2, a distinct and relatively thick (60 cm) floodplain mudstone bed is present in between the adjacent storeys which constitute the rest of the outcrop. Additionally, 1-2 thin mudstone layers frequently separate the sandstone bodies.

Altogether, nine sedimentary logs were taken at this outcrop and thirty-one thin sections represent samples taken in the field seasons. These are listed in Appendices I-II.

Figure 5.22. Outcrop 3 in the stratigraphic record in the Ringerike area. Modified from Davies et al. (2005a).
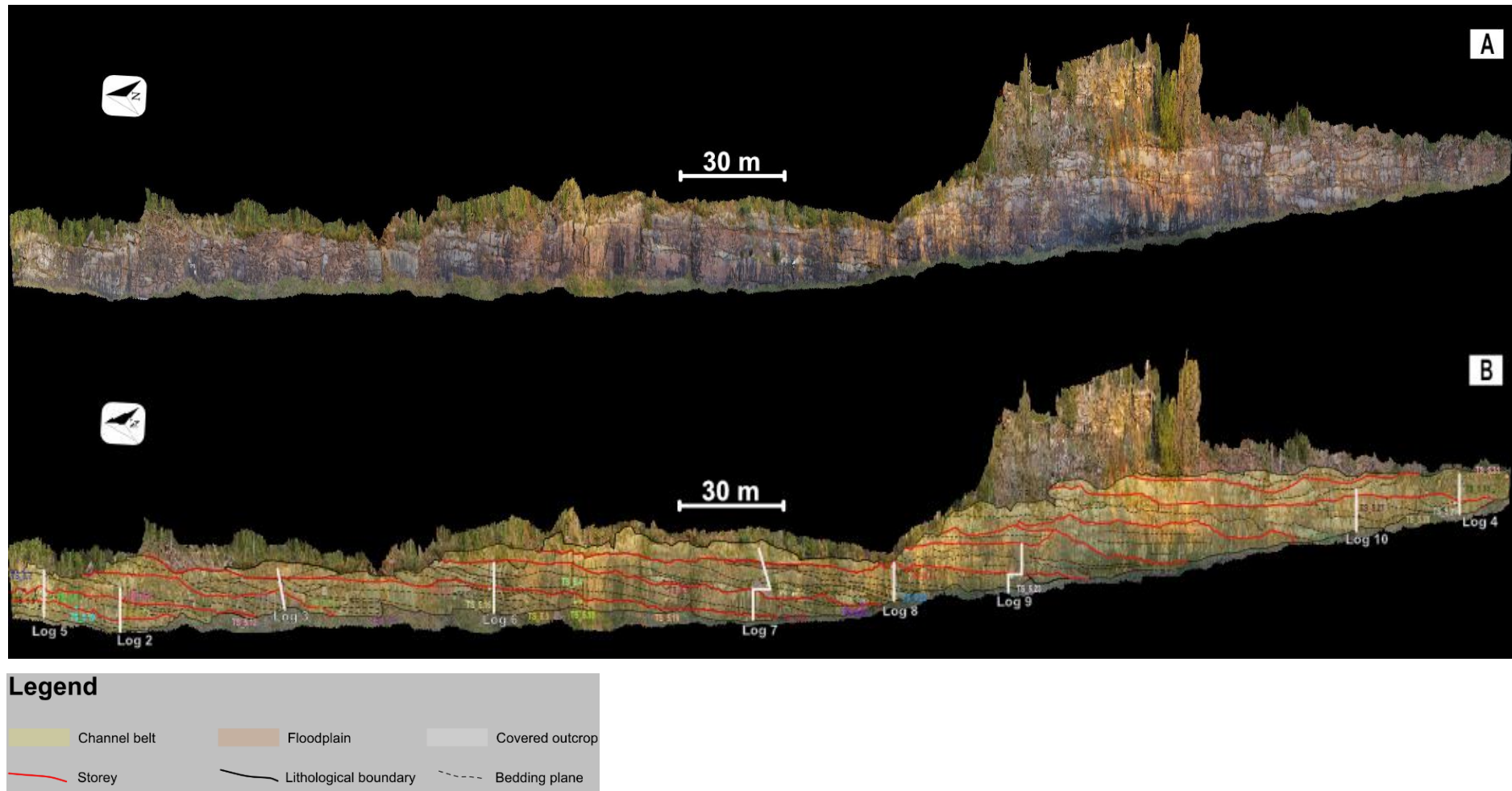
Figure 5.23. Outcrop 3 with 3x vertical exaggeration. The model is presented with A) no interpretation and B) interpretation with associated thin sections (TS) and sedimentary log locations.
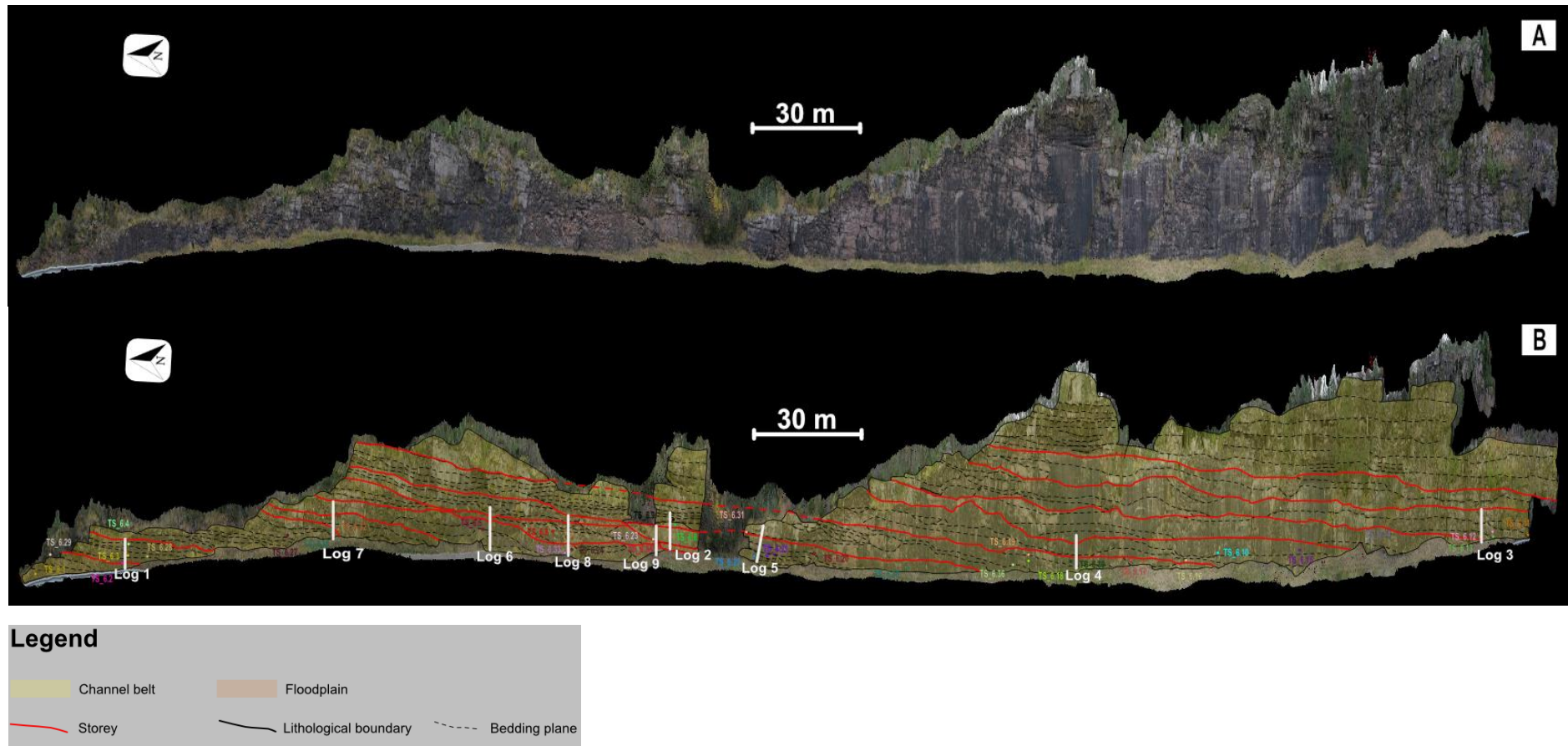
5.2.3 Outcrop 4

This outcrop is situated directly behind outcrop 2 (Fig. 1.2) and represents the Stubdal Formation (Fig. 5.24) in a restricted view horizontally and laterally, though with a closer view of the deposits in the virtual outcrop (Fig. 5.25) contrary to the other outcrops. Outcrop 4 therefore gives more details to the Stubdal Formation than what can be obtained in outcrop 2 & 3, where the thin mudstone beds, bedding surfaces and rip-up mud clasts can be accurately studied.

The outcrop consists of the channel belt-, crevasse splay and floodplain facies associations and is mostly attributed to the channel belt facies association. Storeys herein are restricted to two giving the lack of lateral extension. The two storeys are in the middle divided by floodplain mudstone beds and crevasse splay sandstone beds, likely displaying what also occurs in the deposits in the adjacent outcrop 2. Moreover, rip-up mud clasts are clearly identified in the channel belt facies association in this outcrop.

Altogether, one sedimentary log was taken at this outcrop and ten thin sections represent samples taken in the field seasons. These are listed in Appendices I-II.

Figure 5.24. Outcrop 4 in the stratigraphic record in the Ringerike area. Modified from Davies et al. (2005a).
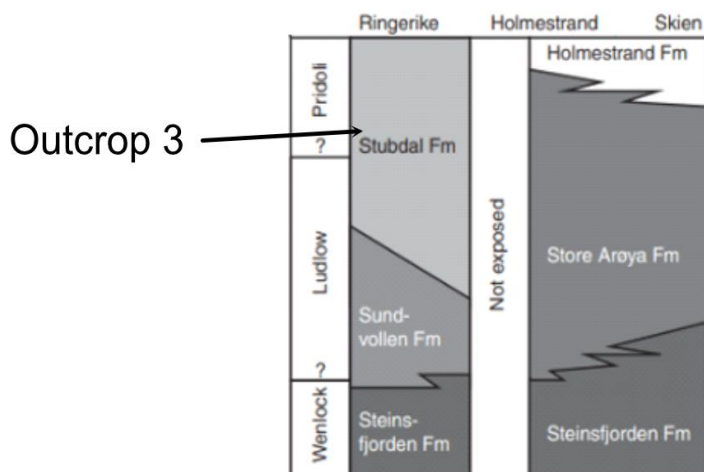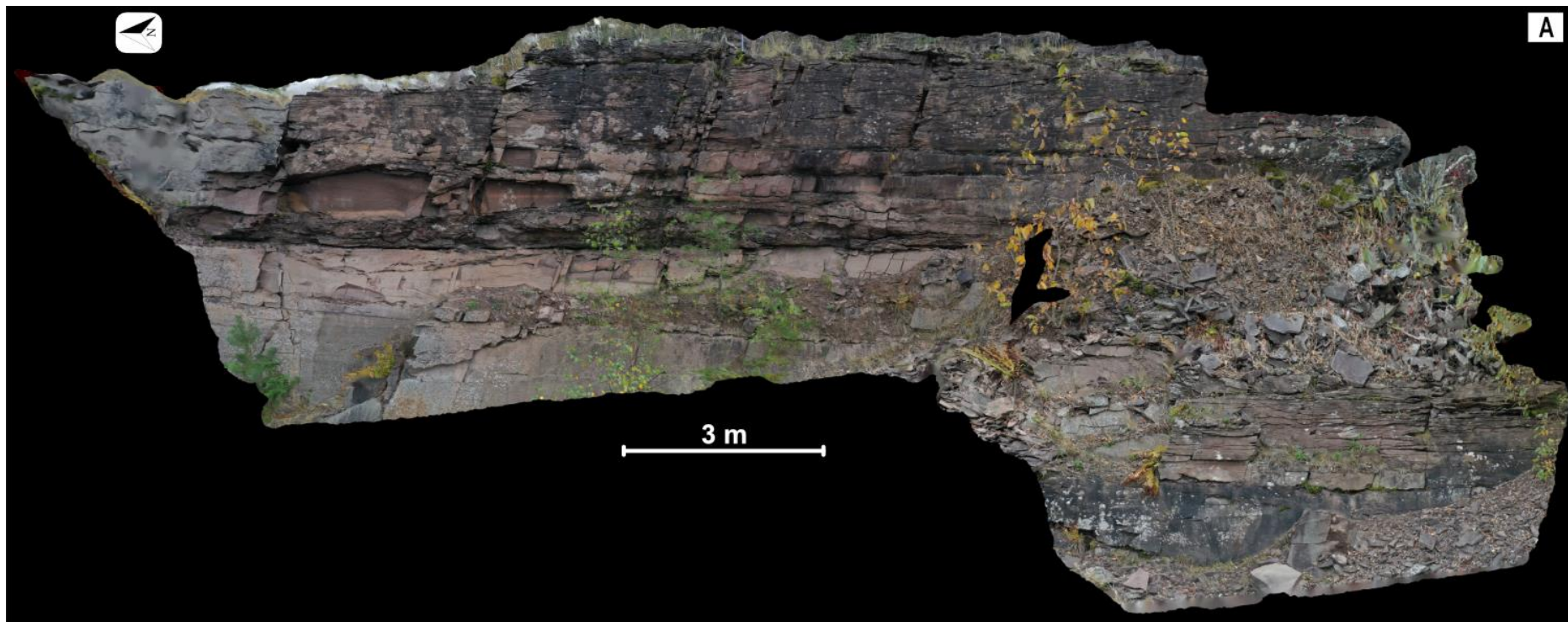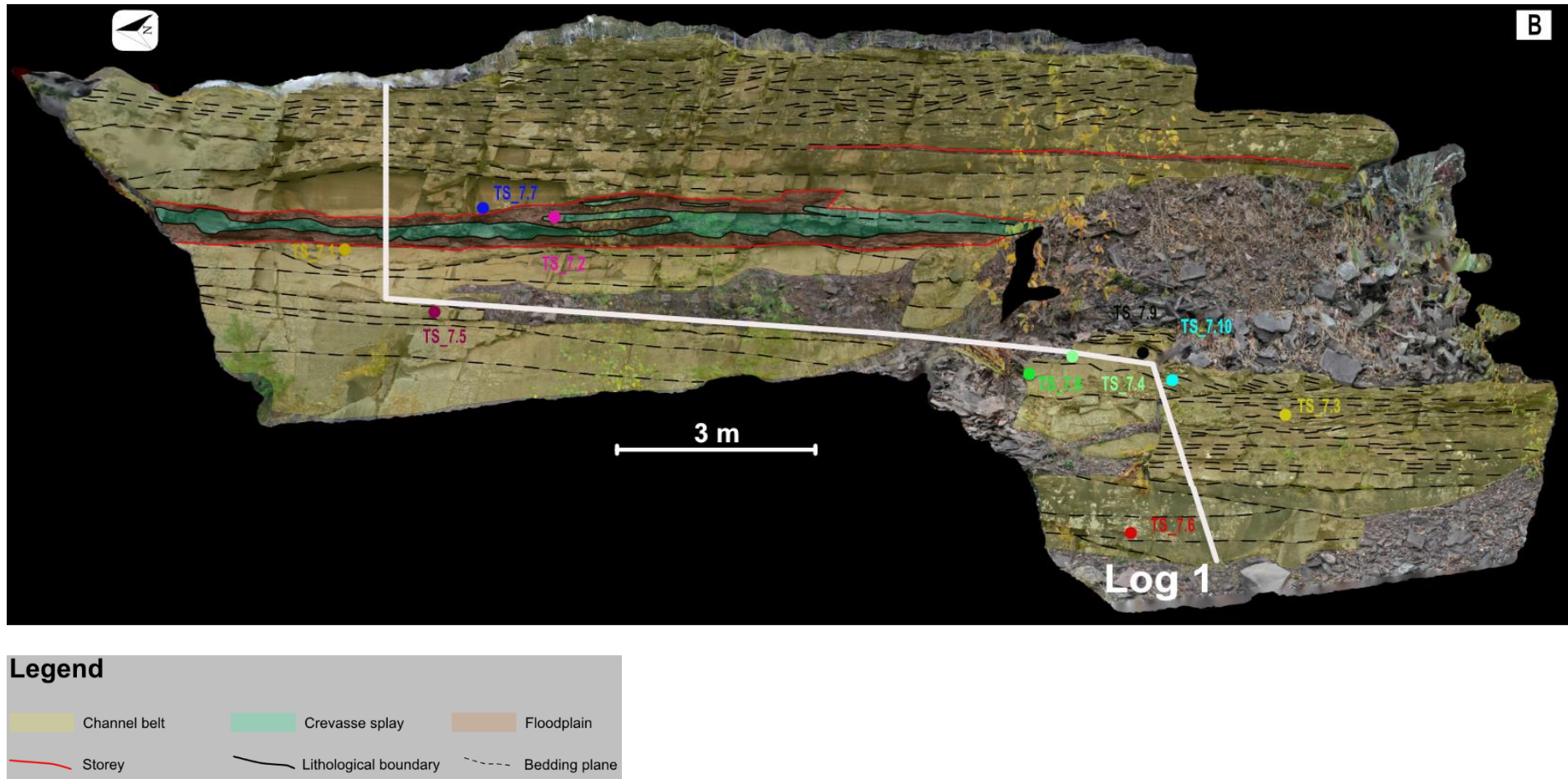
Figure 5.25. Outcrop 4. The model is presented with A) no interpretation and B) interpretation with associated thin sections (TS) and sedimentary log locations.

5.2.5 Outcrop 5

The final outcrop in the study area is the northernmost lying outcrop and is composed of the Sundvollen Formation (Fig. 5.26), situated near Rørvik Camping close to Sundvollen (Fig. 1.2). Outcrop 5 is entirely comprised of the loess facies association which is divided into five beds ranging from 0.3-3 metres in thickness while having a width of 25 metres (Fig. 5.27). The loessite can be followed throughout the Sundvollen Formation in the Ringerike area, though total width is unknown (Davies et al., 2005a). Note the massive appearance of the deposits, tabular bed boundaries and sheet-like sedimentary architecture (Fig. 5.27), clearly distinctive from the other facies associations.

Altogether, two thin sections represent samples taken in the field seasons at this outcrop. These are listed in Appendix II.

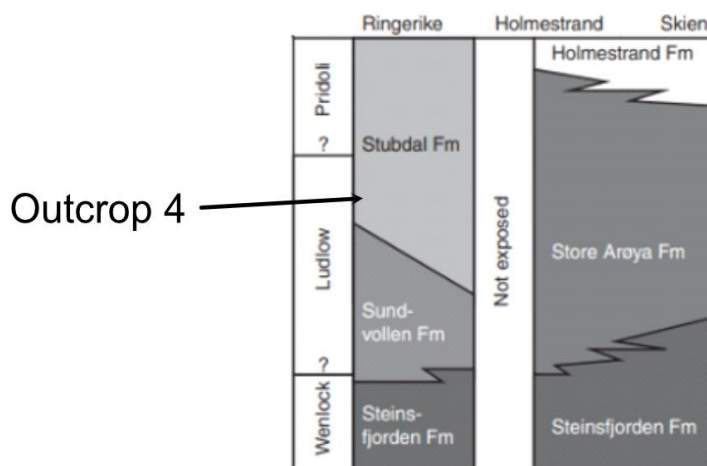**Figure 5.26.** Outcrop 3 in the stratigraphic record in the Ringerike area. Modified from Davies et al. (2005a).
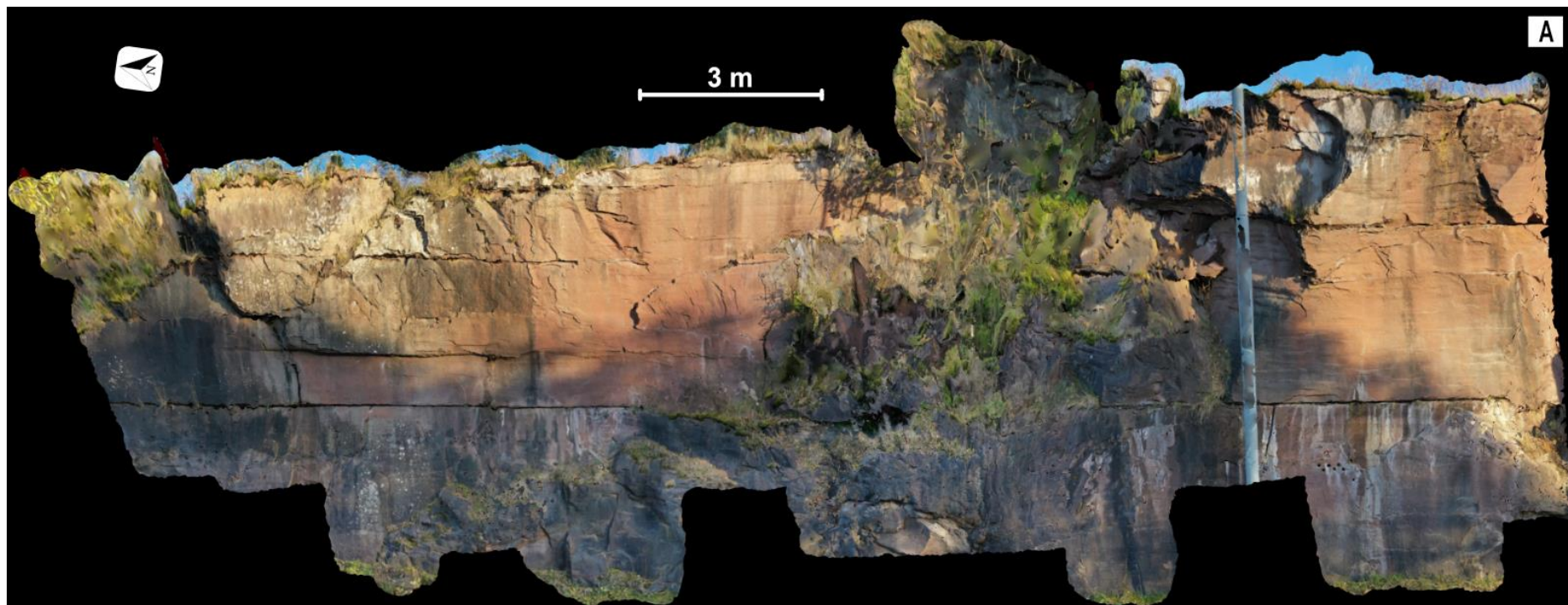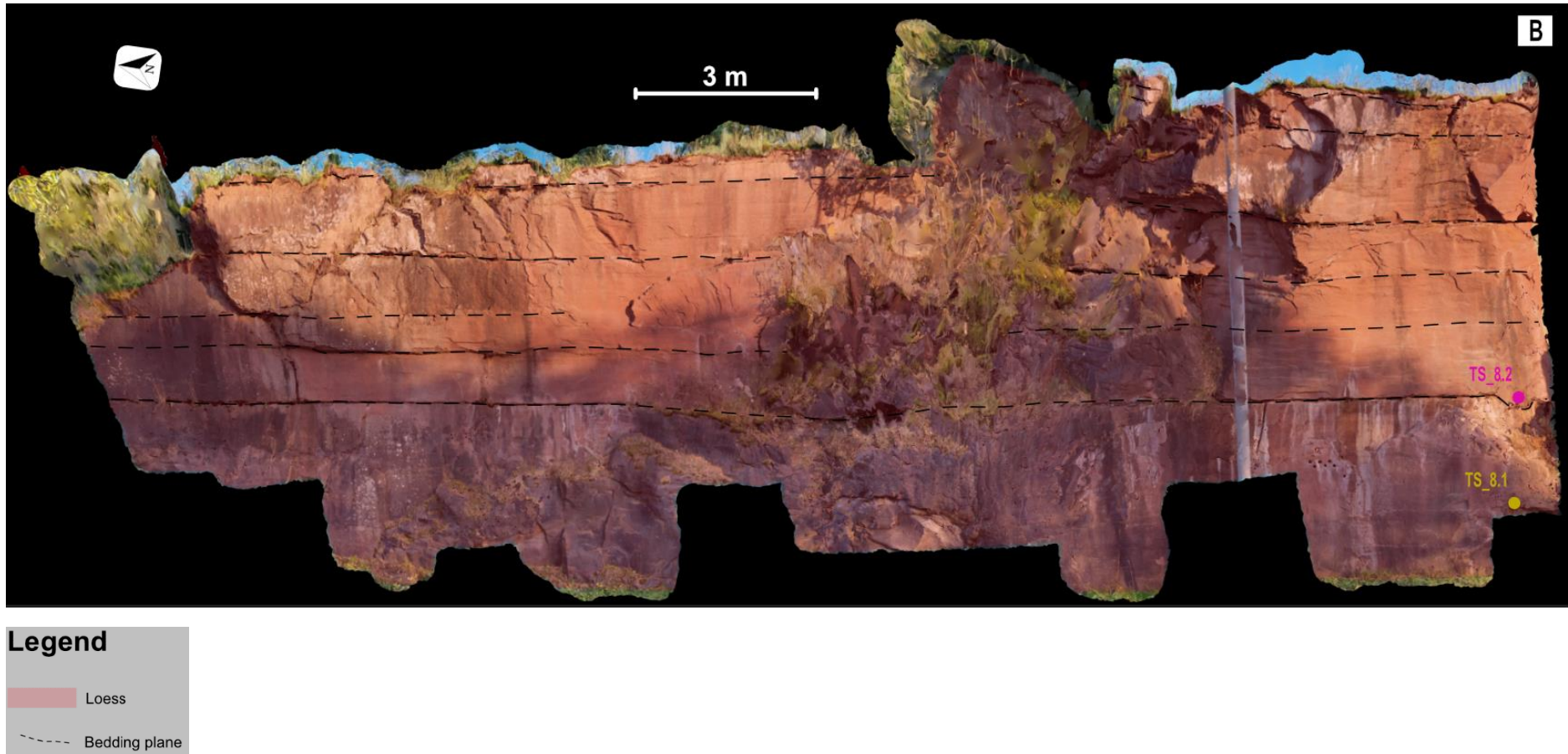
Figure 5.27. Outcrop 5. The model is presented with A) no interpretation B) interpretation with associated thin sections (TS).

5.3 Facies association distribution

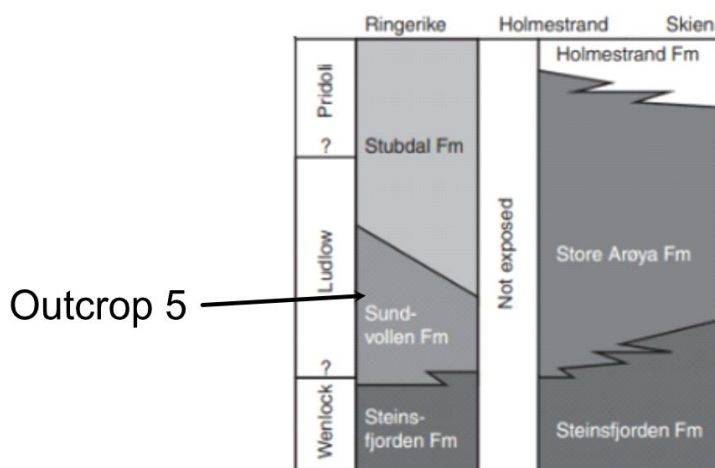The proportion of the different facies associations (Appendix III) have been determined for each of the five outcrops, by quantifying the amounts of the different facies associations on each interpreted outcrop using the ImageJ software (National Institutes of Health, u.y.) shown by the plot in Fig. 5.28.

Outcrop 1 has the most variation in facies associations, containing every recognised facies association in the study area. The abandoned channel and loess facies associations comprise ~19 % and ~17 % of outcrop 1, respectively. However, the channel belt facies association is the dominant facies association in outcrop 1, comprising ~53 % of the facies association distribution.

Contrarily, outcrops 2-3 are richer in the channel belt facies association, comprising ~ 99 % of the facies in the outcrops. Outcrop 4 is additionally rich in the channel belt facies association, comprising ~ 91 % of the facies association distribution.

Floodplain distribution is remarkably different in the outcrops, where outcrop 1 & 4 contain 5% floodplain deposits in sharp contrast to > 0,5 % in outcrops 2 & 3. Moreover, the crevasse splay distribution is also noticeably different within the outcrops, owing to a source of error as the crevasse splay architecture is not detectable in the zoomed-out version of outcrops 2-3 as presented in the model. Nevertheless, in the facies association distribution analyses, the crevasse splay facies association is absent in outcrops 2-3 whereas it comprises 6-4 % of the facies in outcrops 1 & 4. Equivalently, floodplain facies association distribution may not be accurately presented in the plots of outcrops 2-3 due to the similar issue of not detecting certain areas in the zoomed-out versions of the outcrops.

Lastly, outcrop 5 shows no differences in facies and is 100 % comprised of loess facies association.
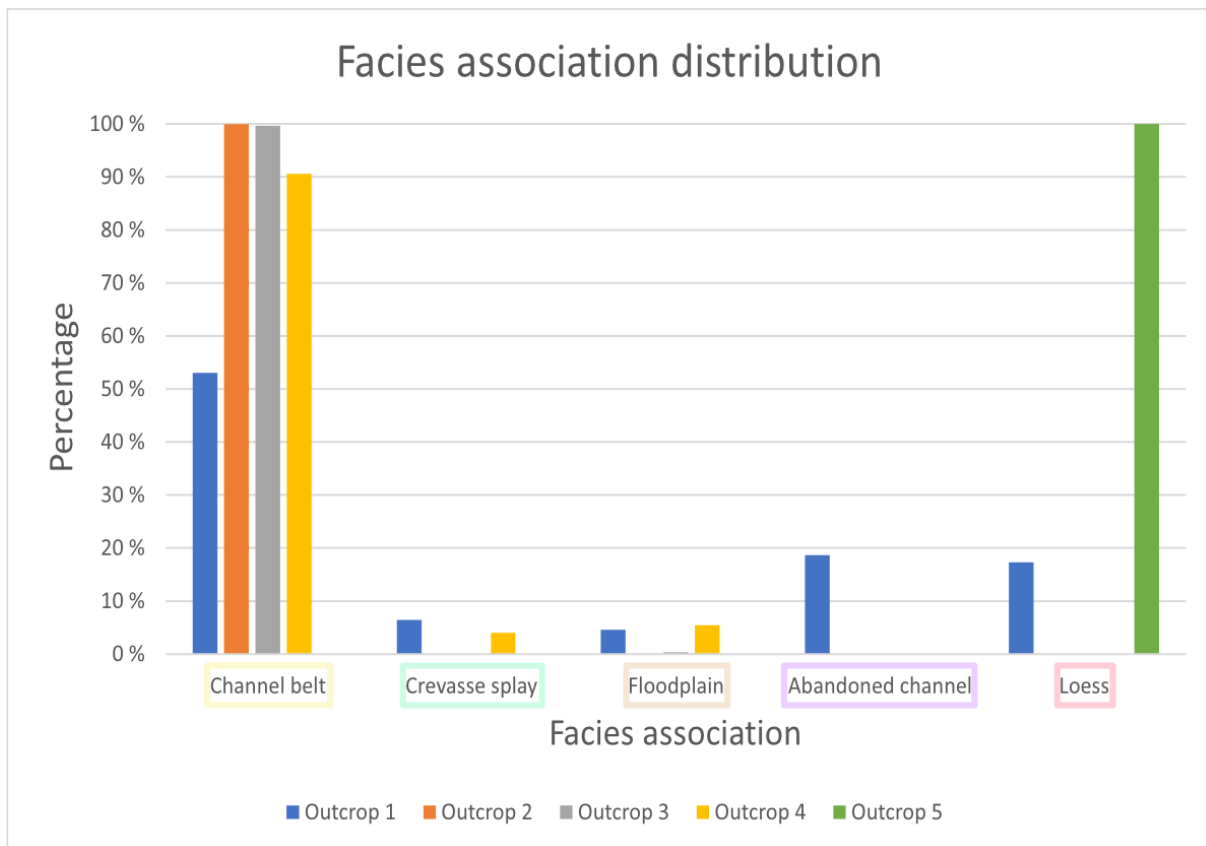
Figure 5.28. Column chart of the facies association distribution in the five outcrops in the study area. Facies associations are in the figure outlined by a coloured box corresponding to their colour in the virtual outcrop models in chapter 5.2.

6.0 Discussion

This chapter aims to discuss the results which were presented in the former chapter and what these imply for 1) the deposits in the Ringerike Group in general and fluvial style differentiation between the Sundvollen and Stubdal Formations, 2) connectivity and reservoir characterisation, 3) tectonic, climatic and vegetation influences on the deposits and 4) mineralogy of the deposits.

6.1 Ringerike Group deposits

The results show a very sandstone-rich alluvial system in the study area, with amalgamated sandstone bodies in a multi-storey complex in both the Sundvollen Formation and in the Stubdal Formation. The multi-storey sandstone deposits in the study area are most likely deposited in the proximal zone of a distributary fluvial system with amalgamated and large sandstone bodies and with minor amounts of floodplain mudstone beds in concordance with the idealised model by Nichols & Fisher (2007).

The development of the piggyback basin contemporaneous with the deposition of the Ringerike Group as argued by several authors (e.g. Halvorsen, 2003; Davies et al., 2005b; Bruton et al., 2010) is observable in the outcrops as both sedimentary structures and architectures mostly display a dipping nature. A model of the piggyback basin is shown in Fig. 6.1 where a syncline structure is interpreted for the Ringerike Group. Such an interpretation is consistent with both the relatively northerly locations of the outcrops and the nature of the deposits as explained above. However, no major metamorphosis of the Ringerike Group deposits was observed during field- and laboratory work, suggesting very mechanically competent deposits all together.
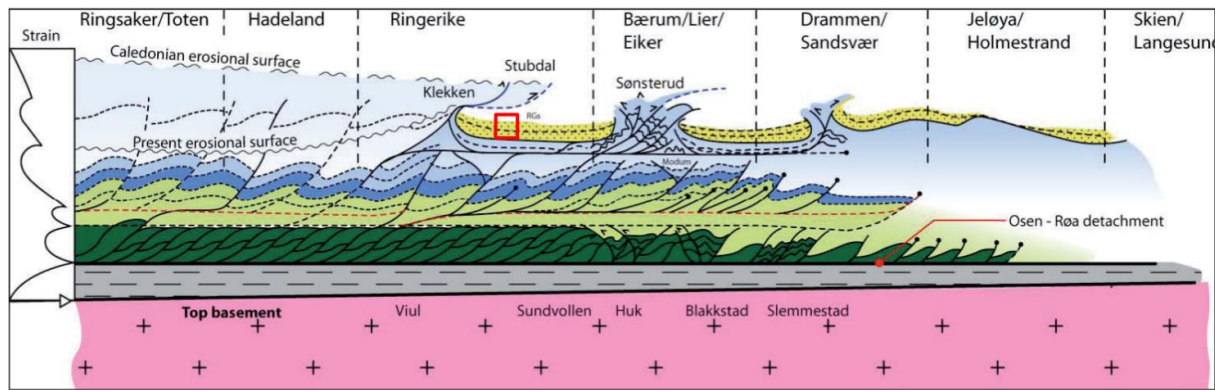
Figure 6.1. Conceptual tectonic model of the Oslo Region showing the entire Lower Palaeozoic sedimentary succession. The study area is represented by the red outlined box, displaying dipping sedimentary beds in a piggyback basin. Modified from Bruton et al. (2010).

Previous studies of the Ringerike Group (Turner, 1974a; Dam and Andreassen, 1990; Davies et al., 2005b) have suggested a northerly/north-westerly provenance of the sediments from palaeoflow measurements, in Late-Silurian times corresponding to the front of Scandinavian Caledonides within the Osen-Røa nappe complex (Nystuen, 1983). Geographical equivalent today is the southern parts of the Jotunheimen/Gudbrandsdalen areas, meaning a source area located approximately 100-120 km away from the depozones in Ringerike.

Facies and sedimentary architecture analysis in the former chapter supports the arguments presented by previous studies (Turner, 1974a;1974b; Halvorsen, 2003; Davies et al., 2005b) in which it is unequivocally believed that the sandstone deposits in the study area are of fluvial character. Moreover, there is a clear distinction between the Sundvollen Formation and the Stubdal Formation, grading upwards from the Sundvollen Formation to the Stubdal Formation somewhere between outcrop 1 and outcrop 2 (Fig. 1.2). This transition is marked by the absence of the abandoned channel and loess facies associations further south in the more sandstone-rich Stubdal Formation. Previous studies (Turner, 1974a; Worsley et al., 1983) have pointed to a shift from deposits in a meandering river environment in the Sundvollen Formation to a braided river environment in the overlying Stubdal Formation. Progradation in the foreland basin system resulting in a more proximal alluvial high energy environment in the study area where fine materials are lesser represented in the outcrops, combined with thick and laterally extensive amalgamated sandstone bodies and higher water discharges have been factors justifying an interpretation of a braided river environment.

The close view of the channel belt deposits in outcrop 4 (Fig. 6.2) display the amalgamation style well, with all the erosional truncations which are cross-cutting each other, clearly different from single channel belts with the idealised lens-shaped sedimentary architecture. Such cross-cutting in the channel belt storeys are also observed in the wider outcrops in outcrop 1-3 (Fig. 5.19, 5.21 & 5.23), however with a smaller resolution compared to outcrop 4. Channel belt deposits in all these outcrops are largely composed of the same grain sizes and sedimentary structures with limited fining-upwards trends (Appendices I-II), thus not displaying any major differences in facies and sedimentary architectures.

Moreover, outcrop 4 (Fig. 5.25) shows how crevasse splay sandstone beds and floodplain mudstone beds are also represented in the Stubdal Formation. The facies distribution in outcrops 2 & 3 (Fig. 5.28), which is composed of the same deposits in the Stubdal Formation, is thus overestimated in channel belt proportions compared to crevasse splay and floodplain proportions. Although outcrop 4 is a small outcrop, it gives valuable information on the meso-scale depositional elements in the Stubdal Formation, making the deposits in the Stubdal Formation more comparable to the more floodplain-rich Sundvollen Formation (Fig. 5.19).

Furthermore, according to the width to thickness (W/T) classification by Gibling (2006) the channel belts arranged in storeys in the Ringerike Group, which are interpreted as unconfined and mobile channel belts, are classified as narrow sheets normally ranging from W/T of 15-20 in the Sundvollen Formation and W/T of 60-70 in the Stubdal Formation. However, such W/T ratios are likely underestimated as outcrops in the study area rarely show the full architecture of the sandstone bodies.

Legend

Channel belt

Bedding plane
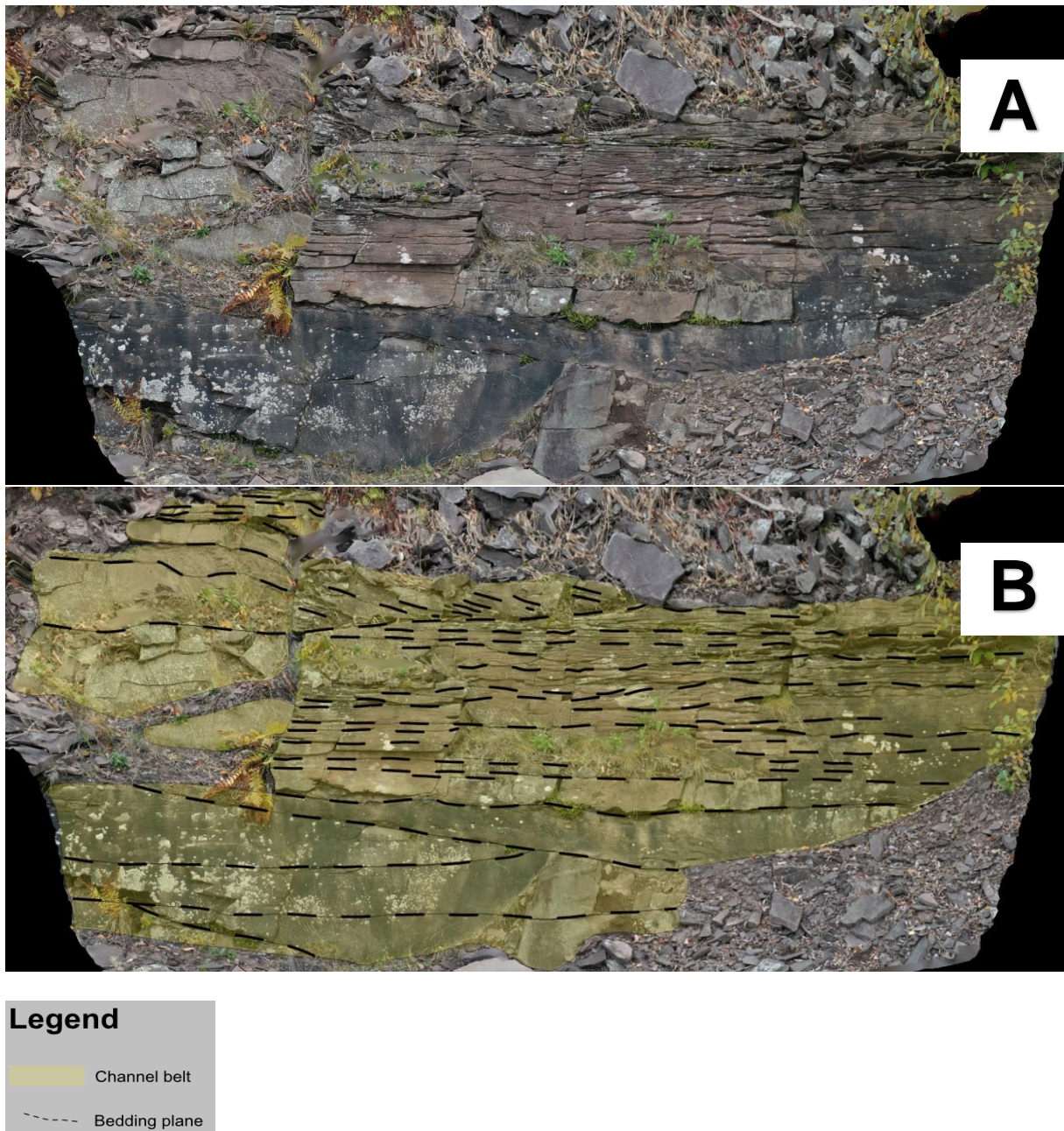
Figure 6.2. Channel belts in outcrop 4. A) Without interpretation and B) with interpretation. Note how the sandstone beds are stacked upon each other as amalgamated sandstone bodies, clearly eroding into one another.

6.1.1 Fluvial style differentiation

It should however be noted that a distinction of these fluvial styles, meandering and braided, is difficult to differentiate between in outcrops of proximal character (Hartley et al., 2015), especially with the weathered outcrops in the study area restricting identification of e.g. grain size trends and sedimentary structures. The simplest way of differentiating the fluvial styles

would be to detect point bars and the associated lateral accretion surfaces. Point bars reflect deposition by meandering rivers and outcrops containing clear point bars would pinpoint the fluvial style as meandering (e.g. Bridge, 2006). However, clearly defined point bars/lateral accretion surfaces are not clearly identified in the outcrops herein, thus making it again difficult to distinguish the sandstone deposits in the Sundvollen Formation and the Stubdal Formation.

Braid bars would be another way of differentiating the fluvial styles, which would reflect deposition by braided rivers. Though in contrast to point bars, the braid bars cannot be exactly pinpointed in outcrops as there is in contrast to point bars no single sequence of shallowing-upwards which applies for braid bar identification (e.g. Bridge, 2006). Due to the higher energy and bedload capacity commonly found in braided rivers, braid bars tend to be more gravel-rich and/or represent sandstone beds with upper flow regime sedimentary structures (e.g. Bridge & Lunt, 2006).

As there are no major differences in sedimentary structures, grain sizes and architecture in the sandstone deposits in the Sundvollen Formation at outcrop 1 (Fig. 5.19) and Stubdal Formation at outcrop 2 & 3 (Fig. 5.21 & 5.24), the distinguishments authors previously have stated about the fluvial styles between the two formations is a bit obscure. The most obvious distinction between the formations is the abandoned channel facies association which is solely present in outcrop 1 (Fig. 1.2) and the fine-grained deposits lying over the abandoned channel. These fine-grained deposits are also likely related to the avulsion of the river, depositing floodplain mudstones and loessites which at the time of deposition most likely were adjacent to the active channel as thick loessites often are deposited near (~50 km) to river channels (Li et al, 2020). The mudstone beds in the abandoned channel facies association likely points to an avulsion given the fine-grained deposits in the mud plug generated by the higher river discharges (Turner, 1974a) up towards the Stubdal Formation, as higher river discharges are acknowledged to induce avulsions of river channels (e.g. Valenza et al., 2020).

Sandstone composition in the interpreted channel belt facies association in both the Sundvollen Formation and the Stubdal Formation is virtually indistinguishable, both with a quartzarenitic composition composed of subangular-subrounded grains often accompanied by rip-up mud clasts. Moreover, grain sizes in both formations range between 0.15-0.4 mm and palaeoflow directions from Davies et al. (2005b) gives a mean vector of 168 ° in the Sundvollen Formation and 171 ° in the Stubdal Formation (Fig. 6.3), i.e. a south-easterly transport direction.
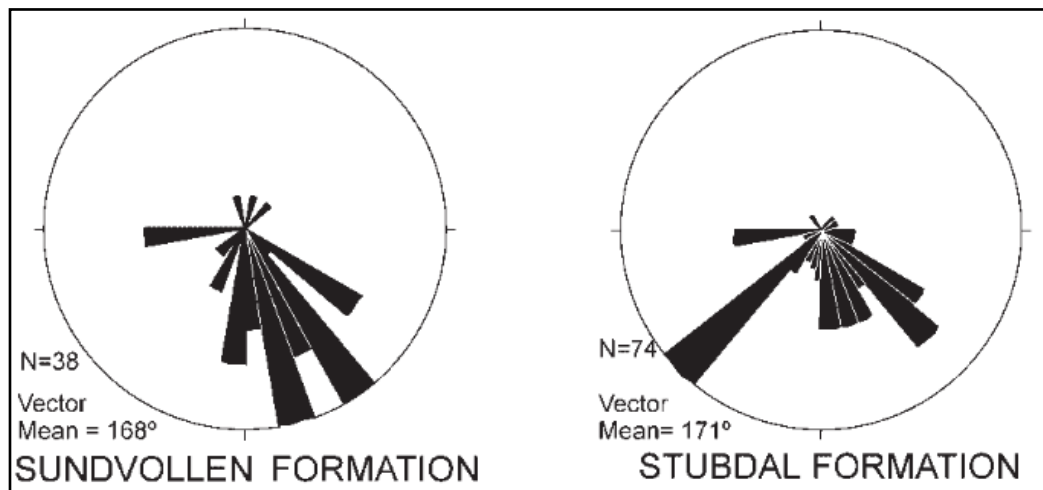
Figure 6.3. Rose diagrams showing palaeoflow directions derived from foreset dip and parting lineation measurements of the Sundvollen Formation and the Stubdal Formation, with a mean vector of 168 ° and 171 °, respectively. Modified from Davies et al. (2005b).

The rose diagrams however show palaeoflow measurements in different directions, ranging from southeast to west. These measurements indicate that axial rivers also were present during deposition of the Ringerike Group, possibly feeding into the larger DFS which constitutes the mean vector in the rose diagrams. The pronounced south-westerly trend in the Stubdal Formation suggests that axial rivers most likely were more present during the deposition of the Stubdal Formation, possibly related to the ongoing development of the piggyback basin in Ludlow-Pridoli as axial rivers are a common feature in such basins (e.g. Weismann et al., 2010; Ghinassi et al., 2014). Suriano et al. (2015) proposed a classification of an open piggyback basin with axial rivers flowing into the larger transference system. Such a piggyback basin can be inferred for the Ringerike area in Late Silurian given the mean vector of southeast palaeoflow (Fig. 6.3), with rivers likely continuing further in the foreland basin system towards the foredeep zone in the foreland basin system (Fig. 6.4).
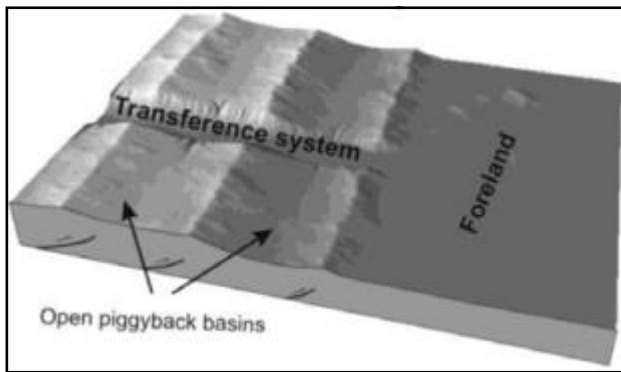
Figure 6.4. Conceptual model displaying an open piggyback basin, with rivers flowing in axial and transference systems. From Suriano et al. (2015).

Due to grain sizes being restricted as outcrops are solely represented by fine-medium grained sandstones, grain size differentiation between the two formations and believed fluvial styles is not applicable. Additionally, Bridge (2006) argues that the believed grain size differences and discharge variability between meandering and braided rivers are inaccurate, as braided rivers can contain large amounts of fines and fine sand in suspension and meandering rivers can contain coarse sand and gravel as bedload. The hypothesis that the rivers in the Stubdal Formation are braided due to the higher discharge is thus also not applicable if Bridge's rationale is followed.

However, Swan et al. (2018) address the dilemma of differentiating braided versus meandering fluvial deposits in a study of the Caineville Wash outcrop in Utah, which is comparable to the outcrops represented in this thesis. Similarly to the Ringerike Group fluvial deposits, the Caineville Wash fluvial deposits consist of amalgamated sandstone bodies with restricted grain sizes and is interpreted to be deposited in the proximal-medial part of a DFS (e.g. Owen et al., 2015; Swan et al., 2018). The sandstone beds of the Caineville Wash outcrop was formerly interpreted as representing braided river deposits (e.g. Peterson, 1978; Robinson & McCabe, 1997). On the other hand, in the study by Swan et al. (2018) arcuate point-bar planform architectures in the virtual outcrop of Caineville Wash (VOG Group, 2022) were observed, clearly indicating meandering river deposits. Sedimentary logs which were taken on the Caineville Wash outcrop consisting of stacked sandstones with no fining-upwards trend however resembled patterns commonly believed to represent typical deposits of braided river (Bridge & Lunt, 2006), in spite of the planform architectures suggesting otherwise. The authors argue that such a distinction between braided and meandering river deposits in a proximal part of a DFS with amalgamated sandstone bodies is an intricate subject as 2D interpretation of proximal fluvial deposits is complicated and can easily be misinterpreted.

Contrarily to the Caineville Wash outcrop, outcrops in the study area of Ringerike are covered by vegetation at the top, consequently restricting identification of the planform sedimentary architectural elements of the deposits. Nonetheless, the arguments by Swan et al. (2018) can be applied to the Ringerike Group, as the deposits between the two analogues is very similar. No certain conclusions can be made about the fluvial style in the Ringerike Group deposits, yet the possibility of meandering rivers depositing sediment in the Stubdal Formation and braided rivers depositing sediment in the Sundvollen Formation cannot be ruled out.

6.1.2 Loess facies association

The FA5, which is interpreted as the loess facies association, occurs only in the Sundvollen Formation represented by outcrop 1 & 5 (Fig. 1.2) and is the most uncertain of the five recognised facies associations in this thesis in regards to interpretation of the depositional environment. Deposits within this facies association is stratigraphically defined as the Dronningveien Siltstone Member as introduced by Turner (1974a). It occurs as a marker horizon between the sandstones in the channel belt facies association, overlying the Sundvollen Formation and underlying the Stubdal Formation. Lithologies in the member are restricted to siltstone and sedimentary structures are either in form of horizontal or wavy lamination.

Previous interpretation of the depositional environment is limited to Halvorsen (2003), who suggest a lacustrine origin of the Dronningveien Siltstone Member. However, it is also plausible that the siltstones represent loessite, deposited from aerosols with a possible Caledonian provenance. As a result of the arid/semi-arid palaeoclimate in the foreland basins southeast of the Caledonides (Kiipli et al., 2016), physical weathering would likely be the dominant weathering force (e.g. Van de Kamp, 2010) in the Caledonian hinterland, generating abundant dust which may have deposited loessites in the Ringerike area. Random grain fabric of subangular-subrounded poorly sorted siltstone samples, an unequivocal characteristic of loessite deposits according to Wilkins et al. (2018), combined with a typical sheet-like sedimentary architecture and lateral continuity of loessites (Johnson, 1989) is comparable with the results presented in chapter 5.1.1.5.

However, there is also evidence of aligned grain fabric in the samples, contrarily to the normal deposition of loessites grains with random grain fabric. These features are though possibly explained by pluvial reworking of loess sediments in monsoonal seasons which likely occurred in the Ringerike area in Late Silurian (Davies et al., 2005b). Nevertheless, the similarity of the

siltstone deposits in this study and the other studies mentioned above therefore suggest an interpretation of an aeolian source for the Dronningveien Siltstone Member.

Furthermore, as the Dronningveien Siltstone Member commonly occurs as thick packages of siltstones uninterrupted by other facies associations, it implies a quiescence of fluvial sedimentation most likely related to the avulsion of the ancient river channel represented by the upper abandoned channel in outcrop 1. Due to a lack of age relationships and bed contact with the loess facies association in the Sundvollen Formation and the channel belt facies association in the Stubdal Formation, a sedimentation rate of the loessites is not possible to calculate. Nevertheless, regarding that the loessites likely were eroded by the overlying channel belts, the total thickness of the loessites presumably exceeded reported (Davies et al., 2005a) thicknesses of 10-15 metres. Such large loess deposits indicate a close proximity to the source area and connected rivers (e.g. Muhs, 2007; Li et al., 2020), in this case the advancing Caledonides, further supporting the interpretation of a proximal alluvial system being represented in the Ringerike Group.

6.1.3 Depositional environment models

With reference to the former chapters and the discussion regarding the deposits identified in outcrops in the study area, four new depositional environment models have been constructed for the Sundvollen Formation and the Stubdal Formation. As definite conclusions have not been made on the fluvial style in the Stubdal Formation, one model is showing a meandering river style whereas the other model shows a braided river style for both the Sundvollen Formation and the Stubdal Formation in the depositional environment models (Fig. 6.5 & 6.6). The models are confined to the study area of Ringerike and only represent the results discussed in this thesis, meaning the marginal marine deposits of the Sundvollen Formation are not included. Furthermore, the models depict the depositional environment contemporaneous with the development of the piggyback basin, represented by the topographic high (source of sediments) and thrust movements in the north and the depozones further south (Fig. 6.5 & 6.6). Note how in contrast to the model of the Sundvollen Formation, the model of the Stubdal Formation has a topographic high further south in response to the south/south-easterly tectonic transport of the piggyback basin (Bruton et al., 2010). The deposits in the subsurface are in reference to the architectural style shown in outcrops combined with the facies associations recognized in the Sundvollen and Stubdal Formations in chapter 5.

6.1.3.1 Sundvollen Formation

The Sundvollen Formation of Wenlock-Ludlow age is in the depositional environment models (Fig. 6.5A & 6.6A) represented by the depositional agents which controlled the deposition of the facies associations recognised in chapter 5.1. Due to the amalgamation of the channel belts and the variation of palaeoflow directions (Fig. 6.3), it is likely that the meandering river contemporaneous with deposition of the Sundvollen Formation avulsed frequently or that braided rivers (with the yellow braid bars in Fig. 6.6) spread throughout the floodplain. In the model, the blue river is the last active river in the study area when depositing the Sundvollen Formation, while the grey rivers with represent the former active river channels. Additionally, the crevasse splay deposits in the Sundvollen Formation are represented by the yellow lobes connected to the river channel, splaying out into the floodplain. The stacking of these crevasse splay deposits in outcrop 1 (Fig. 5.19) indicates river floods were frequent during deposition of the Sundvollen Formation.

Moreover, the mudstone beds in the floodplain facies association and the loessite beds in the loess facies association are represented by the green and beige colours, respectively. The laterally extensive and thick loessite beds in the Sundvollen Formation suggest weathering was strong in the Caledonian orogen, depositing aerosols over a wide area throughout Ringerike with the black arrows pointing to the wind directions toward the depozone in the piggyback basin. These aerosols are depicted by the beige circles which were likely deposited by aeolian forces in the southerly adjacent piggyback basin. The floodplain deposits make up the rest of the depozones in the piggyback basin, however such deposits are scarce in the outcrops due to the erosion caused by the channel belt sandstone bodies.

The deposits in the subsurface representing the Sundvollen Formation may show how the deposits were arranged in the study area shortly after deposition, thus not reflecting post-Caledonian tectonism.

6.1.3.2 Stubdal Formation

The Stubdal Formation of Ludlow-Pridoli age is in the depositional environment models (Fig. 6.5B and 6.6B) represented by the depositional agents which controlled the deposition of the facies associations recognised in chapter 5.1. The depositional environment in the Stubdal Formation is similar to the depositional environment in the Sundvollen Formation (Fig. 6.5A & 6.6A) though without the loess and abandoned channels. However, the palaeoflow directions (Fig. 6.3) points to the presence of an axial river in combination with the transference DFS, displayed by the rivers flowing east-west in the depositional environment models. Moreover, the crevasse splay and floodplain facies associations are similarly to the Sundvollen Formation present in the Stubdal Formation, also displayed by the yellow lobes and green colour in the models under. The absence of abandoned channel and loess facies associations in the outcrops suggest that these were simply eroded away and thus not observed. On the other hand, the mean wind direction could have changed, depositing the thick loess deposits elsewhere.

The deposits in the subsurface representing the Sundvollen Formation and the Stubdal Formation may show how the deposits were arranged in the study area shortly after deposition, thus not reflecting post-Caledonian tectonism.
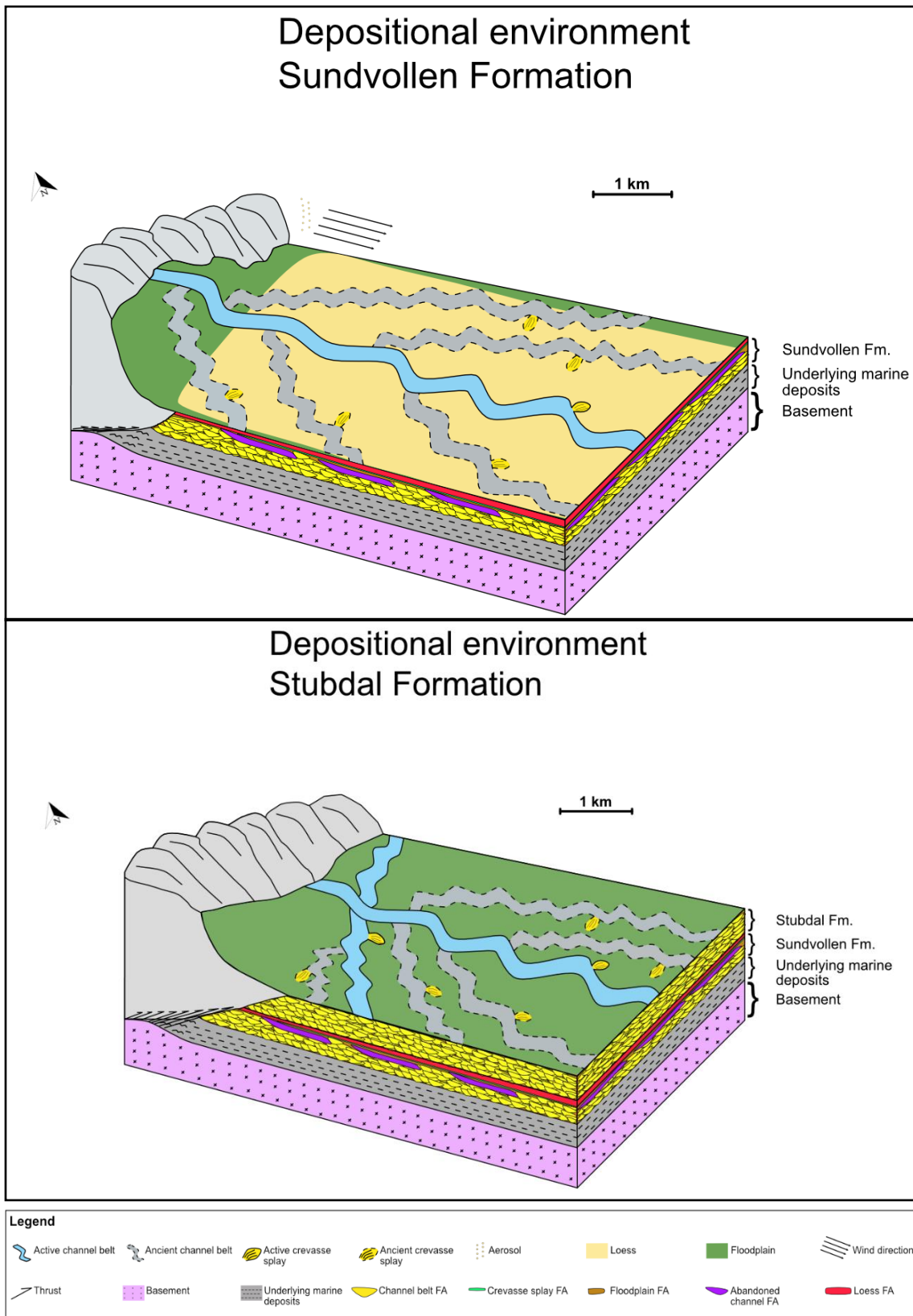
Figure 6.5. Conceptual depositional environment models of A) the Sundvollen Formation and B) the Stubdal Formation with meandering rivers. Active channel belts and crevasse splays are attributed to the last active river channels at the time of deposition.
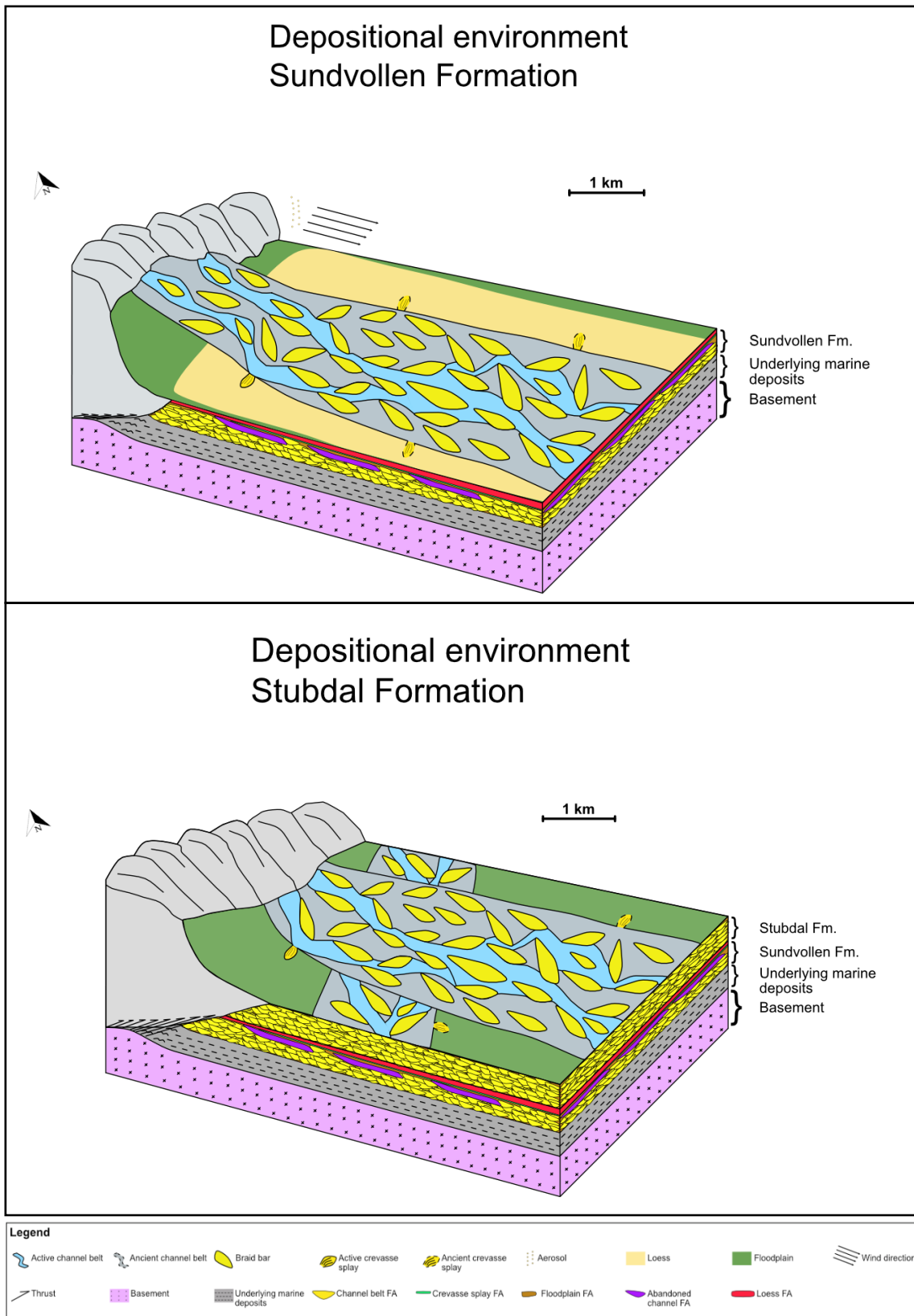
Figure 6.6. Conceptual depositional environment models of A) the Sundvollen Formation and B) the Stubdal Formation with braided rivers. Active channel belts and crevasse splays are attributed to the last active river channels at the time of deposition.

6.2 Connectivity within the outcrops

The results from the facies distribution plots show outcrops which are highly sandstone-rich, except the siltstone abundant outcrop 5 (Fig. 5.27). Outcrop 1 with a sandstone content of 60 % contain the least amount of sandstones whereas outcrop 2 & 3 and outcrop 4 with a sandstone content of ~ 99 % and 95 % contain the most amount of sandstone beds. Disregarding the cemented nature of the sandstone beds in the channel belt and crevasse splay FA due to compaction and deep burial and rather assume all sandstone beds in this analogue have good reservoir properties (i.e. porosity and permeability), net to gross (N/G) can be calculated for each of outcrops 1-4, as shown in Table 6.1. However, as explained in chapter 5.3, these facies distribution plots have inaccurate mudstone values and N/G should therefore be regarded as slightly overestimated if the thin mudstone layers in between channel belts are accounted for.

Table 6.1. Net to gross values of outcrops 1-4.

Outcrop	Sandstone (percentage)	Mudstone (percentage)	Net to gross
1 – Sundvollen Formation	60	40	0.6
2 – Stubdal Formation	~ 99	0.03	0.99
3 – Stubdal Formation	~ 99	0.4	0.99
4 – Stubdal Formation	95	5	0.95

N/G values in the outcrops 2-4 are as shown in Table 6.1 exceptional, with N/G close to 1 whereas outcrop 1 have a slightly worse yet satisfactory N/G of 0.61.

While the N/G values of the outcrops are good qualities for a reservoir, it is additionally crucial to review the architecture of the deposits in order to examine their reservoir qualities. The channel belt deposits are predominantly laterally extensive and amalgamated in the outcrops, thus connecting well from sandstone body to sandstone body. Additionally, the identified crevasse splays are interpreted as pinching out in the channel belts and though not surrounded by mudstone beds in the floodplain or abandoned channel facies associations, helping connectivity as the intercalated mudstones most likely act as fluid baffles in the fluvial system, as mudstones typically do in fluvial reservoirs (e.g. Miall, 1993; Robinson & McCabe, 1997; Pranter et al., 2007).

On the other hand, the thin mudstones in between sand bodies could possibly also affect the connectivity in a negative way. As some of the sandstone bodies were not possible to examine closely in the field due to being located high up on the outcrops, the amount of 1-5 cm thin mudstone drape beds in between sandstone bodies are uncertain. An estimated average of 80-90 % thin mudstone layers between the sandstone bodies in the outcrops can however be established from studying the drone images and virtual outcrops. These thin mudstone layers are likely formed from either 1) waning flow conditions in the river flow, when peak flooding has passed and suspended material were deposited in between the former and next peak flooding (Davies et al., 2005b) or 2) simply a thin and likely short-lived floodplain environment in between the channel belt deposits.

How the actual connectivity within the sandstones in the deposits would be, with the uncertain amounts of mudstone beds, is unfortunately difficult to tell. Mudstone drape deposits and their effect on fluid flow could be great, as these mudstone drapes potentially can act as fluid flow baffles (Willis et al., 2018). The mudstone drapes will however in the study area likely be laterally impersistent in the outcrops as the amalgamated channel belts often erode into one another, thus connecting the sandstone bodies without the interruption of mudstone baffles. Moreover, subsidence in the Ringerike area in the Late Silurian was according to Bjørlykke (1983) relatively high, and sediment flux must therefore also have been high in order to retain a progradation (e.g. Catuneanu et al., 2011) which transpired throughout the Oslo region in the Late Silurian (Worsley et al., 1983), and which is reflected in the over 1000 m thick Ringerike Group deposits (Fig. 2.3). A rapid aggradation with stacked sandstone bodies rather than amalgamated sandstone bodies would therefore might be inferred to represent the sandstones in the Ringerike Group. However, the very erosional style of the channel belts in the Ringerike Group deposits points to amalgamation of the sandstone bodies which as argued by Willis et al. (2018) would significantly enhance connectivity as coarser grained lag deposits and sandstone channel belts are superimposed to one another. The restricted grain size distribution in the channel belts in the Sundvollen and Stubdal Formations would not benefit too much from the amalgamation effect on connectivity as only fine-medium-grained sandstone bodies are present with no extraformational conglomerates. However, similar proximal fluvial deposits with coarse-grained lag deposits certainly would have enhanced connectivity. Everything considered, it can be assumed that the connectivity between each of the individual sandstone bodies is good as N/G is excellent, and that fluid flow within the amalgamated sandstone bodies in the Ringerike Group would have no major baffles.

6.3 Palaeoclimate influences

The presence of plane-parallel stratification, cross-bedding and rip-up mud clasts with amalgamated sandstone bodies suggest that the fluvial sandstone bodies were deposited in a high energy environment, supporting that deposition took place in the proximal zone. However, the absence of coarse-grained sediments is contradictory to the idealised model by Nichols & Fisher (2007), as thin section analyses only reveal fine-medium grained sandstones. The absence of the coarse grains may be due several reasons. Tectonic controls on river discharge and denudation (Gorsline, 1984), low river competences (e.g. Baker & Ritter, 1975) and a source of fine-grained deposits such as aeolian strata being eroded (e.g. Rittersbacher et al., 2014) are for example some of the factors which may explain the solely fine-medium grained sandstone deposits.

Moreover, as Ringerike in Late Silurian was located in the subequatorial zone (Torsvik & Cocks, 2013), it is not clear whether the rivers were perennial or ephemeral giving the semi-arid/arid palaeoclimate. Davies et al. (2005b) suggest an ephemeral river style due to the high surface temperature and monsoonal conditions at the time of deposition (Budyko et al., 1987; Love & Williams, 2000) combined with the presence of angular rip-up mud clasts, where these rip-up mud clasts were easily entrained into the stream due to a lack of vegetation making riverbanks less stable. The angular rip-up mud clasts would thus reflect short transportation. Furthermore, Dam & Andreassen (1990) also argues ephemeral streams in the form of hyperconcentrated flows were present in the Ringerike Group, pointing to the presence of massive sandstone bodies and upper flow regime sedimentary structures in the more southerly Holmestrand Formation. Such massive sandstone bodies and upper flow regime sedimentary structures have also been recognised in the Sundvollen and Stubdal Formations, represented in sedimentary logs in Appendix I. Ephemeral streams existing concurrent with the deposition of the Ringerike Group in the Ringerike area is therefore highly likely.

6.4 Vegetation influences

Thin sections of floodplain and abandoned channel facies associations in chapter 5.1 most likely show evidence of vegetation, represented by what appears to be a rootlet and rhizocretions (Fig. 5.11 & 5.12). The depositional environment of these facies associations are in contact with subaerial agents and thus susceptible to vegetation as running water in the form of streams are rarely present. These thin sections are sampled from the Sundvollen Formation, which deposited alluvial sediments in Wenlock-Ludlow, and vegetation structures herein are attributed to vegetation stage 4 defined by Davies & Gibling (2010). The vegetation stages are divided from 0-6 where stages 0-1 are defined as pre-vegetational in the Proterozoic, stage 2 is defined by the earliest development of terrestrial vegetation in Cambrian-Middle Ordovician strata, stage 3 is defined by simple terrestrial plant signatures in Early Silurian strata, stage 4 is defined by more advanced vascular terrestrial plants in Late Silurian strata and stages 5-6 are defined by even more advanced and developed vegetation signatures in post-Silurian times. The complexity of the rhizocretions identified in chapter 5.1.2.3 is concurrent with the assertion made by the authors in vegetation stage 4 where advanced vascular land plants started to develop as well as being identified in Late Silurian strata. Such vegetation influences may therefore have been pivotal to the existence of meandering rivers in the Late Silurian, as the root systems identified in the results likely aided with stabilising the riverbanks (e.g. Abernethy & Rutherfurd, 2001).

However, there is some dispute to the effect vegetation has on stabilizing riverbanks. Bridge (2006) argues that vegetation has little effect on bank stability and channel pattern whereas Davies & Gibling (2010) refute this argument. It should on the other hand be noted that the existence of meandering rivers has been proved back to the Neoproterozoic when vegetation was not yet developed (McMahon & Davies, 2018), in conflict with previous studies pointing to a shift from strictly braided to more meandering fluvial styles in the Late Silurian-Early Devonian (Gibling & Davies, 2010; Gibling & Davies, 2014). The effect vegetation had on riverbank stability may therefore still be equivocal in the Ringerike Group channel belts and Palaeozoic fluvial deposits in general.

6.5 Tectonic influences

Additional important aspects to discuss are the tectonic influences on the Ringerike Group. Generally, there are not many evidences of tectonism in the study area, however there is one distinct fault which is found in outcrop 1 (Fig. 5.19) in the Sundvollen Formation. As the fault contact is unfortunately concealed due to a break in the outcrop, it is not possible to state the fault type. The deposits may have been affected by tectonics at time of deposition (syn-tectonic sedimentation) or after deposition. The Ringerike Group is believed to be deposited in a piggyback basin as the Sundvollen and Stubdal Formations exhibit a syncline geometry with low-dipping angles (Bruton et al., 2010), and a reverse fault related to the compressional events during the Caledonian orogeny is a possible causation for the fault. However, the later extensional events both during the Devonian collapse of the Caledonides (Andersen, 1998; Fossen, 2000) and during the rifting in Permian caused by the Variscan orogeny forming the Oslo Graben may have affected the study area after deposition.

A normal fault in the identified fault in outcrop 1 (Fig. 5.19) may however be plausible. According to the Geological Survey of Norway (2022a), there is no fault registered in outcrop 1 and adjacent faults are depicted as unknown (Fig. 6.5). Yet on the other hand, the observed fault may be a continuation of the fault stretching through the overlying Krokskogen lava plateau and down into the Ringerike Group. As the fault then would stretch both through the Late Carboniferous-Permian volcanic rocks and the Silurian Ringerike Group, it must be post-Caledonian and most likely a normal fault.
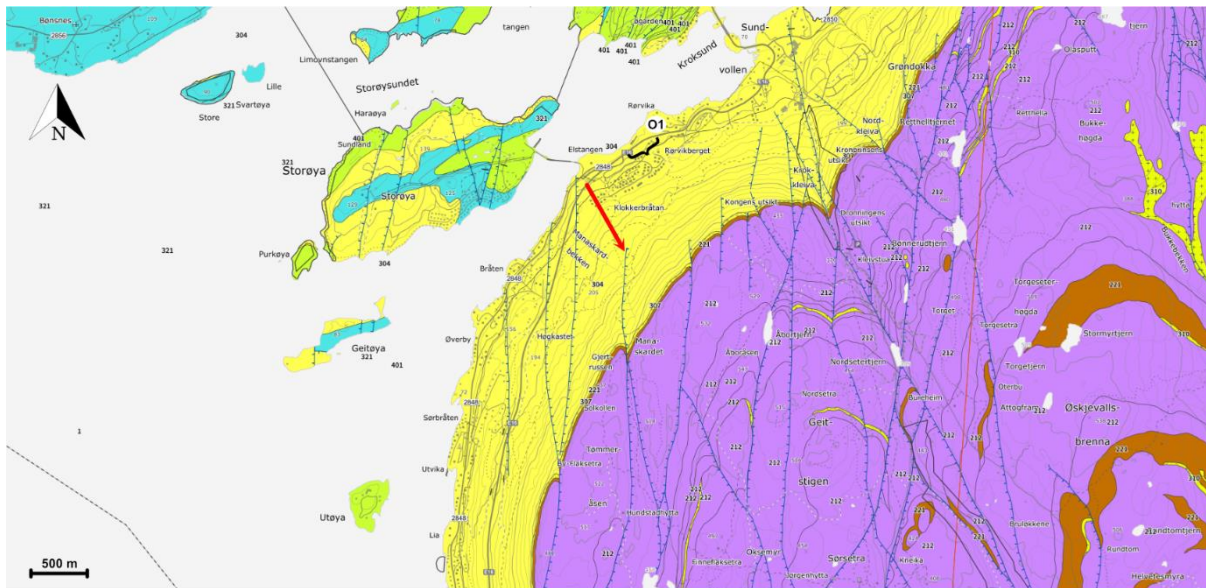
Figure 6.7. Bedrock map of Hole municipality, where the length and occurrence of outcrop 1 (O1 on map) is marked by the black curly brace. A possible link to the fault identified in outcrop 1 can be to trace the fault marked by the red arrow down to the outcrop. Ringerike Group is shown by the yellow colour on the eastern side of Tyrifjorden beneath the Late Carboniferous-Permian rhomb porphyrys (purple), basalts (dark orange) and breccias (light yellow). Shales (lime green), sandstones (yellow) and limestone (turquoise) in the Hole and Bærum Groups underlying the Ringerike Group lie in or on the northern/western side of Tyrifjorden, respectively. Fault symbols are furthermore defined as unknown in the fault styles. Modified from the Geological Survey of Norway (2022a).

6.6 Mineralogy

Moreover, the mineralogy in the collected samples from the Ringerike Group is worth mentioning. Apart from the quartz and feldspar grains, common accessory minerals include (though are not limited to) chlorite, natrolite and fluorite (Appendix II). These minerals are common in relation to hydrothermal veins and magmatic activity (Sheard et al., 2012), possibly either due to magmatic activity pre-, syn- or post-deposition of the Ringerike Group. According to Turner & Whitaker (1976), the radial-shaped natrolite is present as cement, thus implying a post-depositional nature. Moreover, they claim chlorite is present both as cement and as individual grains, with a possible provenance of sparagmites in Valdres and ultramafic/mafic rocks in the Jotun nappes. A lack of other modern and similar petrology studies of the Ringerike Group makes it somewhat difficult to discuss the provenance of these accessory minerals. However, other possible provenances of the chlorites may be due to weathering of clay minerals in the sandstones and low-grade metamorphosis of the Ringerike Group. The frequently

deformed nature of the chlorite grains in the thin sections (Fig. 6.8) might suggest a pre- or syndepositional source and hence eliminate a post-depositional source.
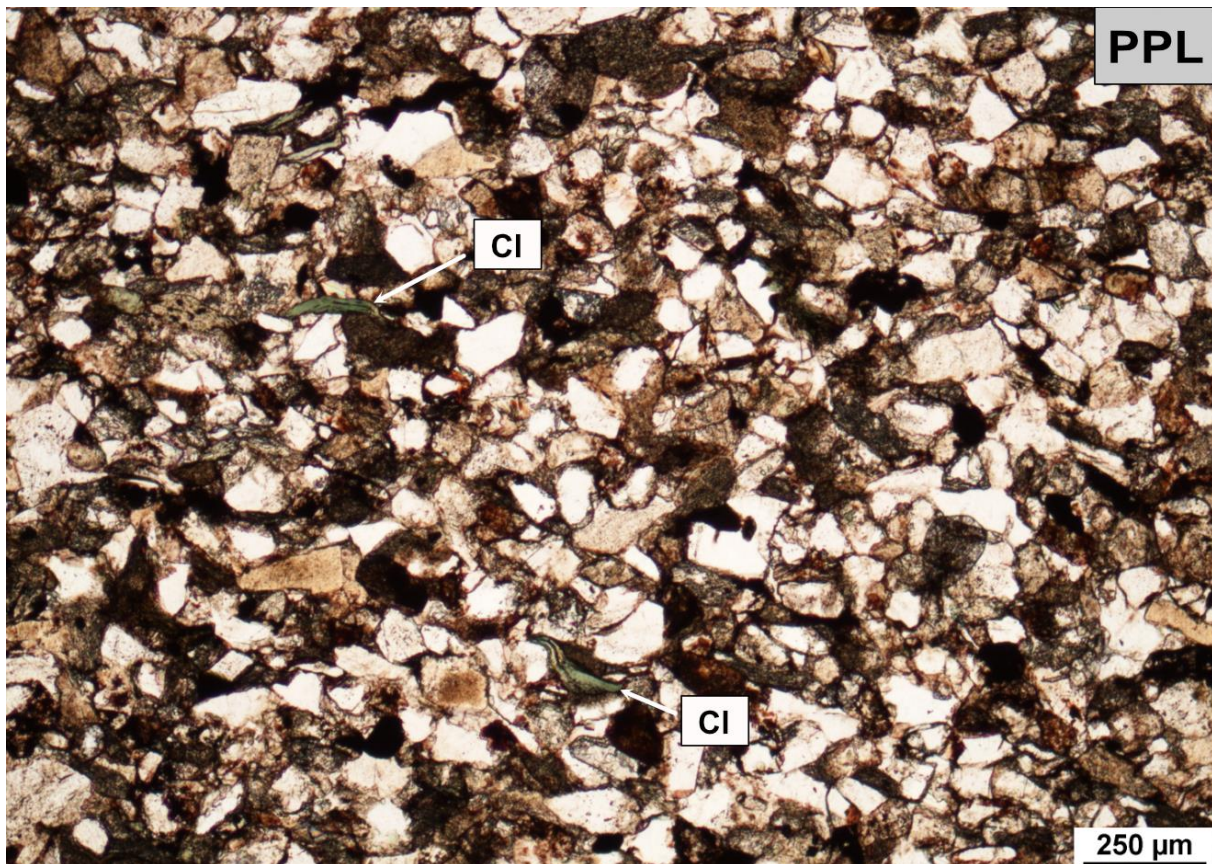
Figure 6.8. Thin section 2.15 showing deformed chlorite grains in a channel belt sample.

The occurrence of fluorite has on the other hand not been discussed previously. Fluorite is common in hydrothermal veins (e.g. Sheard et al., 2012), and the fluorite crystal may be formed after burial of the sandstones. Moreover, opaque minerals have also been identified and blackish coatings are often present in the thin sections. These opaques and coatings are linked to the formation of heavy iron minerals such as hematite, ilmenite and chromite post-depositionally (Turner, 1974a; Turner & Whitaker, 1976).

7.0 Conclusions

In this thesis, the Ringerike Group of Eastern, Norway have been studied by investigating virtual outcrops combined with field work and microscopy. Results from the study and subsequent discussion gives the following conclusions about the alluvial deposits:

- Facies associations in the Ringerike Group in the study area are unequivocally of alluvial character and comprise channel belt-, crevasse splay-, floodplain-, abandoned channel- and loess facies associations from which the Sundvollen Formation contain all of these whereas the Stubdal Formation is restricted to channel belt-, crevasse splay- and floodplain facies associations. The highest proportion of the facies association in both formations is attributed to the channel belt facies association.

- The channel belt deposits in the Sundvollen Formation and the Stubdal Formation are not very different in facies and sedimentary architecture analyses, however no certain conclusions can be made about the fluvial style in the Ringerike Group channel belt deposits.

- The fluvial deposits in the Ringerike Group would likely act as an excellent reservoir with good connectivity and high N/G. The mudstone baffles would most likely not act as baffles to fluid flow regarding the amalgamation of the sandstone bodies which enhances connectivity.

- Channel belt and loess deposits points to an arid/semi-arid palaeoenvironment in which physical weathering likely was dominant and where ephemeral streams likely were present with powerful flow indicated by massive sandstone beds, upper flow regime sedimentary structures and rip-up mud clasts.

- Vegetation influences are observed in the abandoned channel facies association through rhizocretions and a rootlet, concurrent with the vegetation stage 4 in Late Silurian. However, its effect on riverbank stability and sedimentation is inconclusive.

- Tectonic influences on the Ringerike Group are observable through the southerly dipping beds on the outcrops, displaying a syncline structure which likely was generated by the formation of the piggyback basin syn-depositional. A distinct fault is also present in the Sundvollen Formation, likely formed post-depositional.

- Quartz is the most abundant mineral in thin sections, and sandstones in the channel belt facies association have a quartzarenitic composition. Minor amounts of chlorite,

natrolite, plagioclase, opaque minerals and fluorite are additionally identified. Chlorite, natrolite and fluorite are likely secondary minerals, occurring after deposition of the Ringerike Group.

8.0 Further work

This thesis has provided a new and detailed study of the facies and sedimentary architectures of the Sundvollen and Stubdal Formations. However, there are still subjects for further work about the Ringerike Group and proximal alluvial systems in general which may aid in our understanding of proximal alluvial systems.

- Planform sedimentary architectural elements are not observed in outcrops of the Ringerike Group and differentiating braided and meandering deposits is therefore a complicated task. Utilising 3D Ground-Penetrating-Radar (GPR) which would show both planform and subsurface sedimentary architectures could possibly enlighten this issue.
- Photogrammetry modelling of the largest outcrops in this study does not allow for accurate descriptions and identification of thin mudstone layers. Drone date acquisition with a higher resolution measuring these mudstone drapes or studies of other similar proximal alluvial systems analogues where such mudstone drapes can be accurately mapped may further improve our understanding of connectivity and heterogeneity in proximal fluvial systems.
- The studied outcrops are excellent analogues for subsurface, sandstone-rich fluvial deposits. Creating and flow simulating a reservoir model of these deposits, ideally constrained by 3D GPR, would provide insights into how fluids such as oil, gas, water and carbon dioxide could be managed most efficiently in such reservoirs.

References

Abernethy, B., & Rutherfurd, I. D. (2001). The distribution and strength of riparian tree roots in relation to riverbank reinforcement. *Hydrological processes*, *15*(1), 63-79.

Agisoft Metashape. (2021). *Agisoft User Manual: Professional Edition, Version 1.7*. Retrieved 01.06.2022 from: https://www.agisoft.com/pdf/metashape-pro_1_7_en.pdf

Allen, P. A., & Homewood, P. (Eds.). (2009). *Foreland basins*. John Wiley & Sons.

Amoros, C., Roux, A. L., Reygrobellet, J. L., Bravard, J. P., & Pautou, G. (1987). A method for applied ecological studies of fluvial hydrosystems. *Regulated Rivers: Research & Management*, *1*(1), 17-36.

Andersen, T. B. (1998). Extensional tectonics in the Caledonides of southern Norway, an overview. *Tectonophysics*, *285*(3-4), 333-351.

Baker, V. R., & Ritter, D. F. (1975). Competence of rivers to transport coarse bedload material. *Geological Society of America Bulletin*, *86*(7), 975-978.

Beaumont, C. (1981). Foreland basins. *Geophysical Journal International*, *65*(2), 291-329.

Belmar, O., Bruno, D., Martinez-Capel, F., Barquín, J., & Velasco, J. (2013). Effects of flow regime alteration on fluvial habitats and riparian quality in a semiarid Mediterranean basin. *Ecological Indicators*, *30*, 52-64.

Bjørlykke, K. (1983). Subsidence and tectonics in Late Precambrian and Palaeozoic sedimentary basins of southern Norway. *Geological Survey of Norway*. *380*, 159-172.

Bridge, J. S., & Lunt, I. A. (2006). Depositional models of braided rivers. In *Braided rivers: Process, deposits, ecology and management* (Vol. 36, p. 11-50). Oxford: Blackwell Publishing.

Bridge, J.S. (2006). Fluvial facies models: Recent developments. In Posamentier, H.W. & Walker, R.G (Eds.), *Facies Models Revisited* (p. 85-170). SEPM Society for Sedimentary Geology

Bruton, D. L., Gabrielsen, R. H., & Larsen, B. T. (2010). The Caledonides of the Oslo Region, Norway–stratigraphy and structural elements. *Norwegian Journal of Geology/Norsk Geologisk Forening*, *90*(3).

Buckley, S.J., Ringdal, K., Naumann, N., Dolva, B., Kurz, T.H., Howell, J.A. and Dewez, T.J., 2019. LIME: Software for 3-D visualization, interpretation, and communication of virtual geoscience models. *Geosphere*, *15*(1), 222-235.

Budyko, M. I., Ronov, A. B., & Yanshin, A. L. (1987). *History of the Earth's Atmosphere* (p. 139). Berlin: Springer-Verlag.

Burns, C. E., Mountney, N. P., Hodgson, D. M., & Colombera, L. (2017). Anatomy and dimensions of fluvial crevasse-splay deposits: Examples from the Cretaceous Castlegate Sandstone and Neslen Formation, Utah, USA. *Sedimentary Geology*, *351*, 21-35.

Carmona, N. B., Buatois, L. A., Ponce, J. J., & Mángano, M. G. (2009). Ichnology and sedimentology of a tide-influenced delta, Lower Miocene Chenque Formation, Patagonia, Argentina: trace-fossil distribution and response to environmental stresses. *Palaeogeography, Palaeoclimatology, Palaeoecology*, *273*(1-2), 75-86.

References

Catuneanu, O., Galloway, W. E., Kendall, C. G. S. C., Miall, A. D., Posamentier, H. W., Strasser, A., & Tucker, M. E. (2011). Sequence stratigraphy: methodology and nomenclature. *Newsletters on stratigraphy*, *44*(3), 173-245.

Cyples, N. N., Ielpi, A., & Dirszowsky, R. W. (2020). Planform and stratigraphic signature of proximal braided streams: remote-sensing and ground-penetrating-radar analysis of the Kicking Horse River, Canadian Rocky Mountains. *Journal of Sedimentary Research*, *90*(1), 131-149.

Dahlgren, S., & Corfu, F. (2001). Northward sediment transport from the late Carboniferous Variscan Mountains: zircon evidence from the Oslo Rift, Norway. *Journal of the Geological Society*, *158*(1), 29-36.

Dam, G., & Andreasen, F. (1990). High-energy ephemeral stream deltas; an example from the Upper Silurian Holmestrand Formation of the Oslo Region, Norway. *Sedimentary Geology*, *66*(3-4), 197-225.

Davies, N. S., Turner, P., & Sansom, I. J. (2005). A revised stratigraphy for the Ringerike Group (Upper Silurian, Oslo Region). *Norwegian Journal of Geology/Norsk Geologisk Forening*, *85*(3).

Davies, N. S., Turner, P., & Sansom, I. J. (2005). Caledonide influences on the Old Red Sandstone fluvial systems of the Oslo Region, Norway. *Geological Journal*, *40*(1), 83-101.

Davies, N. S., Sansom, I. J., & Turner, P. (2006). Trace fossils and paleoenvironments of a late Silurian marginal-marine/alluvial system: the Ringerike Group (Lower Old Red Sandstone), Oslo Region, Norway. *Palaios*, *21*(1), 46-62.

Davies, N. S., & Gibling, M. R. (2010). Cambrian to Devonian evolution of alluvial systems: the sedimentological impact of the earliest land plants. *Earth-Science Reviews*, *98*(3-4), 171-200.

DeCelles, P. G., & Giles, K. A. (1996). Foreland basin systems. *Basin research*, *8*(2), 105-123.

Dickinson, W. R. (1974). Plate tectonics and sedimentation. In *Tectonics and Sedimentation*. (Vol. 22, p. 1-27). SEPM Society for Sedimentary Geology.

DJI. (2022, May 31st). *Mavic 2: See the Bigger Picture*. Retrieved 31.05.2022 from: https://www.dji.com/no/mavic-2

do Nascimento, D. L., Batezelli, A., & Ladeira, F. S. B. (2019). The paleoecological and paleoenvironmental importance of root traces: Plant distribution and topographic significance of root patterns in Upper Cretaceous paleosols. *Catena*, *172*, 789-806.

Donselaar, M. E., Groenenberg, R. M., & Gilding, D. T. (2015). Reservoir geology and geothermal potential of the Delft Sandstone Member in the West Netherlands Basin. In *Proceedings world geothermal congress* (p. 9).

Donselaar, M. E., & Overeem, I. (2008). Connectivity of fluvial point-bar deposits: An example from the Miocene Huesca fluvial fan, Ebro Basin, Spain. *AAPG bulletin*, *92*(9), 1109-1129.

Douglass, D. N. (1988). Paleomagnetics of Ringerike Old Red Sandstone and related rocks, southern Norway: implications for pre-Carboniferous separation of Baltica and British terranes. *Tectonophysics*, *148*(1-2), 11-27.

Fielding, C. R. (2006). Upper flow regime sheets, lenses and scour fills: extending the range of architectural elements for fluvial sediment bodies. *Sedimentary Geology*, *190*(1-4), 227-240.

References

Fossen, H. (2000). Extensional tectonics in the Caledonides: Synorogenic or postorogenic?. *Tectonics*, *19*(2), 213-224.

Förster, A., Schöner, R., Förster, H. J., Norden, B., Blaschke, A. W., Luckert, J., Beutler, G., Gaupp, R. & Rhede, D. (2010). Reservoir characterization of a CO2 storage aquifer: the Upper Triassic Stuttgart Formation in the Northeast German Basin. *Marine and Petroleum Geology*, *27*(10), 2156-2172.

Ghinassi, M., Nemec, W., Aldinucci, M., Nehyba, S., Özaksoy, V., & Fidolini, F. (2014). Plan-form evolution of ancient meandering rivers reconstructed from longitudinal outcrop sections. *Sedimentology*, *61*(4), 952-977.

Ghinassi, M., D'oriano, F., Benvenuti, M., Fedi, M., & Awramik, S. (2015). Lacustrine Facies In Response To Millennial–Century-Scale Climate Changes (Lake Hayk, Northern Ethiopia). *Journal of Sedimentary Research*, *85*(4), 381-398.

Ghinassi, M., Ielpi, A., Aldinucci, M., & Fustic, M. (2016). Downstream-migrating fluvial point bars in the rock record. *Sedimentary Geology*, *334*, 66-96.

Geological Survey of Norway. (2022). *Bedrock – National bedrock database: Municipality of Hole*. Retrieved 02.05.2022 from: https://geo.ngu.no/kart/berggrunn_mobil/

Geological Survey of Norway. (2022). *Ringeriksgruppen*. Retrieved 24.05.2022 from: https://aps.ngu.no/pls/utf8/geoenhet_SokiDb.Vis_enhet?p_id=145258&p_spraak=N

Gorsline, D. S. (1984). A review of fine-grained sediment origins, characteristics, transport and deposition. *Geological Society, London, Special Publications*, *15*(1), 17-34.

Gibling, M. R. (2006). Width and thickness of fluvial channel bodies and valley fills in the geological record: a literature compilation and classification. *Journal of sedimentary Research*, *76*(5), 731-770.

Gibling, M. R., Davies, N. S., Falcon-Lang, H. J., Bashforth, A. R., DiMichele, W. A., Rygel, M. C., & Ielpi, A. (2014). Palaeozoic co-evolution of rivers and vegetation: a synthesis of current knowledge. *Proceedings of the Geologists' Association*, *125*(5-6), 524-533.

Gulliford, A. R., Flint, S. S., & Hodgson, D. M. (2017). Crevasse splay processes and deposits in an ancient distributive fluvial system: the lower Beaufort Group, South Africa. *Sedimentary Geology*, *358*, 1-18.

Halvorsen, T. (2003). *Sediment infill dynamics of a foreland basin: the Silurian Ringerike Group, Oslo Region, Norway*. [Unpublished master's thesis]. University of Oslo.

Hartley, A. J., Owen, A., Swan, A., Weissmann, G. S., Holzweber, B. I., Howell, J., ... & Scuderi, L. (2015). Recognition and importance of amalgamated sandy meander belts in the continental rock record. *Geology*, *43*(8), 679-682.

Heintz, A. (1969). New Agnaths from Ringerike Sandstone. *Skrifer Utgitt Av Det Norske Videnskapsakademi i Oslo, I. Matematisk-Naturvidenskaps Klasse. Ny Serie. 26.*

Henningsmoen, G. (1978). Sedimentary rocks associated with the Oslo region lavas. *The Oslo paleorift. A review guide to excursions. Norges Geologiske Undersøkelse Bulletin*, *337*, 17-24.

Henstra, G. A. (2018). *Geologien på Ringerike*. Koltopp Forlag.

Ingersoll, R. V. (1988). Tectonics of sedimentary basins. *Geological Society of America Bulletin*, *100*(11), 1704-1719.

References

Johnson, S. Y. (1989). Significance of loessite in the Maroon Formation (middle Pennsylvanian to lower Permian), Eagle basin, Northwest Colorado. *Journal of Sedimentary Research*, *59*(5), 782-791.

Kiipli, E., Kiipli, T., Kallaste, T., & Märss, T. (2016). Chemical weathering east and west of the emerging Caledonides in the Silurian–Early Devonian, with implications for climate. *Canadian Journal of Earth Sciences*, *53*(8), 774-780.

Kiær, J. (1908). Das Obersilur im Kristianiagebiete. *Videnskapsselskapets Skrifter i Matematisk-Naturvidenskapelig Klasse*, *7*, 1-22.

Kristoffersen, M., Andersen, T., & Andresen, A. (2014). U–Pb age and Lu–Hf signatures of detrital zircon from Palaeozoic sandstones in the Oslo Rift, Norway. *Geological Magazine*, *151*(5), 816-829.

Lang, S. C., Grech, P., Root, R., Hill, A., & Harrison, D. (2001). The application of sequence stratigraphy to exploration and reservoir development in the Cooper-Eromanga-Bowen-Surat Basin system. *The APPEA Journal*, *41*(1), 223-250.

Li, Y., Shi, W., Aydin, A., Beroya-Eitner, M. A., & Gao, G. (2020). Loess genesis and worldwide distribution. *Earth-Science Reviews*, *201*, 102-947.

Love, S. E., & Williams, B. P. (2000). Sedimentology, cyclicity and floodplain architecture in the Lower Old Red Sandstone of SW Wales. *Geological Society, London, Special Publications*, *180*(1), 371-388.

Martin, B., Owen, A., Nichols, G. J., Hartley, A. J., & Williams, R. D. (2021). Quantifying downstream, vertical and lateral variation in fluvial deposits: Implications from the Huesca Distributive Fluvial System. *Frontiers in Earth Science*, *8*, 733-751.

McMahon, W. J., & Davies, N. S. (2018). The shortage of geological evidence for pre-vegetation meandering rivers. In Ghinassi, M., Colombera, L., Mountney, N.P., Reesink, A.J.H. & Bateman, M (Eds.), *Fluvial meanders and their sedimentary products in the rock record*, (p. 119-148). International Association of Sedimentologists.

Miall, A. D. (1993). The architecture of fluvial-deltaic sequences in the upper Mesaverde Group (Upper Cretaceous), Book Cliffs, Utah. *Geological Society, London, Special Publications*, *75*(1), 305-332.

Miall, A. D. (2006). Reconstructing the architecture and sequence stratigraphy of the preserved fluvial record as a tool for reservoir development: A reality check. *AAPG bulletin*, *90*(7), 989-1002.

Mitten, A. J., Howell, L. P., Clarke, S. M., & Pringle, J. K. (2020). Controls on the deposition and preservation of architectural elements within a fluvial multi-storey sandbody. *Sedimentary Geology*, *401*, 105629.

Morley, C. K. (1986). The Caledonian thrust front and palinspastic restorations in the southern Norwegian Caledonides. *Journal of Structural geology*, *8*(7), 753-765.

Moscariello, A. (2018). Alluvial fans and fluvial fans at the margins of continental sedimentary basins: geomorphic and sedimentological distinction for geo-energy exploration and development. *Geological Society, London, Special Publications*, *440*(1), 215-243.

Muhs, D. R. (2007). Loess deposits, origins and properties. The Encyclopedia of Quaternary Sciences, Elsevier, p. 1405-1418.

References

National Institutes of Health, (u.y.). *ImageJ: Image Processing and Analysis in Java*. Retrieved 21.05.2022 from https://imagej.nih.gov/ij/

Nichols, G. J., & Fisher, J. A. (2007). Processes, facies and architecture of fluvial distributary system deposits. *Sedimentary geology*, *195*(1-2), 75-90.

Nystuen, J. P. (1981). The late Precambrian "sparagmites" of southern Norway; a major Caledonian allochthon; the Osen-Røa nappe complex. *American Journal of Science*, *281*(1), 69-94.

Nystuen, J. P. (1983). Nappe and Thrust Structures in the Sparagmite Region, Southern Norway. *Geological Survey of Norway*, *380*, 67-83.

Oftedahl, C. (1978). Main geologic features of the Oslo Graben. In Ramberg, I.B. & Neumann, E.R (Eds.), *Tectonics and geophysics of continental rifts* (p. 149-165). Springer, Dordrecht.

Ori, G. G., & Friend, P. F. (1984). Sedimentary basins formed and carried piggyback on active thrust sheets. *Geology*, *12*(8), 475-478.

Owen, A., Nichols, G. J., Hartley, A. J., Weissmann, G. S., & Scuderi, L. A. (2015). Quantification of a distributive fluvial system: the Salt Wash DFS of the Morrison Formation, SW USA. *Journal of Sedimentary Research*, *85*(5), 544-561.

Paredes, J. M., Foix, N., Allard, J. O., Valle, M. N., & Giordano, S. R. (2018). Complex alluvial architecture, paleohydraulics and controls of a multichannel fluvial system: Bajo Barreal Formation (Upper Cretaceous) in the Cerro Ballena anticline, Golfo San Jorge Basin, Patagonia. *Journal of South American Earth Sciences*, *85*, 168-190.

Peterson, F. (1978). Measured sections of the lower Member and Salt Wash Member of the Morrison Formation (Upper Jurassic) in the Henry Mountains mineral belt of southern Utah, **78**-1094, (p. 97). *US Geological Survey Report*.

Plint, A. G., & Wadsworth, J. A. (2003). Sedimentology and palaeogeomorphology of four large valley systems incising delta plains, western Canada Foreland Basin: Implications for mid-Cretaceous sea-level changes. *Sedimentology*, *50*(6), 1147-1186.

Pranter, M. J., Ellison, A. I., Cole, R. D., & Patterson, P. E. (2007). Analysis and modeling of intermediate-scale reservoir heterogeneity based on a fluvial point-bar outcrop analog, Williams Fork Formation, Piceance Basin, Colorado. *AAPG bulletin*, *91*(7), 1025-1051.

Rittersbacher, A., Howell, J. A., & Buckley, S. J. (2014). Analysis of fluvial architecture in the Blackhawk Formation, Wasatch Plateau, Utah, USA, using large 3D photorealistic models. *Journal of Sedimentary Research*, *84*(2), 72-87.

Robinson, J. W., & McCabe, P. J. (1997). Sandstone-body and shale-body dimensions in a braided fluvial system: Salt Wash Sandstone Member (Morrison Formation), Garfield County, Utah. *AAPG bulletin*, *81*(8), 1267-1291.

Sheard, E. R., Williams-Jones, A. E., Heiligmann, M., Pederson, C., & Trueman, D. L. (2012). Controls on the concentration of zirconium, niobium, and the rare earth elements in the Thor Lake rare metal deposit, Northwest Territories, Canada. *Economic Geology*, *107*(1), 81-104.

Spjeldnæs, N. (1966). Silurian tidal sediments from the base of the Ringerike Formation, Oslo Region, Norway. *Norsk Geologisk Tidsskrift*, *46*, 497-509.

Størmer, L. (1954). New discoveries of ostracoderms and eurypterids at Ringerike, near Oslo. In *Proceedings of the Geological Society of London* (Vol. 1505, p. 21-22).

References

Suriano, J., Limarino, C. O., Tedesco, A. M., & Alonso, M. S. (2015). Sedimentation model of piggyback basins: Cenozoic examples of San Juan Precordillera, Argentina. *Geological Society, London, Special Publications*, *399*(1), 221-244.

Swan, A., Hartley, A. J., Owen, A., & Howell, J. (2018). Reconstruction of a sandy point-bar deposit: implications for fluvial facies analysis. In Ghinassi, M., Colombera, L., Mountney, N.P., Reesink, A.J.H. & Bateman, M (Eds.), *Fluvial meanders and their sedimentary products in the rock record*, (p. 445-474). International Association of Sedimentologists.

Thayer, J. B., & Ashmore, P. (2016). Floodplain morphology, sedimentology, and development processes of a partially alluvial channel. *Geomorphology*, *269*, 160-174.

Torsvik, T. H., & Cocks, L. R. M. (2013). New global palaeogeographical reconstructions for the Early Palaeozoic and their generation. *Geological Society, London, Memoirs*, *38*(1), 5-24.

Turner, P. (1974). Lithostratigraphy and Facies Analysis of the Ringerike Group of the Oslo Region. *Geological Survey of Norway*, *314*, 101-131.

Turner, P. (1974). *The Stratigraphy and Sedimentology of the Ringerike Group of Norway*. [Doctoral dissertation, University of Leicester].

Turner, P., & Whitaker, J. M. (1976). Petrology and provenance of late Silurian fluviatile sandstones from the Ringerike Group of Norway. *Sedimentary Geology*, *16*(1), 45-68.

University of Bergen. (2020, October 7th). *Thin Section lab: Thin section and polishing laboratory*. Retrieved 19.05.2022 from https://www.uib.no/en/geo/111547/thin-section-lab

Valenza, J. M., Edmonds, D. A., Hwang, T., & Roy, S. (2020). Downstream changes in river avulsion style are related to channel morphology. *Nature Communications*, *11*(1), 1-8.

Van De Kamp, P. C. (2010). Arkose, subarkose, quartz sand, and associated muds derived from felsic plutonic rocks in glacial to tropical humid climates. *Journal of Sedimentary Research*, *80*(10), 895-918.

VOG Group. (2022). *Caineville Wash*. Retrieved 09.05.2022 from https://v3geo.com/model/88

Weissmann, G. S., Hartley, A. J., Nichols, G. J., Scuderi, L. A., Olson, M., Buehler, H., & Banteah, R. (2010). Fluvial form in modern continental sedimentary basins: distributive fluvial systems. *Geology*, *38*(1), 39-42.

Wentworth, C. K. (1922). A Scale of Grade and Class Terms for Clastic Dediments. *The Journal of Geology*, *30*(5), 377-392.

Whitaker, J. M. (1964). Mud-crack diapirism in the Ringerike Sandstone of Southern Norway. *Norsk Geologisk Tidsskrift*, *44*, 19-30.

Whitaker, J.M. (1965). Primary sedimentary structures from the Silurian and Lower Devonian of the Oslo Region, Norway. *Nature, 4998*, 709-711.

Whitaker, J. M. (1980). A new trace fossil from the Ringerike Group, Southern Norway. *Proceedings of the Geologists' Association*, *91*(1-2), 85-89.

Willis, B. J., & Sech, R. P. (2018). Quantifying impacts of fluvial intra-channel-belt heterogeneity on reservoir behaviour. In Ghinassi, M., Colombera, L., Mountney, N.P., Reesink, A.J.H. & Bateman, M (Eds.), *Fluvial meanders and their sedimentary products in the rock record*, (p. 543-572). International Association of Sedimentologists.

References

Wilkins, A. D., Hurst, A., Wilson, M. J., & Archer, S. (2018). Palaeo-environment in an ancient low-latitude, arid lacustrine basin with loessite: The Smith Bank Formation (Early Triassic) in the Central North Sea, UK Continental Shelf. *Sedimentology*, *65*(2), 335-359.

Worsley, D., Aarhus, N., Bassett, M. G., Howe, M. P. A., Mørk, A., & Olaussen, S. (1983). *Geological Survey of Norway*, *384*, 1-57

Appendix

Appendices are attached in the separate zip-folders, ranging from Appendices I-IV.

- Appendix I contains the sedimentary logs.
- Appendix II contains thin section images.
- Appendix III contains ImageJ facies association distribution details.
- Appendix IV contains the virtual outcrops and related technical details.